

TEL AVIV UNIVERSITY

The Iby and Aladar Fleischman Faculty of Engineering
The Zandman-Slaner Graduate School of Engineering

**A study of the use of synchronverters
for grid stabilization using
simulations in SimPower**

A thesis submitted toward the degree of Master of
Science in Electrical and Electronic Engineering

by

Eitan Brown

July 2015

TEL AVIV UNIVERSITY

The Iby and Aladar Fleischman Faculty of Engineering
The Zandman-Slaner Graduate School of Engineering

**A study of the use of synchronverters
for grid stabilization using
simulations in SimPower**

A thesis submitted toward the degree of Master of
Science in Electrical and Electronic Engineering

by

Eitan Brown

This research was carried out in the Department of
Electrical Engineering – Systems
Under the supervision of Prof. George Weiss

July 2015

Acknowledgements

I would like to thank my advisor, Professor George Weiss, who introduced me the fields of control and power electronics. Professor Weiss has guided me throughout my studies both in research and during my courses selection. He had also helped me financially by increasing my university scholarship from his grants. The company Synvertec has sponsored my research by paying my bursary for about one year, and this is gratefully acknowledged. This help has given me the opportunity to devote my time to research. I also wish to thank Vivek Natarajan, a post-doc who gave me guidance and advice throughout my work and also in proofreading the drafts of this thesis. Finally I must mention Elad Venaezian, an MSc student with whom we collaborated on many aspects of this work.

Abstract

Synchronous generators (SG) have the following useful property: once synchronized, they stay synchronized even without any control, unless strong disturbances destroy the synchronism. This is one of the features that have enabled the development of the AC electricity grid at the end of the XIXth century. Today, the stability of networks of synchronous generators that are coupled with various types of loads and other types of power sources (such as renewables) and are operated with the help of multiple control loops, is an area of high interest and intense research, see for instance [1], [3], [12], [16], [26]. This is partly due to the proliferation of power sources that are not synchronous generators, which threatens the stability of the power grid. These power sources use inverters to deliver power to the grid. Most inverters are designed to deliver maximum power from the source and they do not contribute to grid stability, quite the contrary: they introduce disturbances due to the intermittent nature of the power source and they increase the sensitivity of the grid to other disturbances such as faults.

An inverter which behaves like a synchronous generator can simplify the modelling of the overall system and the overall system behavior during sudden disturbances or faults will be as stable as it would be without the inverter or even better. Such inverters, sometimes called *synchronverters*, have been proposed in [2], [6], [27], [32]. (Actually, the control algorithms proposed in these papers are different and the term synchronverter refers to inverters controlled as in [33].) The grid operator can relate to synchronverters in the same way as to classical generators, which makes the transition to the massive penetration of renewable and other distributed energy sources easier and smoother.

Contents

Acknowledgements	3
Abstract.....	4
Contents.....	5
List of Figures	6
List of Tables	8
1. Introduction.....	9
2. Model of a synchronous generator.....	11
2.1. Electrical part	11
2.2. Mechanical part	14
3. Model of a synchronous generator connected to infinite bus	15
3.1. Linearization of the SG model	16
3.2. Reduced order SG model	20
3.3. Linearization of the reduced order SG model	23
4. Introduction to synchronverters	26
5. Additional improvements to the synchronverter algorithm.....	34
6. Some simulation results for synchronverters.....	36
7. Inter-area oscillations	42
7.1. Power system stabilizers	44
7.2. Synchronverters with virtual friction.....	45
7.3. The Pogaku-Prodanovic-Green (PPG) inverter and inter-area oscillations	53
8. Eilat –Ktura grid section: a case study	55
9. A synchronverter based energy storage device for grid stabilization	65
10. Future work and conclusions	74
11. Bibliography.....	75
12. Appendix - synchronverter parameters.....	77
12.1. Basic system for detecting grid faults.....	82

List of Figures

Figure 1. Structure of an idealized three-phase round-rotor synchronous generator.....	11
Figure 2. Linearization of synchronous generator connected to infinite bus devided ..	19
Figure 3. Bode diagram of the linearized subsystem	20
Figure 4. Nyquist diagram of the Linearized subsystem.....	20
Figure 5. Bode diagram of the linearized subsystem described in (3.18)	25
Figure 6. Nyquist diagram of the linearized subsystem described in (3.18).	26
Figure 7. Electronic part of a synchronverter (without control)	27
Figure 8. Proposed controller for a self-synchronized synchronverter	29
Figure 9. Scheme of a 2-level 3 phase inverter with neutral line	31
Figure 10. Neutral clamp inverter topology for one phase of a 3 phase inverter	31
Figure 11. Schematic of a 2-level 3 phase inverter connected to the grid via an LCL ..	32
Figure 12. Reactive power profile of a synchronverter connected to an infinite bus ...	33
Figure 13. Active power profile of a synchronverter connected to an infinite bus	33
Figure 14. Frequency of a synchronverter connected to an infinite bus with PWM ...	33
Figure 15. Updated scheme of the synchronverter algorithm.....	35
Figure 16. Synchronverter grid frequency tracking, frequency decrease.....	36
Figure 17. Synchronverter active power profile when traking grid frequency.....	37
Figure 18. Synchronverter grid frequency tracking, frequency increase.	37
Figure 19. Synchronverter active power profile when traking grid frequency.....	37
Figure 20. Voltage profile of the infinite bus and the synchronverter terminals.....	38
Figure 21. Synchronverter frequency remains constant when the voltage changes.	39
Figure 22. The reactive power of the synchronverter stabilizes	39
Figure 23. Two synchronverters micro grid scheme.....	41
Figure 24. Two synchronverters grid active power profile.	41
Figure 25. Two synchronverters grid frequency profile.....	41
Figure 26. Two synchronverters grid voltage profile	42
Figure 27. The simple power network (without synchronverters).....	43
Figure 28. Power oscillations in the system from Figure 27.	43
Figure 29. General model of a PSS	44
Figure 30. Comparison of power oscillations using three types of PSS	45
Figure 31. The network from Figure 27 after adding synchronverters.	45
Figure 32. Comparison of power oscillations with and without virtual friction.....	46
Figure 33. Comparison of system power flow with synchronverter and PSS	48
Figure 34. Comparison of system voltage profile with synchronverter or PSS.	48
Figure 35. Comparison of system power flow with synchronverter and PSS	49
Figure 36. Comparison of system voltage profile with synchronverter or PSS	49
Figure 37. Synchronverter with PSS controller	50
Figure 38. Synchronverter with PSS controller, proof of concept.....	50
Figure 39. Synchronverter with PSS controller and virtual friction, comparison	50
Figure 40. PPG inverter general scheme.	53
Figure 41. Power controller.	53
Figure 42. Voltage controller.....	54
Figure 43. Current controller.....	54
Figure 44. Comparison of PPG inverter and synchronverter.....	55
Figure 45. Schematics of Eilat-Ktura grid section.	56
Figure 46. Updated power controller of the inverter designed in [23].	57
Figure 47. Synchronization of the inverter at Ktura to the grid.....	57
Figure 48. Frequency in Eilat 10Ω short circuit at Eilat	58
Figure 49. Frequency in Ktura 10Ω short circuit.....	58

Figure 50. Voltage in Eilat 10Ω short circuit at Eilat.....	58
Figure 51. Voltage in Ktura 10Ω short circuit at Eilat.....	59
Figure 52. Power supply in Ktura 10Ω short circuit at Eilat.....	59
Figure 53. Reactive power supply in Ktura 10Ω short circuit at Eilat.....	59
Figure 54. Frequency in Eilat 1Ω short circuit at Eilat.....	60
Figure 55. Frequency in Ktura 1Ω short circuit at Eilat.....	60
Figure 56. Voltage in Eilat 1Ω short circuit at Eilat	60
Figure 57. Voltage in Ktura 1Ω short circuit at Eilat.....	61
Figure 58. Power supply in Ktura 1Ω short circuit at Eilat.....	61
Figure 59. Reactive power supply in Ktura 1Ω short circuit at Eilat.....	61
Figure 60. Frequency in Eilat 0.1Ω short circuit at Eilat	62
Figure 61. Frequency in Ktura 0.1Ω short circuit at Eilat.....	62
Figure 62. Voltage in Eilat 0.1Ω short circuit at Eilat	63
Figure 63. Voltage in Ktura 0.1Ω short circuit at Eilat.....	63
Figure 64. Power supply in Ktura 0.1Ω short circuit at Eilat.....	63
Figure 65. Reactive power supply in Ktura 0.1Ω short circuit at Eilat.....	64
Figure 66. Ktura-Eilat simulation with a synchronverter in Ktura and power delay	65
Figure 67. Scheme of power grid with low, medium and high voltage parts.....	66
Figure 68. Output power of synchronous generator and synchronverter attached	68
Figure 69. Input power of 1MW synchronous motor and 5 MW load.....	69
Figure 70. Synchronverters with any virtual friction shows a small improvement	70
Figure 71. Synchronverters without one sided virtual friction generator frequency	70
Figure 72. Synchronverters with one sided virtual friction generator frequency	71
Figure 73. Synchronverters without one sided virtual friction motor frequency.....	71
Figure 74. Voltage amplitude at motor terminals no one sided virtual friction.....	72
Figure 75. Voltage amplitude at motor terminals with one sided virtual friction.....	72
Figure 76. Comparison of one sided virtual friction to increase of the droop factor	73

List of Tables

Table 1. Typical values for a 5kW synchronous generator	19
Table 2. Parameters for a 40 MW PPG inverter	54
Table 3. Summary of the 6 tested scenarios for synchronverter.....	69
Table 4. Parameters for 5 kW synchronverter	77
Table 5. Parameters for PSS and virtual friction in the synchronverter	78
Table 6. Parameters for a 1 MW synchronverter.....	79
Table 7. Parameters for additional filters for the synchronverter.....	81

1. Introduction

Synchronous generators are a fundamental component of the AC power grid. From a control systems perspective, synchronous generators have the following useful feature: once the generators are synchronized to the grid, they remain synchronized without need for any external control. The AC power grid delivers high power at high voltages using AC/AC transformers which, as of today, is very difficult to accomplish using a DC grid with DC/DC transformers due to the limitations of the electronic switches they use.

The power grid must maintain constant frequency and voltages. In a physical grid, where the loads vary frequently, this is achieved using control algorithms that regulate grid operation. One control loop in the synchronous generator modifies the power set point of the generator in response to frequency changes in the grid using a constant droop coefficient. Another control loop regulates the voltage through the reactive power (although it is more complex). In the European grid the nominal frequency is 50 Hz and the droop coefficient is 3%, this means that when the grid frequency drops by 3% from the nominal value, the power output of the generator is required to go up by 100%. Similarly a 3% frequency rise must lead to a 100% power decrease. The power is changed so as to bring the frequency back to the nominal value. There are physical limitations to the performance of these control loops. For instance, there is a delay in the loop due to the slow response of the mechanical components and the excess energy initially comes from inertia, meaning the stored mechanical energy in the rotor. In order to stabilize the voltage the generator supplies or absorbs reactive power from the grid. The regulation here is less critical, since there are other devices in the power grid for stabilizing the voltage (by supplying or absorbing reactive power). There is also a relation between voltage and frequency but usually the control system decouples them.

Inverters are used for connecting renewable energy sources to the grid. They try to participate in the frequency and voltage regulation in the grid, but due to limitations related to the system architecture and financial constraints (renewable energy as of today is more expensive) often the regulation objectives are sacrificed in favor of other objectives such as harvesting more energy. Inverters are not only used by renewable sources. Today in some countries there are high power DC lines. These lines are good for connecting electrical grids from different countries with different regulations or for simply delivering electricity without radiation in the cables. In the near future, energy storage units will also play a role in the power grid to ensure that power is available during high demands and generator faults. These units will also require inverters to connect to the grid.

Another significant change today is in the nature of the loads. While in the past loads were usually linear resistive (lighting bulbs, etc.) and linear inductive (washing machine for example), today we have computers, and large batteries (electrical cars or storage units) which are nonlinear loads. These new loads require converters (AC/DC) which have their own control systems and limitations. This means that unlike in the past, the grid today is less predictable and experiences faster load changes, is subject to harmonics and interacts with many different controllers.

For now when the renewable energy market is small, around 10% in most countries, the influence of introducing inverters to the grid is negligible and can be handled by strict regulation for any power source in the grid. In the future it is likely that the percentage contribution of renewable energy will be much larger and the grid will contain a large number of nonlinear loads.

There are two approaches to solve this issue, changing the concept of power grid operation and power grid control or introducing a controller for inverters and converters that force them to behave like a synchronous generator.

In this work I will briefly introduce the synchronous machine and derive the equations of a synchronous generator with a constant mechanical torque, i.e. no prime mover or mechanical control of any sort is modelled. The prime mover system will not be discussed here but one can find additional information on [16]. After deriving the mathematical model of a synchronous generator, I will explore the local stability of a synchronous generator connected to an infinite bus and introduce a reduced model with model reduction techniques (additional info on such techniques can be found in [13]). Then after taking some approximations and additional assumptions the concept of synchronverter will be introduced.

I will present some known problems and solutions regarding power grids and demonstrate how synchronverters help the grid to recover from faults and reduce unwanted oscillations better than popular known solutions. The end of my thesis will discuss an additional practical use of the synchronverter for energy storage units. Relevant simulations with a suggested explanation as to how a synchronverter can use the energy storage for increasing grid robustness are included. Due to time limitations I was not able to provide a proper mathematical reasoning for some concepts presented here.

All the variables in this thesis are in SI units, unless specified otherwise.

2. Model of a synchronous generator

In this section, we develop a model for a round rotor synchronous generator starting from first principles. We assume that the generator has one pair of poles per phase and one pair of poles on the rotor, i.e., $p=1$. The machine is assumed to be perfectly built and therefore we ignore magnetic-saturation effects, iron core losses and Eddy currents in our model. Section 2.1 considers the electrical part of the generator while Section 2.2 focuses on the mechanical part. Our derivations follow Grainger and Stevenson [11], Zhong and Weiss [33]. A more detailed model taking into account cogging and other nonlinear effects is in Mandel and Weiss [18], see also Sauer and Pai [24].

2.1. Electrical part

The structure of an idealized three-phase generator is shown in Figure 1. The currents in the three stator windings are denoted by i_a , i_b and i_c and the voltages across them by v_a , v_b and v_c . The current and voltage across the rotor winding are i_f and v_f , respectively. The stator windings can be regarded as concentrated coils with self-inductance L , mutual inductance $-M$ and resistance R_s . Define $L_s = M + L$. The rotor windings are also regarded as a concentrated coil with self-inductance L_f and resistance R_f . M_f is the amplitude of the mutual inductance between the rotor and each of the stators windings. The rotor angle is denoted by θ , as shown in Figure 1.

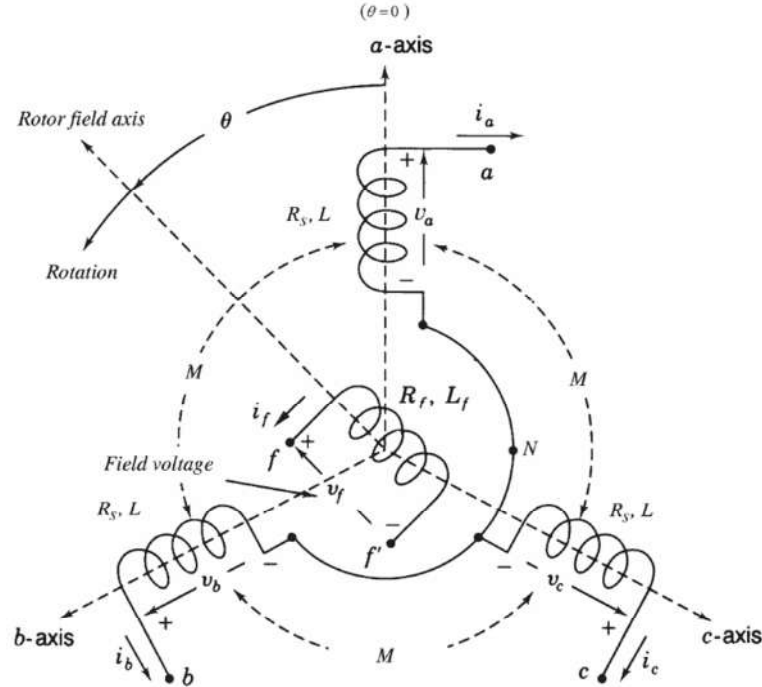


Figure 1. Structure of an idealized three-phase round-rotor synchronous generator with $p=1$, modified from [11], Figure 3.4.

We assume that the neutral line is absent and therefore

$$i_a + i_b + i_c = 0.$$

Denote the stator fluxes by Φ_a , Φ_b and Φ_c . Define the vectors

$$\begin{aligned} i &= \begin{bmatrix} i_a \\ i_b \\ i_c \end{bmatrix}, \quad \Phi = \begin{bmatrix} \Phi_a \\ \Phi_b \\ \Phi_c \end{bmatrix}, \quad v = \begin{bmatrix} v_a \\ v_b \\ v_c \end{bmatrix}, \\ \widetilde{\cos} \theta &= \begin{bmatrix} \cos \theta \\ \cos(\theta - 2\pi/3) \\ \cos(\theta - 4\pi/3) \end{bmatrix}, \quad \widetilde{\sin} \theta = \begin{bmatrix} \sin \theta \\ \sin(\theta - 2\pi/3) \\ \sin(\theta - 4\pi/3) \end{bmatrix}. \end{aligned}$$

The stator flux linkages are given by

$$\Phi = L_s i + M_f i_f \widetilde{\cos} \theta$$

and the rotor flux linkage Φ_f is given by

$$(2.1) \quad \Phi_f = L_f i_f + M_f \langle i, \widetilde{\cos} \theta \rangle.$$

The phase terminal voltage vector v satisfies

$$(2.2) \quad v = e - R_s i - L_s \frac{di}{dt},$$

where $e = [e_a \ e_b \ e_c]^T$ is the back EMF due to the rotor movement and it is given by

$$(2.3) \quad e = M_f i_f \omega \widetilde{\sin} \theta - M_f \frac{di_f}{dt} \widetilde{\cos} \theta,$$

where $\omega = \dot{\theta}$ is the angular velocity of the rotor. e is also called the *synchronous internal voltage*. Similarly, the field terminal voltage is

$$(2.4) \quad v_f = -R_f i_f - \frac{d\Phi_f}{dt}.$$

By applying the Park transformation

$$(2.5) \quad U(\theta) = \sqrt{\frac{3}{2}} \begin{bmatrix} \cos \theta & \cos\left(\theta - \frac{2\pi}{3}\right) & \cos\left(\theta + \frac{2\pi}{3}\right) \\ -\sin \theta & -\sin\left(\theta - \frac{2\pi}{3}\right) & -\sin\left(\theta + \frac{2\pi}{3}\right) \\ \frac{1}{\sqrt{2}} & \frac{1}{\sqrt{2}} & \frac{1}{\sqrt{2}} \end{bmatrix}$$

to (2.2), we get the following expression:

$$(2.6) \quad L_s U(\theta) \frac{di}{dt} + R_s U(\theta) i = U(\theta) e - U(\theta) v.$$

We denote $e_{dq} = U(\theta) e$, whose components are e_d , e_q and e_0 (in this order). The vectors v_{dq} and i_{dq} are defined similarly. It is easy to verify that

$$(2.7) \quad \frac{d}{d\theta} \begin{bmatrix} i_d \\ i_q \\ i_0 \end{bmatrix} = U(\theta) \frac{di}{d\theta} + \begin{bmatrix} i_q \\ -i_d \\ 0 \end{bmatrix}$$

which can be rewritten as

$$(2.8) \quad \frac{d}{dt} \begin{bmatrix} i_d \\ i_q \\ i_0 \end{bmatrix} = U(\theta) \frac{di}{dt} + \omega \begin{bmatrix} i_q \\ -i_d \\ 0 \end{bmatrix}.$$

Using this, we can rewrite (2.6) as follows:

$$(2.9) \quad L_s \frac{d}{dt} \begin{bmatrix} i_d \\ i_q \\ i_0 \end{bmatrix} - L_s \omega \begin{bmatrix} i_q \\ -i_d \\ 0 \end{bmatrix} + R_s \begin{bmatrix} i_d \\ i_q \\ i_0 \end{bmatrix} = \begin{bmatrix} e_d - v_d \\ e_q - v_q \\ e_0 - v_0 \end{bmatrix}.$$

Since there is no neutral line, $i_0 = 0$ and hence $e_0 = v_0$. From (2.9)

$$(2.10) \quad \frac{d}{dt} \begin{bmatrix} i_d \\ i_q \end{bmatrix} = \omega \begin{bmatrix} i_q \\ -i_d \end{bmatrix} - \frac{R_s}{L_s} \begin{bmatrix} i_d \\ i_q \end{bmatrix} + \frac{1}{L_s} \begin{bmatrix} e_d - v_d \\ e_q - v_q \end{bmatrix}.$$

Applying the Park transform to (2.3) we get

$$(2.11) \quad \begin{bmatrix} e_d \\ e_q \end{bmatrix} = -\sqrt{\frac{3}{2}} \begin{bmatrix} M_f \frac{di_f}{dt} \\ M_f i_f \omega \end{bmatrix} = -\sqrt{\frac{3}{2}} M_f \begin{bmatrix} \frac{di_f}{dt} \\ i_f \omega \end{bmatrix}.$$

In (2.4), substituting for Φ_f from (2.1) and using the identity $\langle i, \cos \theta \rangle = \sqrt{3/2} i_d$ (recall that $i_{dq} = U(\theta)i$ where $U(\theta)$ is defined in (2.5)) it follows that

$$(2.12) \quad L_f \frac{di_f}{dt} + \sqrt{\frac{3}{2}} M_f \frac{di_d}{dt} + R_f i_f = -v_f.$$

Using the equation for $\frac{di_d}{dt}$ from (2.9) in (2.12) we get

$$(2.13) \quad \left(1 - \frac{3M_f^2}{2L_f L_s}\right) \frac{di_f}{dt} = -\sqrt{\frac{3}{2}} \frac{M_f}{L_f} \left(\omega i_q - \frac{R_s}{L_s} i_d - \frac{1}{L_s} v_d\right) - \frac{R_f}{L_f} i_f - \frac{1}{L_f} v_f,$$

where $1 - M_f^2/(L_f L_s) > 0$ and $L = 2L_s/3$. By defining

$$(2.14) \quad \alpha = \left(1 - \frac{3M_f^2}{2L_f L_s}\right)^{-1}, \quad m = \sqrt{\frac{3}{2}} M_f,$$

(2.13) can be written as

$$(2.15) \quad \frac{di_f}{dt} = \frac{\alpha m}{L_f} \left(\omega i_q - \frac{R_s}{L_s} i_d - \frac{1}{L_s} v_d\right) - \frac{\alpha R_f}{L_f} i_f - \frac{\alpha}{L_f} v_f.$$

Now we obtain the following equation for i_d and i_q from (2.10) by substituting for e_d and e_q from (2.11) and for di_f/dt from (2.15):

$$(2.16) \quad \frac{d}{dt} \begin{bmatrix} i_d \\ i_q \end{bmatrix} = \omega \begin{bmatrix} i_q \\ -i_d \end{bmatrix} - \frac{R_s}{L_s} \begin{bmatrix} i_d \\ i_q \end{bmatrix} - \frac{m}{L_s} \begin{bmatrix} -\frac{\alpha m}{L_f} \left(\omega i_q - \frac{R_s}{L_s} i_d - \frac{1}{L_s} v_d \right) - \frac{\alpha R_f}{L_f} i_f - \frac{\alpha}{L_f} v_f \\ \omega i_f \end{bmatrix}.$$

2.2. Mechanical part

The energy stored in the machine's magnetic field is

$$E_{mag} = \frac{1}{2} \langle i, \Phi \rangle + \frac{1}{2} i_f \Phi_f = \frac{1}{2} \langle i, L_s i \rangle + M_f i_f \langle i, \cos \theta \rangle + \frac{1}{2} L_f i_f^2.$$

The electromagnetic torque can be calculated as shown below (see [7], [10] and [11] for details), where we use the relation $\theta = p\theta_m$, θ_m is the mechanical rotor angle and $p=1$ (as explained at the beginning of this chapter):

$$(2.17) \quad T_e = \frac{\partial E_{mag}}{\partial \theta_m} \Big|_{\Phi, \Phi_f \text{ constant}} = \frac{\partial E_{mag}}{\partial \theta_m} \Big|_{i, i_f \text{ constant}} = -p \frac{\partial E_{mag}}{\partial \theta} \Big|_{i, i_f \text{ constant}} = -p M_f i_f \left\langle i, \frac{\partial \cos \theta}{\partial \theta} \right\rangle = p M_f i_f \langle i, \sin \theta \rangle = -\sqrt{\frac{3}{2}} M_f i_f i_q = -m i_f i_q.$$

Usually the mechanical torque is produced/regulated by a prime mover which often consists of a turbine and a controller, see Chapter 9 in [16] for different types of prime movers. In our model, we ignore the dynamics of the prime mover and instead assume that the specified mechanical torque T_m (plus the droop correction, explained below) acts on the rotor. If we assume no cogging torque, which is the torque due to the interaction between the permanent magnets or electromagnets of the rotor and the stator slots, then the mechanical part of the machine is governed by

$$(2.18) \quad J \dot{\omega} = T_m - T_e - D_p \omega,$$

where J is the moment of inertia of all parts rotating, D_p is the damping factor and the rotation frequency ω is the first derivative of the rotor angle. The term $-D_p \omega$ is due in part to viscous friction, but mostly it is due to the droop controller of the prime mover, which adjusts the active torque depending on ω . The kinetic energy of the rotor is $E_{kin} = J \omega^2 / 2$. It follows that

$$\dot{E}_{kin} = J \dot{\omega} \omega = \omega (T_m - T_e - D_p \omega) = \omega (T_m + m i_f i_q - D_p \omega).$$

In the absence of any external torque ($T_m = 0$) and short circuit in all terminals, the change in the total energy $E = E_{mag} + E_{kin}$ of the system, must be equal to the loss of energy due to mechanical damping (including the droop correction) and electrical resistance. It is easy to check that

$$(2.19) \quad \dot{E} = \dot{E}_{mag} + \dot{E}_{kin} = -R_s(i_d^2 + i_q^2) - R_f i_f^2 - D_p \omega^2 \leq 0.$$

This validates our energy calculations. Note that, if we neglect the viscous friction, then the active torque acting on the generator is $T_m - D_p \omega$.

Using (2.15), (2.16), (2.17) and (2.18) we obtain the following system which models the dynamics of a perfectly built synchronous generator with one pair of poles:

$$(2.20) \quad \begin{aligned} \frac{d}{dt} \begin{bmatrix} L_s i_d \\ L_s i_q \\ L_f i_f \\ J\omega \end{bmatrix} &= \begin{bmatrix} -\alpha R_s & \alpha \omega L_s & \alpha m R_f & 0 \\ -\omega L_s & -R_s & 0 & -m i_f \\ \alpha m R_s / L_s & -\alpha m \omega & -\alpha R_f & 0 \\ 0 & m i_f & 0 & -D_p \end{bmatrix} \begin{bmatrix} i_d \\ i_q \\ i_f \\ \omega \end{bmatrix} \\ &+ \begin{bmatrix} -\alpha & 0 & \alpha m / L_f & 0 \\ 0 & -1 & 0 & 0 \\ \alpha m / L_s & 0 & -\alpha & 0 \\ 0 & 0 & 0 & 1 \end{bmatrix} \begin{bmatrix} v_d \\ v_q \\ v_f \\ T_m \end{bmatrix}. \end{aligned}$$

We mention that this system can be represented as a port-hamiltonian system, see Fiaz, Zonetti, Ortega, Scherpen and van der Schaft [9].

3. Model of a synchronous generator connected to an infinite bus

In this section we develop a model for a single synchronous generator (SG) connected to the power grid. The grid is assumed to be an infinite bus, i.e., a constant three-phase AC voltage source. This is a reasonable assumption since the influence of a single generator on a grid consisting of many equivalent generators is typically small. To simplify the presentation, the constants L_s and R_s are redefined to include the resistance and inductance of the line leading to the bus. Thus the stator terminal voltage v is the voltage of the bus. The bus voltage $v = [v_a \ v_b \ v_c]^T$ depends on the bus angle θ_{bus} as follows:

$$v_a = \sqrt{2/3} V \cos \theta_{bus}, \quad v_b = \sqrt{2/3} V \cos(\theta_{bus} - 2\pi/3), \quad v_c = \sqrt{2/3} V \cos(\theta_{bus} + 2\pi/3).$$

Here $V > 0$ is the line to line rms voltage. Define

$$\delta = -\pi/2 - (\theta_{bus} - \theta),$$

where θ is the rotor angle of the synchronous generator. This is the well-known *power angle*, the angle by which the synchronous internal voltage e is ahead of the bus voltage v . We apply the Park transform (2.5) to v . Using the definition $v_{dq} = U(\theta)v$, we get that

$$(3.1) \quad v_d = -V \sin \delta, \quad v_q = -V \cos \delta.$$

It is easy to see that

$$(3.2) \quad \dot{\delta} = \omega - \omega_g,$$

where ω_g is the constant bus frequency. Thus $\ddot{\delta} = \dot{\omega}$. From (2.17) and (2.18) we get

$$(3.3) \quad J\ddot{\delta} + D_p(\dot{\delta} + \omega_g) = mi_f i_q + T_m.$$

If we can express i_q as a (possibly approximate) function of δ , then from the above equation an ODE in δ that resembles the classical swing equation can be obtained. We will derive such an ODE using model reduction in Section 3.2.

We remember (2.20) for the dynamics of the full system. Now we add the state variable δ with the state equation (3.2) and assign the values of v_d and v_q from (3.1) to get the following ODE system with 5 state variables:

$$(3.4) \quad \begin{aligned} \frac{d}{dt} \begin{bmatrix} L_s i_d \\ L_s i_q \\ L_f i_f \\ J\omega \\ \delta \end{bmatrix} &= \begin{bmatrix} -\alpha R_s & \alpha\omega L_s & \alpha m R_f / L_f & 0 & 0 \\ -\omega & -R_s & 0 & -mi_f & 0 \\ \alpha m R_s / L_s & -\alpha m \omega & -\alpha R_f & 0 & 0 \\ 0 & mi_f & 0 & -D_p & 0 \\ 0 & 0 & 0 & 1 & 0 \end{bmatrix} \begin{bmatrix} i_d \\ i_q \\ i_f \\ \omega \\ \delta \end{bmatrix} \\ &+ \begin{bmatrix} -\alpha & 0 & \alpha m / L_f & 0 & 0 \\ 0 & -1 & 0 & 0 & 0 \\ \alpha m / L_s & 0 & -\alpha & 0 & 0 \\ 0 & 0 & 0 & 1 & 0 \\ 0 & 0 & 0 & 0 & 1 \end{bmatrix} \begin{bmatrix} -V \sin \delta \\ -V \cos \delta \\ v_f \\ T_m \\ -\omega_g \end{bmatrix}. \end{aligned}$$

3.1. Linearization of the SG model on an infinite bus

We analyze the local stability of (3.4) by linearizing it near its equilibrium points in this section. **We assume that i_f is constant** (this assumption is made to simplify the calculations). Then the nonlinear equations (3.4) reduce to

$$(3.5) \quad \begin{aligned} \frac{d}{dt} \begin{bmatrix} L_s i_d \\ L_s i_q \\ J\omega \\ \delta \end{bmatrix} &= \begin{bmatrix} -R_s & \omega L_s & 0 & 0 \\ -\omega L_s & -R_s & -mi_f & 0 \\ 0 & mi_f & -D_p & 0 \\ 0 & 0 & 1 & 0 \end{bmatrix} \begin{bmatrix} i_d \\ i_q \\ \omega \\ \delta \end{bmatrix} + \begin{bmatrix} V \sin \delta \\ V \cos \delta \\ T_m \\ -\omega_g \end{bmatrix}. \end{aligned}$$

We compute the equilibrium points $[i_{d0} \ i_{q0} \ \omega_0 \ \delta_0]^T$ for (3.5) by setting the derivatives of all the state variables to be 0. Letting $\dot{\delta} = 0$, it follows from the fourth equation in (3.5) that $\omega_0 = \omega_g$. The third equation in (3.5) (setting $\dot{\omega} = 0$) gives

$$\begin{aligned} mi_f i_{q0} - D_p \omega_g + T_m &= 0 \\ \Rightarrow i_{q0} &= -\frac{1}{mi_f} (T_m - D_p \omega_g). \end{aligned}$$

It follows from the second equation in (3.5) that

$$-R_s i_{d0} + \omega_g L_s i_{q0} + V \sin \delta_0 = 0$$

$$\Rightarrow i_{d0} = \frac{V}{R_s} \sin \delta_0 - \frac{\omega_g L_s}{R_s m_i f} (T_m - D_p \omega_g).$$

Finally we get from the first equation in (3.5) that

$$(3.6) \quad -\omega_g L_s i_{d0} - R_s i_{q0} - m_i f \omega_g + V \cos \delta_0 = 0.$$

We define Z and ψ as follows: $Z = R_s + j\omega_g L_s = |Z| e^{j\psi}$, so that

$$(3.7) \quad |Z| = \sqrt{R_s^2 + \omega_g^2 L_s^2}, \quad \psi = \arctan(\omega_g L_s / R_s).$$

After substituting for i_{d0} and i_{q0} in (3.6), using the definitions in (3.7), the power angle δ at the equilibrium is given by the expression

$$(3.8) \quad \delta_0 = \arccos \left(\frac{m_i f \omega_g R_s}{|Z| V} - \frac{|Z|(T_m - D_p \omega_g)}{V m_i f} \right) - \psi.$$

This equation may have 0, 1 or 2 solutions modulo 2π . If there are two solutions, then there are two equilibrium points and they are either both unstable or one stable and one unstable. We want to linearize the system near a stable equilibrium point. For this we compute the equilibrium points and check if any of them is stable. The linearized system will be of the form

$$(3.9) \quad \dot{x} = Ax.$$

Define

$$\tilde{i}_d = i_d - i_{d0}, \quad \tilde{i}_q = i_q - i_{q0}, \quad \tilde{\omega} = \omega - \omega_0, \quad \tilde{\delta} = \delta - \delta_0,$$

where $x_{eq} = [i_{d0} \ i_{q0} \ \omega_0 \ \delta_0]^T$ is an equilibrium point of (3.5), and denote $x = [\tilde{i}_d \ \tilde{i}_q \ \tilde{\omega} \ \tilde{\delta}]^T$.

Define $z = [i_d \ i_q \ \omega \ \delta]^T$ and rewrite (3.5) in the form $\dot{z} = f(z)$, then A in (3.9) is the

Jacobian defined by $A_{ij} = \frac{\partial f(z)_i}{\partial z_j} \Big|_{z=x_{eq}}$. We calculate the Jacobian from (3.5) and get

$$A = \begin{bmatrix} -R_s/L_s & \omega_g & i_{q0} & V \cos \delta_0 / L_s \\ -\omega_g & -R_s/L_s & -(i_{d0} + m_i f / L_s) & -V \sin \delta_0 / L_s \\ 0 & m_i f / J & -D_p / J & 0 \\ 0 & 0 & 1 & 0 \end{bmatrix}.$$

We need to assign parameter values to compute the equilibrium points of (3.5) and check if they are stable, by computing the eigenvalues of the resulting Jacobian matrix. For the nominal values of the parameters shown in Table 1, we obtain a pair of equilibrium points $x_{eq} = [i_{d0} \ i_{q0} \ \omega_0 \ \delta_0]^T$ shown below:

$$x_{eq}^1 = [-6.7181 \ -12.2190 \ 100\pi \ 0.0398], \quad x_{eq}^2 = [-578.2614 \ -12.2190 \ 100\pi \ -2.9624].$$

For x_{eq}^1 the matrix A is

$$A = \begin{bmatrix} -34.5455 & 314.1593 & -12.2190 & 90467 \\ -314.1593 & -34.5455 & -289.3083 & -3602.5 \\ 0 & 6.5126 & -8.5 & 0 \\ 0 & 0 & 1 & 0 \end{bmatrix}$$

and the eigenvalues of A are:

$$\lambda_1 = -34.88 + 314.23j, \lambda_2 = -34.88 - 314.23j, \lambda_3 = -3.92 + 43j, \lambda_4 = -3.92 - 43j.$$

For x_{eq}^2 the matrix A is

$$A = \begin{bmatrix} -34.5455 & 314.1593 & -12.2190 & -89089 \\ -314.1593 & -34.5455 & 282.3083 & 16138 \\ 0 & 6.5126 & -8.5 & 0 \\ 0 & 0 & 1 & 0 \end{bmatrix}$$

and the eigenvalues of are:

$$\lambda_1 = -34.87 + 314.22j, \lambda_2 = -34.87 - 314.22j, \lambda_3 = -47.23, \lambda_4 = 39.38.$$

Notice that in both cases λ_1 and λ_2 are almost equal to $-R_s/L_s \pm j\omega_g$.

Hence (3.5) has two equilibrium points, where x_{eq}^1 is stable and x_{eq}^2 is unstable. This is true for typical values of the parameters. For some set of parameter vectors, it is possible to show that the synchronous generator model (3.5) is almost globally asymptotically stable, meaning that almost all the trajectories converge to the stable equilibrium point, see [20].

We remark that (3.4) can be linearized without the assumption of constant rotor current, but the expressions become extremely complex and the model is very difficult to analyze.

In order to compare (3.5) to a reduced model that will be introduced in Section 3.2 we will manipulate the linearized system $\dot{x} = Ax$, where $x = [\tilde{i}_d \ \tilde{i}_q \ \tilde{\omega} \ \tilde{\delta}]^T$ and A is as calculated above. We can write $\dot{x} = Ax$ as a feedback interconnection of an integrator (with input $\tilde{\omega}$ and output $\tilde{\delta}$) with the third order system

$$(3.10) \quad \dot{z} = A_3 z + B_3 z, \quad y = C_3 z,$$

where $z = [\tilde{i}_d \ \tilde{i}_q \ \tilde{\omega}]^T$ and

$$A_3 = \begin{bmatrix} -R_s/L_s & \omega_g & i_{q0} \\ -\omega_g & -R_s/L_s & -(i_{d0} + mi_f/L_s) \\ 0 & mi_f/J & -D_p/J \end{bmatrix}, \quad B_3 = \begin{bmatrix} V \cos \delta_0 / L_s \\ -V \sin \delta_0 / L_s \\ 0 \end{bmatrix}, \quad C_3 = [0 \ 0 \ -1],$$

as shown in Figure 2.

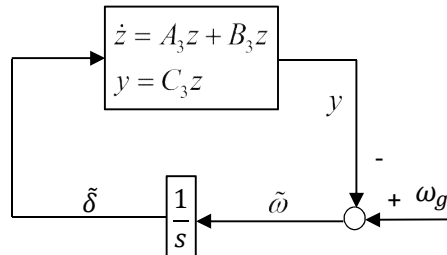


Figure 2. The linearization of a synchronous generator connected to an infinite bus, divided into two subsystems.

The transfer function of the third order system is

$$G(s) = C_3(sI - A_3)^{-1} B_3.$$

The Bode and Nyquist plots for this transfer function, with A_3 , B_3 and C_3 evaluated at x_{eq}^1 , are in Figure 3 and 4. The eigenvalues of A_3 for x_{eq}^1 are:

$$\lambda_1 = -34.43 + 317.13j, \lambda_2 = -34.43 - 317.13j, \lambda_3 = -8.74.$$

The eigenvalues of A_3 for x_{eq}^2 are:

$$\lambda_1 = -34.92 + 311.25j, \lambda_2 = -34.92 - 311.25j, \lambda_3 = -77.5.$$

In Section 3.3 we will derive a feedback interconnection, similar to that shown in Figure 2, but using a reduced model for the SG. We plot its Bode and Nyquist plots and compare it with the plots in Figures 3 and 4. We do this comparison to ascertain the fidelity of the reduced model.

Parameter	Value
V - line to line rms value	$230\sqrt{3} = 398.37$ V
$P_n = 5\text{kW}$, $T_m = P_n/\omega_g + D_p\omega_g$	549.986 Nm
ω_g	$100\pi \text{ s}^{-1}$
R_s	0.152Ω
L_s	4.4 mH
R_f	0.6Ω
L_f	0.3 H
M_f	0.025 H
J (for $J\omega^2 / 2P \approx 2$ seconds)	0.2 Kgm^2
D_p (100% increase of P for 3% decrease of ω)	1.7 Js
i_f	42.54 A

Table 1. Nominal values for a 5kW synchronous generator connected to a 50 Hz low voltage line in a European or similar power grid.

The resulting parameters, α, m , and mi_f at equilibrium are:

$$\alpha = 3.451, m = 0.0306 \text{ H}, mi_f = 1.304 \text{ Vs}, e_{rms} = M_f i_f \omega / \sqrt{2} = 236.8 \text{ V} \text{ V}.$$

Some of the values in Table 1 are obtained from regulation requirements in Europe (for instance the values of D_p , J , ω_g and V). The values of R_s and L_s are selected to be the same as those of the 5 kW synchronverter on which experiments are being conducted at Tel Aviv University. The values of R_f , L_f and M_f were chosen intuitively to match the other parameters. The value of mi_f was found via simulation of a simple system consisting of a synchronous generator and an ideal voltage source. The Bode and Nyquist plots below were obtained using standard MATLAB commands.

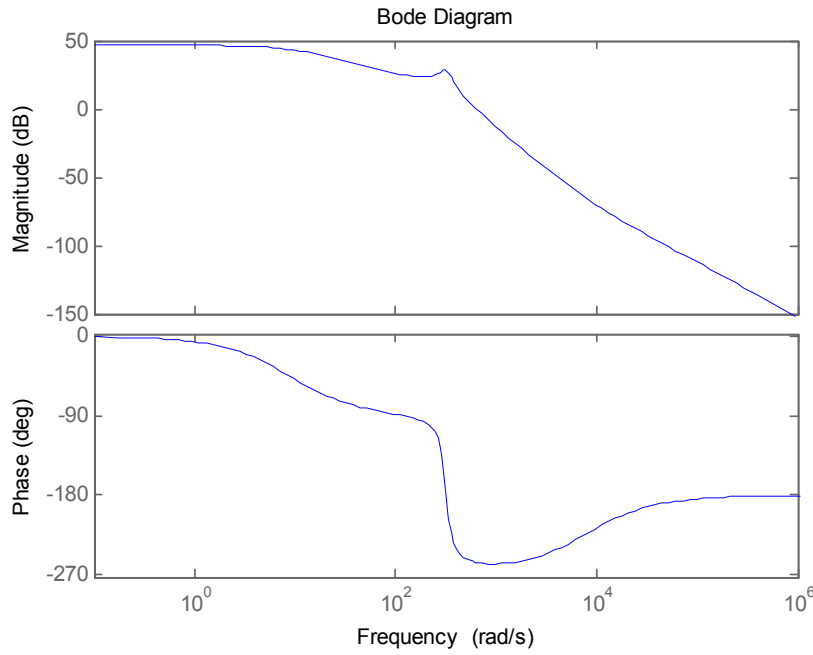


Figure 3. Bode diagram of the linearized subsystem described in (3.10) around the stable equilibrium point x_{eq}^1 of the nonlinear model (3.5).

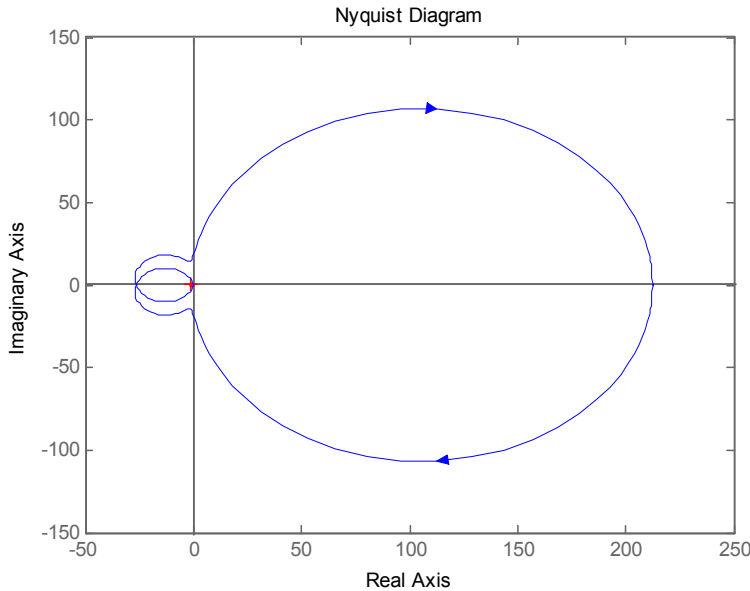


Figure 4. Nyquist diagram of the linearized subsystem described in (3.10) around the stable equilibrium point x_{eq}^1 of the nonlinear model (3.5).

3.2. The reduced order SG model

We develop a reduced order model for the fifth order system in (3.4). As mentioned below (3.3), the idea is to express i_q as a function of δ . Since L_s is typically small, following the singular perturbation theory (see Chapter 11 in [13]), we let $L_s di_d / dt = 0$

and $L_s \frac{di_q}{dt} = 0$ in (3.4). In other words, i_d and i_q are assumed to be fast variables. This gives:

$$(3.11) \quad i_d = \frac{\omega L_s}{R_s} i_q + \frac{m R_f}{R_s L_f} i_f + \frac{V \sin \delta}{R_s} + \frac{m}{L_f R_s} v_f,$$

$$(3.12) \quad i_q = -\frac{\omega L_s}{R_s} i_d - \frac{m \omega}{R_s} i_f + \frac{V \cos \delta}{R_s}.$$

We define the stator impedance $Z_\omega = R_s + j\omega L_s$, so that $|Z_\omega| = \sqrt{R_s^2 + \omega^2 L_s^2}$.

Solving for i_q from (3.11) and (3.12) gives

$$i_q = \frac{1}{|Z_\omega|^2} \left[-\frac{m \omega}{L_f} (R_f L_s + R_s L_f) i_f + V (R_s \cos \delta - \omega L_s \sin \delta) - \frac{m \omega L_s}{L_f} v_f \right].$$

Substituting for i_q in (3.3) gives

$$\begin{aligned} J \ddot{\delta} + D_p (\dot{\delta} + \omega_g) &= \\ T_m + \frac{m i_f}{|Z_\omega|^2} \left[-\frac{m \omega}{L_f} (R_f L_s + R_s L_f) i_f + V (R_s \cos \delta - \omega L_s \sin \delta) - \frac{m \omega L_s}{L_f} v_f \right], \end{aligned}$$

which can be equivalently expressed as

$$(3.13) \quad \begin{aligned} J \ddot{\delta} + D_p (\dot{\delta} + \omega_g) &= T_m + \\ \left(\frac{V R_s}{|Z_\omega|^2} \cos \delta - \frac{V \omega L_s}{|Z_\omega|^2} \sin \delta \right) m i_f - \frac{\omega (R_f L_s + R_s L_f)}{|Z_\omega|^2 L_f} m^2 i_f^2 - \frac{\omega L_s}{|Z_\omega|^2 L_f} m^2 i_f v_f. \end{aligned}$$

By definition $\omega_g L_s = |Z| \sin \psi$ and $R_s = |Z| \cos \psi$ (Z and ψ are defined before (3.7)). We assume that $\omega \approx \omega_g$ and therefore $|Z_\omega| \approx |Z|$. By replacing $|Z_\omega|$ with $|Z|$ in (3.13) and using the identity $\cos(\psi + \delta) = \cos \psi \cos \delta - \sin \psi \sin \delta$ and $\omega = \omega_g + \dot{\delta}$, we get:

$$(3.14) \quad \begin{aligned} J \ddot{\delta} + \left(D_p + \frac{m^2 (R_f L_s + R_s L_f)}{|Z|^2 L_f} i_f^2 + \frac{m^2 L_s}{|Z|^2 L_f} i_f v_f \right) \dot{\delta} - \frac{m i_f V}{|Z|} \cos(\psi + \delta) &= \\ T_m - \left(D_p + \frac{m^2 (R_f L_s + R_s L_f)}{|Z|^2 L_f} i_f^2 + \frac{m^2 L_s}{|Z|^2 L_f} i_f v_f \right) \omega_g. \end{aligned}$$

This ODE is coupled with another ODE that expresses i_f , see (3.15) below.

From (3.4), the dynamics of i_f is described by the equation

$$\frac{di_f}{dt} = \frac{\alpha m R_s}{L_f L_s} i_d - \frac{\alpha m \omega}{L_f} i_q - \frac{\alpha R_f}{L_f} i_f - \frac{v_f \alpha}{L_f} - \frac{\alpha m}{L_f L_s} V \sin \delta.$$

After substituting i_q and i_d with their reduced model expressions (3.11) and (3.12), we get:

$$\frac{di_f}{dt} = \frac{\alpha R_f}{L_f} \left(\frac{m^2}{L_f L_s} - 1 \right) i_f + V \sin \delta \left(\frac{\alpha m}{L_s} \right) \left(\frac{1}{L_f} - \frac{1}{L_s} \right) - \frac{1}{L_f} v_f,$$

which can be simplified to

$$(3.15) \quad \frac{di_f}{dt} = -\frac{R_f}{L_f} i_f - \frac{1}{L_f} v_f.$$

Irrespective of initial conditions, i_f stabilizes to a final value that depends only on v_f and the values of the rotor parameters. The final value is

$$\lim_{t \rightarrow \infty} i_f(t) = -v_f / R_f.$$

In other words the equilibrium value is $i_{f0} = -v_f / R_f$. Since we are interested in the long time behavior of (3.14), we replace i_f with i_{f0} and rewrite it as

$$(3.16) \quad J \ddot{\delta} + \left(D_p + \frac{m^2 R_s}{|Z|^2 R_f^2} v_f^2 \right) \dot{\delta} + \frac{mv_f V}{|Z|R_f} \cos(\psi + \delta) = T_m - \left(D_p + \frac{m^2 R_s}{|Z|^2 R_f^2} v_f^2 \right) \omega_g.$$

For the almost global stability of (3.16) it is necessary that

$$D_p + \frac{m^2 R_s}{|Z|^2 R_f^2} v_f^2 > 0,$$

which holds trivially since both the terms on the left side are positive. For more information on the stability of pendulum like equations, see [17]. To calculate the equilibrium points, we let $\ddot{\delta} = 0$ and $\dot{\delta} = 0$ in (3.16) and get the following expression for the equilibrium value of δ :

$$\delta_0 = \arccos \left(\frac{(T_m - D_p \omega_g) |Z| R_f}{m V v_f} - \frac{m v_f \omega_g R_s}{V |Z| R_f} \right) + \psi,$$

which is equivalent to (3.8) if we use $i_f = -v_f / R_f$. From here we get an additional **stability condition**:

$$-1 \leq \frac{T_m + D_p \omega_n |Z| R_f}{m V v_f} - \frac{m v_f \omega_g R_s}{V |Z| R_f} \leq 1.$$

This condition appears to hold for most typical generator parameter values and in most cases the system (3.16) has one stable equilibrium point.

In the above analysis we have made several assumptions, the most significant of them being $\omega \approx \omega_g$. In the absence of this assumption, but still using the steady state value $i_f = -v_f / R_f$, (3.16) had to be replaced with

$$(3.17) \quad J \ddot{\delta} + \left(D_p + \frac{m^2 R_s}{|Z_\omega|^2 R_f^2} v_f^2 \right) \dot{\delta} + \frac{mv_f V}{R_f |Z_\omega|} \cos(\psi_\omega + \delta) = T_m - \left(D_p + \frac{m^2 R_s}{|Z_\omega|^2 R_f^2} v_f^2 \right) \omega_g,$$

where ψ_ω is the stator impedance angle, $\psi_\omega = \arctan(\omega L_s / R_s)$.

The global stability of this system is an open question. But it is quite straightforward to analyze the local stability of this system around an equilibrium point (the procedure for local stability analysis was demonstrated in Section 3.1 for a more complex model). Future work will focus on estimating the domain of attraction of the stable equilibrium point, whenever it exists. Note that in this section the rotor current was not assumed to be constant like it was in Section 3.1. However as seen from (3.15) the rotor current does not depend on other state variables in the reduced model. Therefore in the stability analysis, the rotor current can be regarded as a constant with value equal to its equilibrium value i_{f0} .

3.3. Linearization of the reduced order SG model

While analyzing the dynamics of a network of synchronous generators it is convenient to use reduced order models. But it is not clear if the reduced models capture the primary dynamics of the network. In Section 3.2 a reduced model (3.13), (3.15) was obtained for a synchronous generator connected to an infinite bus. In this section we try to evaluate the quality of this reduction. To do this we linearize the reduced model around a stable equilibrium point and represent it as a feedback interconnection of a second order system and an integrator (similar to that in Figure 2). We plot the Bode and Nyquist plots of the second order system and compare it with the corresponding plots of the third order system in Figure 2 so as to compare the reduced model to the full model with constant i_f , (3.5). In the reduced model i_f is not assumed to be constant, but in the full model in Section 3.1 it is assumed to be constant.

Define $x_{eq} = [i_{f0} \ \omega_0 \ \delta_0]^T$ to be an equilibrium point of the reduced model (3.13), (3.15)

and define $z = [i_f \ \omega \ \delta]^T$. We calculate the Jacobian $A_{ij} = \left. \frac{\partial f(z)_i}{\partial z_j} \right|_{z=x_{eq}}$, where

$$f(y) = \begin{bmatrix} -i_f R_f / L_f - v_f / L_f \\ \frac{(i_f m V (R_s \cos \delta - \omega L_s \sin \delta) - \omega m^2 (i_f^2 (R_s L_f + R_f L_s) + i_f v_f L_s) / L_f) + T_m - D_p \omega}{|Z_\omega|^2} \\ \omega - \omega_g \end{bmatrix}$$

is defined using (3.15), (3.2) and (3.13). We get that

$$A = \begin{bmatrix} -R_f / L_f & 0 & 0 \\ A_{21} & A_{22} & -m V i_{f0} \sin(\delta_0 + \psi) / J |Z| \\ 0 & 1 & 0 \end{bmatrix},$$

where

$$A_{21} = \frac{L_f m V (R_s \cos \delta_0 - L_s \omega_g \sin \delta_0) - \omega_g v_f L_s m^2 - 2m^2 i_{f0} (R_s L_f + R_f L_s) \omega_g}{J |Z|^2 L_f}$$

$$A_{22} = \frac{-2L_s^2\omega_g mVL_f R_s i_{f0} \cos\delta_0}{J|Z|^4 L_f} + \frac{-(R_s^2 - \omega_g^2 L_s^2) \left(m^2 i_{f0}^2 (R_s L_f + R_f L_s) + m^2 i_{f0} v_f L_s - L_f i_{f0} m V L_s \sin\delta_0 \right)}{J|Z|^4 L_f} - \frac{D_p}{J}.$$

The equilibrium value of i_f is $-v_f/R_f$ and for δ we use (3.17) by letting $\ddot{\delta} = 0$, $\dot{\delta} = 0$ and substituting v_f with $-i_{f0} R_f$ to get :

$$\delta_0 = \arccos \left(\frac{i_{f0} R_s m \omega_g}{V |Z|} - \frac{|Z| (T_m - D_p \omega_g)}{m V i_{f0}} \right) - \psi,$$

which is equivalent to (3.8). Again we have used the values from Table 1 and have checked if there are equilibrium points. We have found two equilibrium points, where the first point is $x_{eq}^1 = [42.54 \ 100\pi \ 0.0398]^T$ and the second is $x_{eq}^2 = [42.54 \ 100\pi \ -2.9624]^T$. We can use (3.11) and (3.12) to compute the values of i_d and i_q according to x_{eq}^1 and get $i_d = -6.7181$ and $i_q = -12.2190$. We see that the values of i_d and i_q along with δ and ω have identical values to the values i_{d0} , i_{q0} , ω_0 and δ_0 in the stable equilibrium point x_{eq}^1 of the fourth order system (3.5). For the first equilibrium x_{eq}^1 the matrix A is

$$A = \begin{bmatrix} -2 & 0 & 0 \\ -7.08 & -8.9 & 517.6 \\ 0 & 1 & 0 \end{bmatrix},$$

and the eigenvalues are:

$$\lambda_1 = -4.45 + 22.31j, \lambda_2 = -4.45 - 22.31j, \lambda_3 = -2.$$

For the second equilibrium x_{eq}^2 the matrix A is

$$A = \begin{bmatrix} -2 & 0 & 0 \\ -7.08 & -7.614 & 517.6 \\ 0 & 1 & 0 \end{bmatrix}$$

and the eigenvalues are:

$\lambda_1 = 19.26$, $\lambda_2 = -26.87$, $\lambda_3 = -2$. We see that x_{eq}^1 is the stable equilibrium, which corresponds to the similarity in values.

Define $x = [\tilde{i}_f \ \tilde{\omega} \ \tilde{\delta}]^T$, where $\tilde{i}_f = i_f - i_{f0}$, $\tilde{\omega} = \omega - \omega_0$ and $\tilde{\delta} = \delta - \delta_0$. We examine the linearized system $\dot{x} = Ax$, where $x = [\tilde{i}_f \ \tilde{\omega} \ \tilde{\delta}]^T$ and A is the 3x3 Jacobian matrix calculated previously. We can write this system as a feedback interconnection of an integrator (with input $\tilde{\omega}$ and out output $\tilde{\delta}$) with the second order system

$$(3.18) \quad \dot{z} = A_2 z + B_2 z, \quad y = C_2 z,$$

where $z = [\tilde{i}_f \ \tilde{\omega}]^T$ and

$$A_2 = \begin{bmatrix} -R_f/L_f & 0 \\ A_{21} & A_{22} \end{bmatrix}, \quad B_2 = \begin{bmatrix} 0 \\ -mVi_{f0} \sin(\delta_0 + \psi)/JZ \end{bmatrix}, \quad C_2 = [0 \quad -1],$$

identical to what was done in Figure 2 and receive the following transfer function for the second order plant:

$$G(s) = C_2(sI - A_2)^{-1} B_2.$$

We plot Bode and Nyquist diagrams using the values from Table 1 and get:

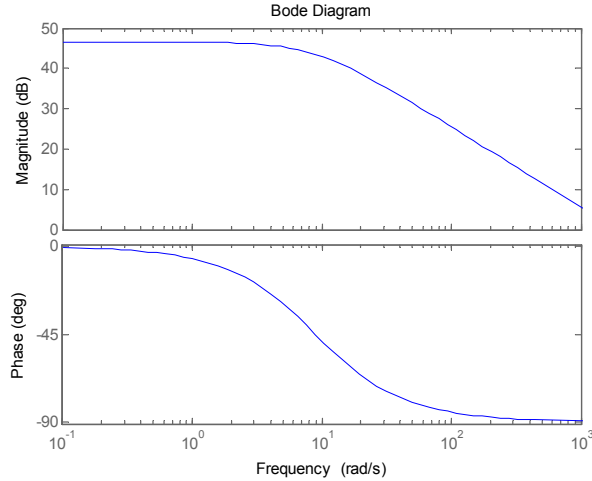


Figure 5. Bode diagram of the linearized subsystem described in (3.18) around the stable equilibrium point x_{eq}^1 of the nonlinear reduced model (3.13), (3.15). This should be compared to Figure 3.

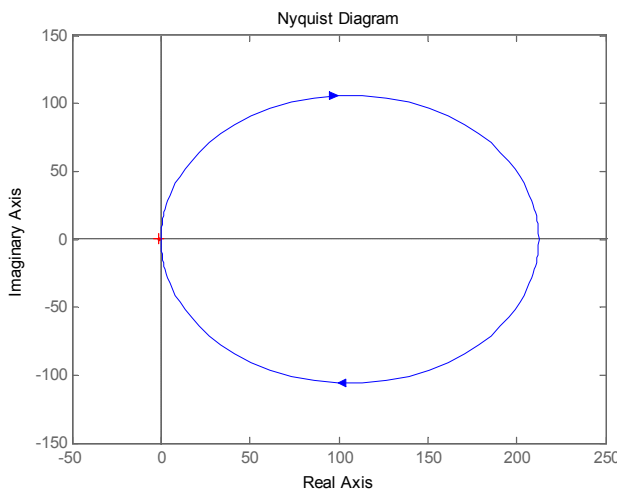


Figure 6. Nyquist diagram of the linearized subsystem described in (3.18) around the stable equilibrium point x_{eq}^1 of the nonlinear reduced model (3.13), (3.15). This should be compared with Figure 4.

The reduced model is almost identical to the full model in the low frequency region. This means that for the generator connected to the infinite bus, near an equilibrium point we can use the model reduction to analyze the synchronous generator. In the future, we hope to show that taking the rotor current to be constant (or slowly varying) is a good approximation of the full fifth order system in (3.4).

4. Introduction to synchronverters

In this chapter we will use the model of the synchronous generator from Chapter 1 to build the model of a synchronverter. The *synchronverter* is an inverter with a special control algorithm that causes it to mimic the operation of a synchronous generator. We use the same model of a synchronous machine as in Figure 1 with no neutral line connected. (However we mention that synchronverters can be built also with a neutral line connected to the grid.) Now we can take equations (2.2), (2.3), (2.4), (2.17) and (2.18) from Chapter 2 for our synchronverter model. We add an additional assumption of a constant rotor current to simplify calculations. As mentioned in Section 3.3 this is not necessarily a good approximation but it is required to simplify the design of the controller. If we consider the synchronverter to be a small inverter (power wise) in a very large grid then the grid may be regarded as an infinite bus, so that the equations of the system should be similar to (3.5). Future work should include a comparison of these two models. We get the following equations for our synchronverter:

$$(4.1) \quad v = -R_s i - L_s \frac{di}{dt} + e,$$

$$(4.2) \quad e = \omega M_f i_f \widetilde{\sin \theta},$$

$$(4.3) \quad T_e = M_f i_f \langle i, \widetilde{\sin \theta} \rangle,$$

$$(4.4) \quad J \dot{\omega} = T_m - T_e - D_p \omega,$$

$$\omega = \dot{\theta}.$$

The active and reactive power are defined by $P = \langle i, e \rangle$ and $Q = \langle i, e_{quad} \rangle$, where $e_{quad} = -\omega M_f i_f \widetilde{\cos \theta}$. We can calculate the active power and the reactive power using the simple equations:

$$(4.5) \quad P = \omega M_f i_f \langle i, \widetilde{\sin \theta} \rangle,$$

$$Q = -\omega M_f i_f \langle i, \widetilde{\cos \theta} \rangle.$$

These equations give us the basic algorithm of the synchronverter shown in Figure 7:

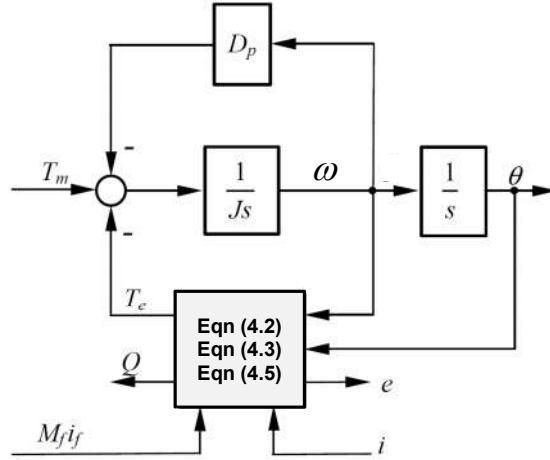


Figure 7. Electronic part of a synchronverter (without control), typically running on a DSP.

Note that, if we assume no viscous friction, then the virtual active torque acting on the rotor is $T_m - D_p \omega$. The fact that this expression depends on ω means that it is actually a feedback loop, called *frequency droop*. As was mentioned in Section 2.2 (about the model of the synchronous generator), we consider the torque T_m to be constant or an input which changes by user demand. To avoid sharp transients, we add an LPF for the signal T_m . If we denote $T_n = T_m - D_p \omega_n$, which is the active torque at the nominal frequency ω_n , then

$$T_m = T_n - D_p (\omega - \omega_n).$$

Since the frequency of the synchronverter follows the frequency of the grid, the synchronverter will change its output power so that for frequencies above nominal the power will be less than the nominal power, while for frequencies below nominal, the power will be more than the nominal power. We would like to choose the droop coefficient D_p so that it matches the real droop coefficients used in synchronous generators. For example for most generators in the European grid, for a 3% change in frequency the power will change 100% from nominal. Obviously for a real system this cannot always be obtained. We don't always have enough energy stored or the ability to absorb energy in our system. Later on we will show how to handle this problem.

The importance of J should also be noted. J should receive a value that allows the machine to have an inertia time constant that fits an actual synchronous generator. For the synchronverter we prefer the lowest of values of J , since it slows down system response time and may cause stability problems. Let H be the *inertia time constant* of a synchronous generator, defined as $H = \frac{1}{2} J \omega_n^2 / P_n$. It is known that: $2\text{ sec} \leq H \leq 12\text{ sec}$.

This leads to $J \geq 4P_n / \omega_n^2$ and $D_p = P_n / (\text{droop rate} \times \omega_n^2)$, where the droop rate is the proportion of ω_n that will cause a 100% change in T_m (typically around 0.03).

For voltage and reactive power control an additional control loop is required. The rotor current is considered constant or at least slowly changing, and as we have seen the rotor flux has a strong influence on the voltage amplitude in the synchronous generator, see

(4.2). Indeed, the synchronous internal voltage e is the most significant component in the voltage v from (4.1) since we can assume small resistance and inductance of the stator. We use the approximate relation

$$(4.6) \quad Q = 3 \left[\frac{VE}{X} \cos(\delta) - \frac{V^2}{X} \right]$$

derived in [16], where V is the rms voltage value on one phase of the synchronverter terminals, E is the rms value of e , δ is the power angle as defined in (3.1) and $X = \omega L_s$ is the absolute value of the stator impedance when R_s is neglected. We see from (4.2) that we can use the rotor flux to control E and so also the reactive power using a simple integral controller. We can see this also directly from (4.5). We want to enable a change in Q using a change of rotor flux with minimum changes to P , which we have already controlled using the frequency droop part. Most synchronous generators operate in a PV (power-voltage) control scheme. This means that the generator will help stabilize voltage by supplying or absorbing reactive power. For this we add another droop loop for voltage dependent reactive power

$$D_q = -\frac{Q - Q_{set}}{V - V_n} = -\frac{\Delta Q}{\Delta V} \geq 0.$$

Here Q is the output reactive power, Q_{set} is the desired reactive power for nominal voltage, V is the measured rms voltage on the synchronverters terminals and V_n is the nominal rms voltage. The integrator on the rotor flux control loop (shown in Figure 8) has a gain $1/K > 0$. Choosing K and D_q depends on the application, by tuning. Larger K means a slower system but usually more stable. Larger D_q means that the synchronverter will try harder correcting the voltages at the expense of accurately tracking the desired Q_{set} . In order to work in a *PQ* (*power-reactive power*) control scheme, only reactive power control, the user can take $D_q = 0$. Measuring the amplitude of the voltage on the synchronverter terminals requires extra work in the algorithm. Here we make the assumptions that the system is symmetric, balanced and has no higher harmonics. Under these assumptions the voltage amplitude detection is very simple (see [33] for more information):

$$(4.7) \quad V_g = \sqrt{2/3} \times \sqrt{-(v_a v_b + v_b v_c + v_c v_a)},$$

where v_a, v_b and v_c are the measured voltages on the synchronverters terminals. In software implementation one should check that the sum inside the square root is indeed positive to avoid Nan (not a number) errors. Since this expression doesn't always hold, if the grid is unbalanced, it is recommended to pass the measured voltages through an LPF. The same is true for Q and T_e , see Figure 8. This LPF is a tunable filter, my chosen values for simulations will be discussed in Section 12. The initial condition for the rotor flux should be the approximate steady state value which can be calculated from

$$(4.8) \quad M_f i_f = |e| / \omega_n,$$

where $|e|$ is the expected amplitude of e from (2.3), (about 10% higher than the amplitude of the nominal grid voltage).

Synchronization of the synchronconverter to the grid can be done by using a PLL, but there is a better way. The paper [32] presents the design of a self-synchronizing synchronconverter. This is implemented by adding 3 software implemented switches. The first switch, S_Q turns off the voltage control part, D_q . The second switch S_C connects a virtual resistor and inductor R_{vir} and L_{vir} , where a virtual current is calculated from measured grid voltage, instead of a measured current. This is done since without synchronization we can't connect the synchronconverter to the grid, to avoid a large current and a large transient at the moment of grid connection. In our equations, see (4.3) and (4.4) we see that the measured current plays an important role. This means we must find a suitable replacement. Usually we select the virtual resistor to be twice the stator resistor and the virtual inductor is identical in size to the actual inductor. The calculation of the current is as follows:

$$\hat{i}_{vir}(s) = \frac{\hat{e}(s) - \hat{v}_g(s)}{L_{vir}s + R_{vir}},$$

where a $\hat{\cdot}$ denotes the Laplace transform, s is the complex variable, e is the internal synchronous voltage vector, v_g is the measured grid voltage vector and i_{vir} is a vector replacing i . The third and last switch S_p connects a PI controller to the frequency droop loop in order to replace the nominal frequency of the grid, which is 50Hz for Europe and 60Hz in North America, with the actual grid frequency ω_g estimated via ω_r . This calculation is required because the grid frequency may deviate from nominal values by a small portion. During the entire synchronization process P_{set} and Q_{set} are set to be 0. The purpose is to make the synchronconverter create a mirror image of the grid where no power is delivered to or from the grid. The result is a smooth connection to the grid and afterwards we can slowly increase $|P_{set}|$ and $|Q_{set}|$. It is recommended to give different values for the synchronconverter constants when synchronizing. **Smaller inertia constant will significantly reduce the synchronization time. Increasing the integrator constant K in the reactive power control loop will slow synchronization but will help stabilize the process. Choosing these new values must be done carefully since the system can become unstable!** For instance, if $\omega_g L_{vir}$ is small compared to R_{vir} and if K is relatively small, then the system will oscillate.

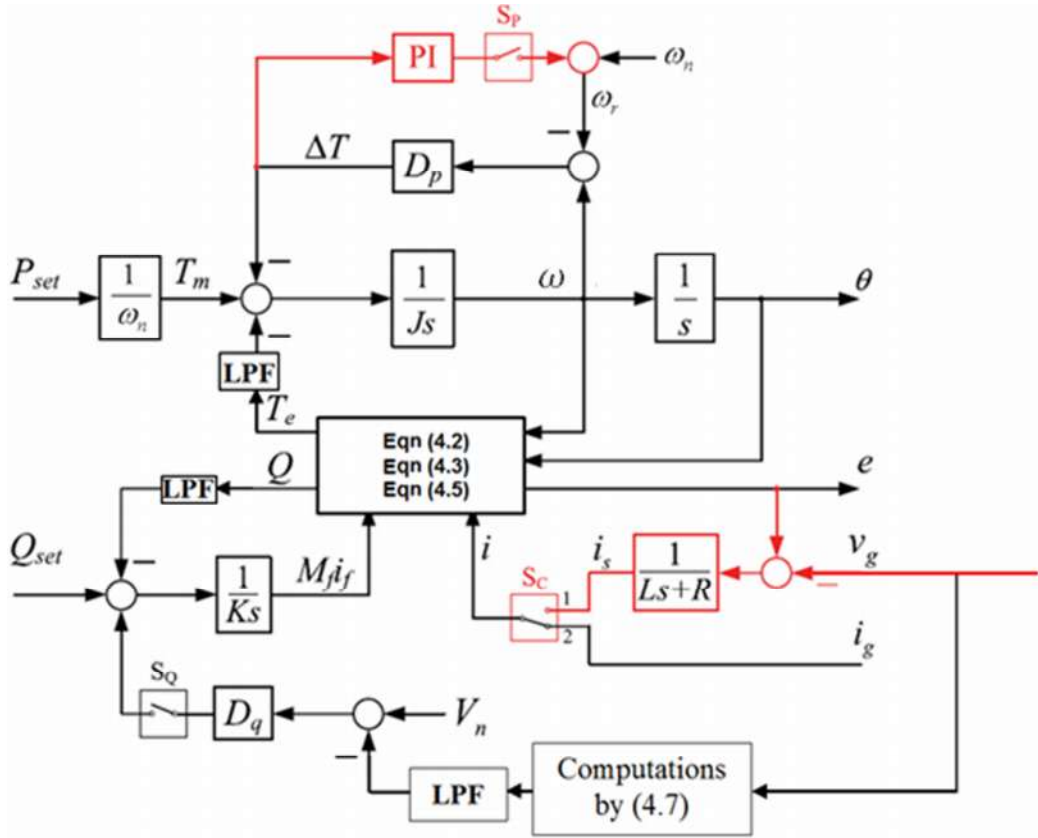


Figure 8. Proposed controller (electronic part) for a self-synchronized synchronverter, following [32].

Finally we mention briefly the PWM (Pulse Width Modulation, see [8]) part and the filters that connect the inverter to the grid. The desired signal e computed by (4.2) is sent to a PWM signal generator that opens and closes electronic switches (IGBT or MOSFET, see [14]) in order to generate an approximation of a sine wave in the low frequency range. The switching frequency must satisfy two conditions. We want the switching frequency to be high enough so that the *Total Harmonic Distortion* (THD) will be sufficiently low, the exact value depends on regulations and application. We want our filter resonant frequency to be at least five times lower than the switching frequency, so that switching noises won't be increased due to resonance. As an upper bound we want to minimize our losses on the switches which we know increase with frequency. A switching frequency of 10 kHz is good enough for a 5 kW inverter that was tested in our simulations and later on in the lab. Before giving a detailed description of the PWM system used, we will give a short background on three phase inverter topology. The topology shown below in Figure 9 is based on the model of the canonical switching cell, see [22] and it is used for most power converters. This allows a two way power flow.

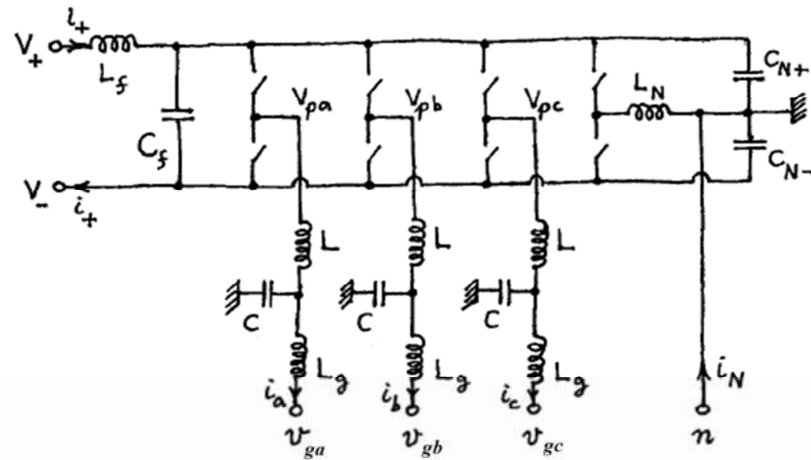


Figure 9. Scheme of a 2-level 3 phase inverter with neutral line based on the model of the basic switching cell.

The figure also shows a neutral line. In our simulations that line was not included. In order to reduce losses and noise we have improved the switches for each phase and implemented a neutral point clamped inverter topology with three DC voltage levels (the neutral is represented as ground):

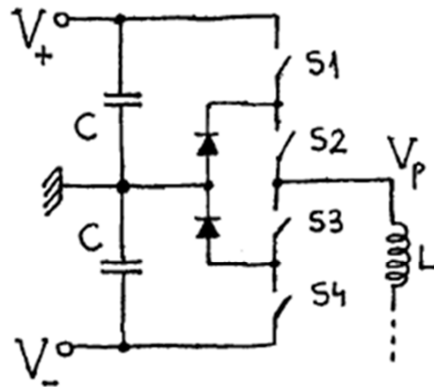


Figure 10. Neutral clamped inverter topology for one phase of a 3-level, 3 phase inverter.

On each phase there is a fast switch between neutral and V_+ when the desired sine wave e is positive, and between neutral and V_- when e is negative. Usually the voltages are symmetric, meaning that $V_+ = |V_-|$, to generate a symmetric sine wave around 0. The circuit in Figure 10 is operated as follows:

$$V_P = V_+ \rightarrow S_1 \text{ and } S_2 \text{ are closed,}$$

$$V_P = 0 \rightarrow S_2 \text{ and } S_3 \text{ are closed,}$$

$$V_P = V_- \rightarrow S_3 \text{ and } S_4 \text{ are closed.}$$

The filter used to connect the inverter to the grid is an LCL filter. This is a very well-known filter used in many inverters. This filter also has the role of being similar to the stator R_s, L_s if we neglect the capacitor (which is needed to reduce the ripple).

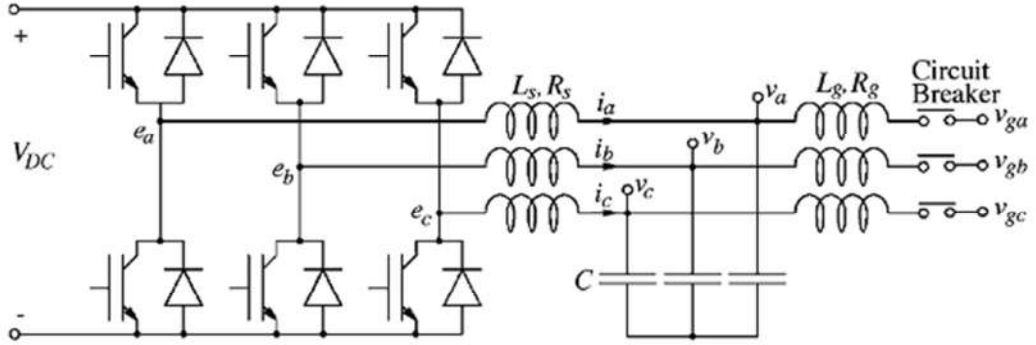


Figure 11. Schematic of a 2-level 3 phase inverter connected to the grid via an LCL filter and a circuit breaker.

The LCL filter is mainly meant to reduce harmonics and make the output current smoother. There are a few basic rules for selecting the filters capacitor and inductors. We want less than 5% current ripple, less than 10% voltage drop on the inductors and a resonance frequency of about 20 times more than the grid frequency 50 Hz. This will allow second and third harmonics to pass but higher harmonics, which include harmonics caused by the switching, will be blocked. The formulas for L_g and C below were calculated by a basic calculation of the ripple of the current and voltage drop on both inductors, the formula for L_s is taken from the model of the basic switching cell:

$$L_s = V_+ T_s / (2 \Delta i), \quad L_g = V_L / (i_n \omega_n) - L_s \quad \text{and} \quad C = 1 / ((L_g \parallel L_s)(20 \omega_n)^2).$$

Here Δi is the current ripple, V_L is the voltage on the two inductors, T_s is the switching period and ω_n is the nominal frequency. The last formula insures that the resonant frequency of the LCL filter is around $20\omega_n$. Typically V_L is 5% - 10% of V_n (the nominal rms phase voltage). Once the filter values (L_s, L_g, C) are calculated for an inverter that transfers power P_1 , the filter values (L_{s2}, L_{g2}, C_2) for another inverter that transfers power P_2 , with identical ripple characteristics and switching frequency, are given by:
 $L_{s2} = L_s P_1 / P_2, \quad L_{g2} = L_g P_1 / P_2 \quad \text{and} \quad C_2 = C P_2 / P_1$.

Since simulations with the exact switching model take a very long time to run, it is desirable to replace the switching model with an average model average model that contains a controlled voltage source instead of switches. To validate this replacement, we have run simulations of a synchronverter with the switches and with the average model. In the simulations we have used a self-synchronized synchronverter with the nominal power 5kW connected to an infinite bus. The solver used was ode23tb, which was recommended when working with SimPower elements. We let $P_{set} = 3.5 \text{ kW}$ and $Q_{set} = 500 \text{ VAr}$. The voltage was 404.158 V line to line rms. Figures 12 and 13 show the active power and reactive power profiles from the two simulations:

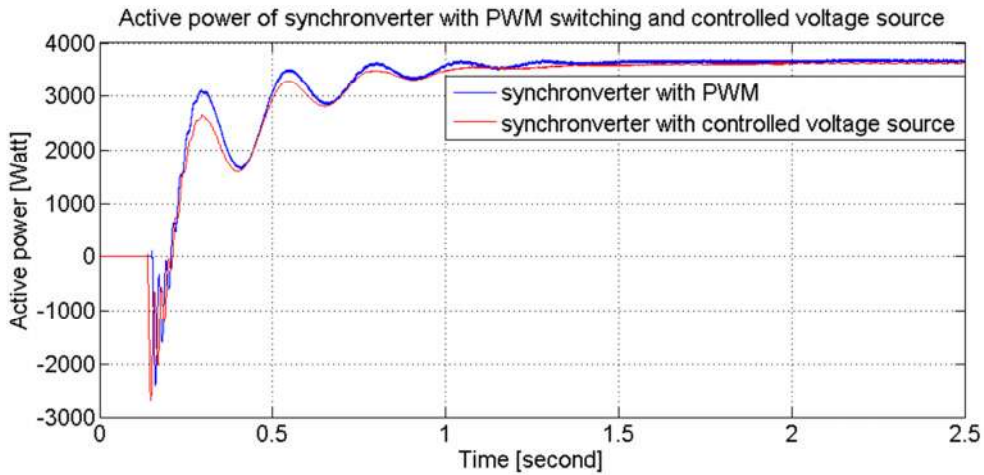


Figure 12. Active power profile of a synchronverter connected to an infinite bus simulated with PWM and with an average model using a controlled voltage source.

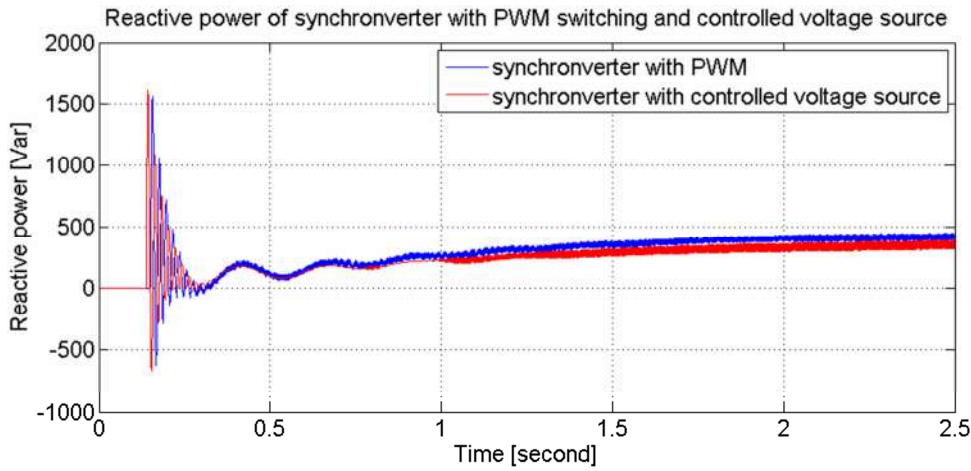


Figure 13. Reactive power profile of a synchronverter connected to an infinite bus simulated with PWM and with an average model using a controlled voltage source.

Figure 14 shows the frequency from the two simulations:

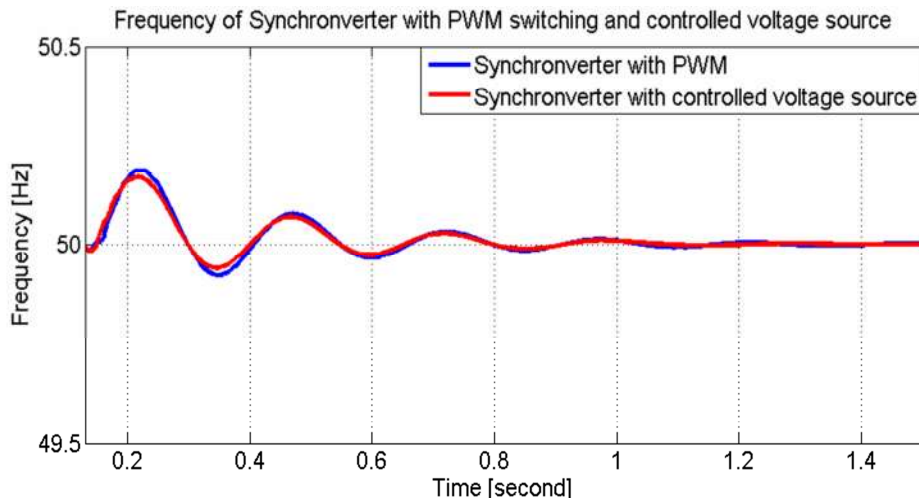


Figure 14. Frequency of a synchronverter connected to an infinite bus simulated with PWM and with an average model using a controlled voltage source.

5. Additional improvements to the synchronverter algorithm

Chapter 4 presented the background on synchronverters, mainly based on [32] and [33]. In this chapter we propose several improvements for the synchronverter model. As mentioned earlier the power supplied by any real source cannot change instantaneously. In order to prevent the inverter from requiring the battery or PV array to change their outputs instantaneously, we filter P_{set} and Q_{set} with LPFs before further processing. The filter bandwidth has been chosen to be 4 rad/s.

Another practical problem arises when the frequency deviation from the nominal value is large and the power that the synchronverter is required to supply or absorb is more than physically possible. To solve this problem we divide the frequency droop loop into two branches: a high and a low pass branch. All the torques except the torque from the high pass branch and T_e are saturated (see Figure 15) thereby limiting the power requirements. We chose 20 rad/sec to be the cutoff frequency for the filter in the low branch of the frequency droop loop.

The final change made to the algorithm is the addition of an over current protection before the PWM. We estimate the current by first computing the vector $e - v$ (the notation is as in (2.2) so that v is now the voltage vector on the filter capacitor). In order to calculate the current i , we also need to estimate the impedance of the inductor nearest to the switches. We assume that the frequency is almost the same as the nominal grid frequency and compute the inductor impedance Z using (3.7). It follows that $|e - v| \approx |Z||i|$. From here we get that the maximal voltage difference $|e - v|$ allowed, based on the maximal current allowed to pass through the inverter using $|e - v|_{max} = |Z||i|_{max}$. Using a saturation block, we ensure that $|e - v| < |Z||i|$ component-wise. This does not replace the usual overcurrent protections for the inverter, but it can give an additional layer of protection provided that the current can be saturated without distorting the signal significantly and that our assumption of the frequency, i.e., it is near nominal grid frequency, is correct.

All these new changes give us the updated synchronverter scheme shown in Figure 15.

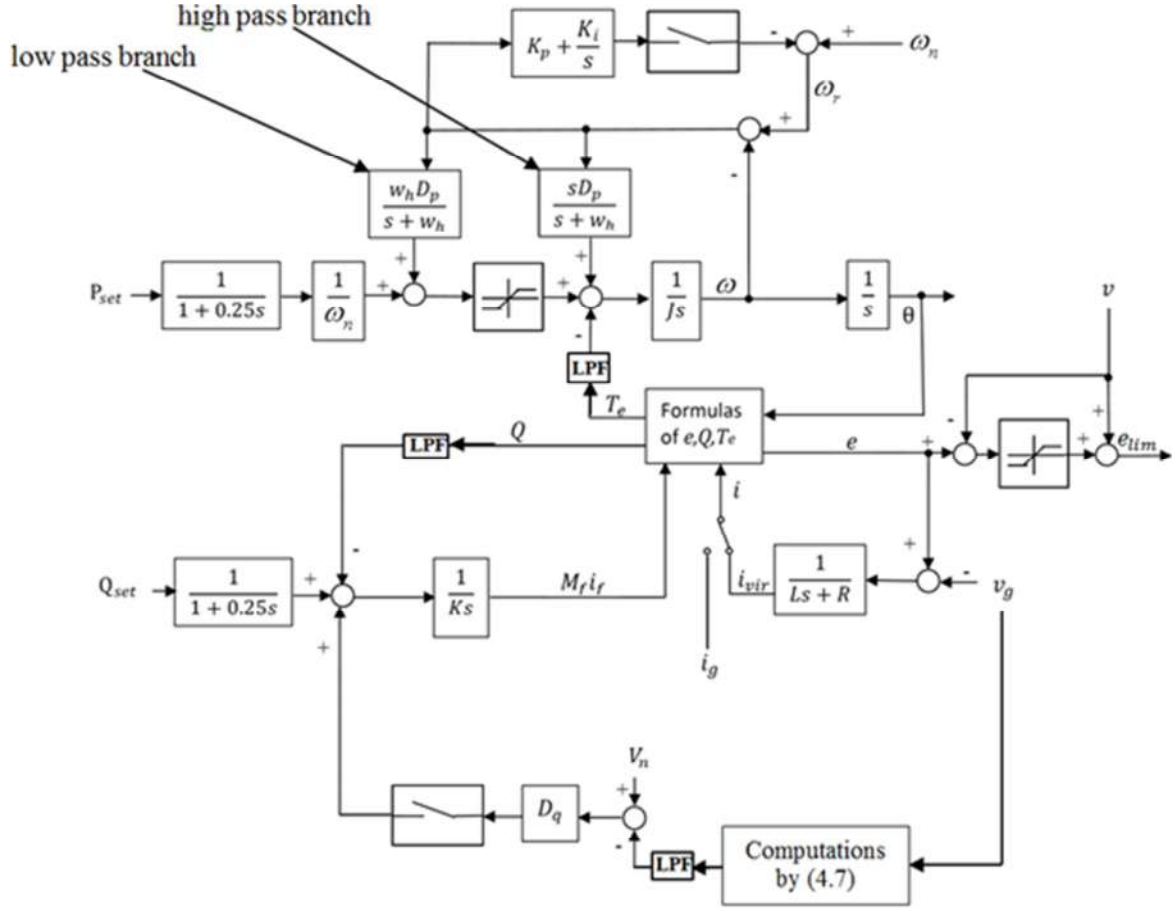


Figure 15. Updated scheme of the synchronconverter algorithm including filters on P_{set} and Q_{set} , saturation of output power and extra protection from high currents.

Another possible change to the synchronconverter structure is an additional LPF before the saturation block of the torque loop. This LPF can simulate the delay caused by additional mechanisms such as an MPPT (controller that tracks the most efficient voltage to be acting on a PV cell for maximum power generation) for a PV array (due to the fact that the DC/DC transformer that delivers power to the inverter is delayed by the MPPT control in case additional power from a storage unit is also required) or a DC/DC transformer that is supposed to discharge an energy storage unit, such as a battery or super capacitor. This LPF should be conditioned to work only if the required output power is greater than the power available nominally to the synchronconverter. This is because we will not need to discharge energy from a storage unit if the required power is smaller to or equal to the power generated nominally by the energy source, usually a PV array.

6. Some simulation results for synchronverters

In this chapter we will show that the synchronverter works like a synchronous generator in a simple grid containing either another synchronverter or an infinite power source (infinite bus) with a transformer of ratio 1:1 and loads modeled as power sinks equal to more or less the nominal power of the synchronverter. This will be done by simulations in Matlab using the average model of a synchronverter designed for 5kW nominal output power. We will show 4 scenarios. The first 3 consider a single synchronverter and a grid with loads and a transformer of ratio 1:1 as described above with an additional line impedance of $1 \text{ m}\Omega$ and 2 mH between the infinite bus and the loads. The last one considers a grid composed of 2 synchronverters, where the first generates the grid by working in island mode with constant voltage and frequency references and the second synchronverter synchronizes and joins.

In the first scenario we connect the synchronverter to an infinite bus and slowly decrease the bus frequency at the rate of 1Hz per second until it reaches 48 Hz. We would like to see that the synchronverter tracks the grid frequency and maintains a power-frequency droop of 100% power increase per 3% frequency decrease. We would also like to see that the power does not exceed a maximum of 8kW. The active power of the synchronverter will be set to 3kW, while its nominal power is 5kW. So when the grids frequency decreases to 48.5Hz synchronverter should reach 8kW and saturate.

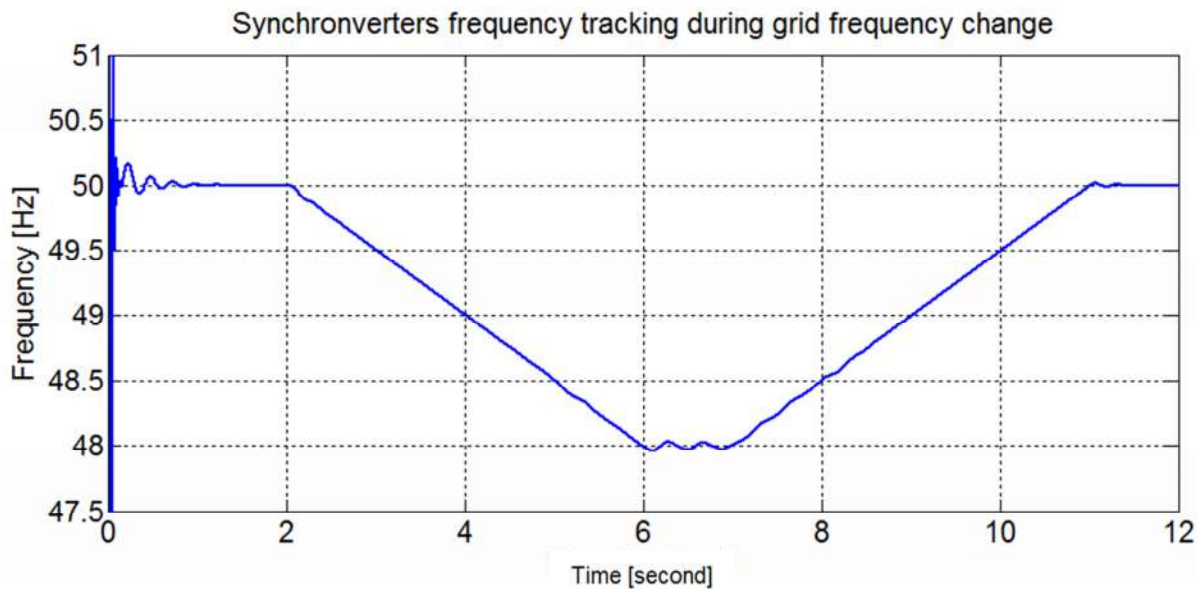


Figure 16. The synchronverter connects to the infinite bus at $t=0.14\text{s}$. The grid frequency starts decreasing at $t=2\text{s}$ at a rate of 1 Hz per second until it reaches 48 Hz at $t=6\text{s}$. At $t=7\text{s}$ the grid frequency starts climbing back to its nominal value at a rate of 1 Hz per second. We see that the synchronverter tracks the grid frequency changes.

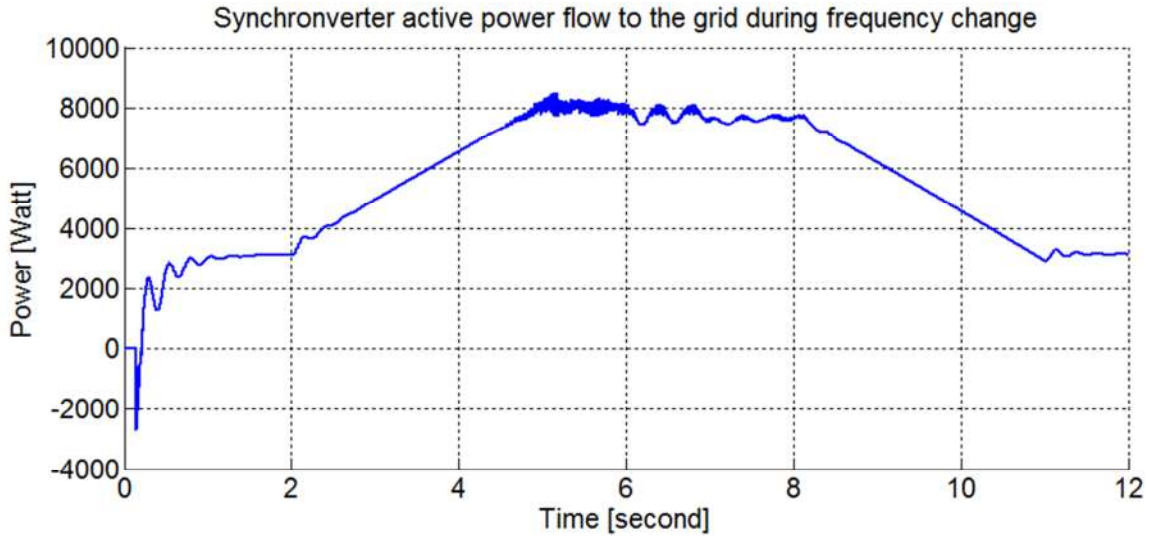


Figure 17. The synchronconverter connects to the infinite bus at $t=0.14s$. The active power stabilizes to $P_{set} = 3kW$. When the grid frequency starts decreasing at $t = 2s$, the synchronconverter starts increasing its power until reaching saturation at $t=5.5s$, while the grid frequency goes down to 48.5 Hz. The grid frequency starts increasing to its nominal value at $t = 8s$ and shortly afterwards the synchronconverter starts decreasing power back to its nominal value.

In the second scenario a synchronconverter is connected to an infinite bus and we slowly increase the bus frequency at the rate of 1Hz per second until it reaches 52 Hz. We would like to see that the synchronconverter tracks the grid frequency and maintains a power-frequency droop of 100% power decrease per 3% frequency increase. We would also like to see that the power does not go below the minimum of 0kW. The active power of the synchronconverter will be set to 3kW and the nominal power is 5kW. So when the grids frequency increases to 51.5Hz synchronconverter should reach 0kW and saturate.

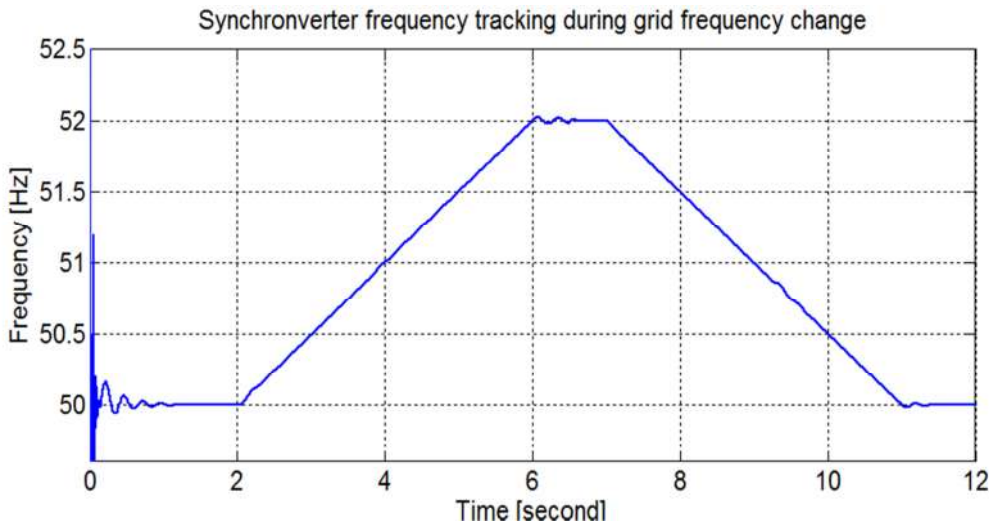


Figure 18. The synchronconverter connects to the infinite bus at $t=0.14s$. The grid frequency starts increasing at $t=2s$ at a rate of 1 Hz per second until it reaches 52 Hz at $t=6s$. At $t=7s$ the grid frequency starts falling back to its nominal value again at a rate of 1 Hz per second. We see that the synchronconverter tracks the grid frequency changes.

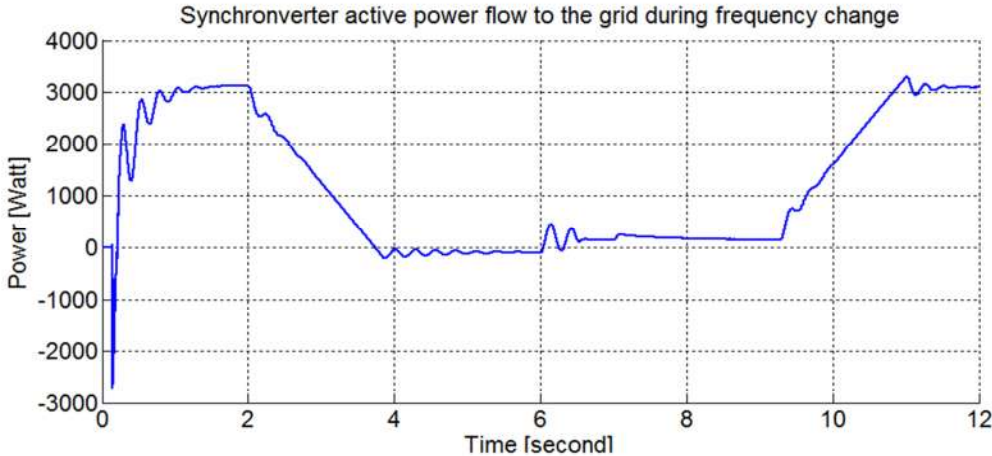


Figure 19. The synchronverter connects to the infinite bus at $t=0.14s$. The synchronverter active power stabilizes to $P_{set} = 3kW$. When the grid frequency starts increasing, the synchronverter decreases its output power until reaching saturation at $t= 4s$ at which time the grid frequency rises above 51 Hz. When the grid frequency starts decreasing to its nominal value, the synchronverter output power starts increasing back to its nominal value.

From these two scenarios we see that the synchronverter is indeed capable of tracking grid frequency under a frequency-power droop loop whose rate can be altered according to practical needs. We have also seen that we can saturate the synchronverter power according to application requirements which in our case was 8kW maximum and 0 kW minimum.

Another important attribute of a synchronverter is that it can stabilize voltage using reactive power, like a synchronous generator. To verify this in simulations we connected the synchronverter to an infinite bus via a line impedance of $1m\Omega$ and $2mH$ and a transformer with ratio 1:1, and slowly changed the voltage from nominal value to 90% of this value. The voltage was decreased at a rate of 16.5 volts per second and was later on increased at the same rate until it reached the nominal value. Since this is an actual electrical system with loads and a transformer (1:1 transformation rate) we see that the voltage in the synchronverter terminals is not identical to the voltage of the infinite bus. The results of this simulation are shown in Figures 20, 21 and 22.

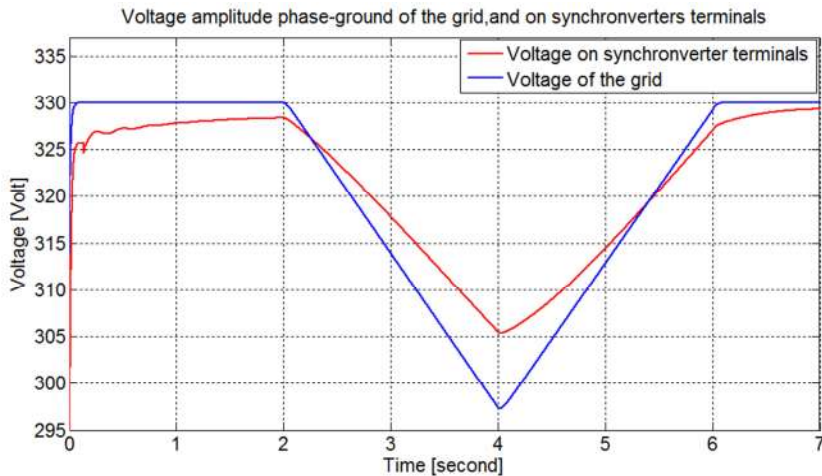


Figure 20. Voltage profile of the grid measured on the terminals of the infinite bus and on the synchronverter terminals. The grid voltage decreases from $t=2s$ until $t =4s$ and then climbs back to its nominal value.

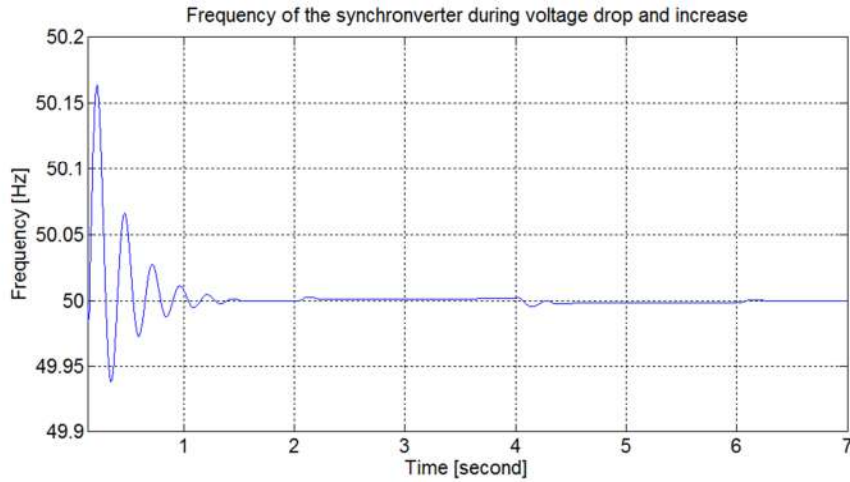


Figure 21. In the same experiment as in Figure 20, the synchronconverter connects to the grid at $t=0.14\text{s}$ and its frequency remains constant when the voltage changes.

We see in Figure 20 that the synchronconverter is able to slightly improve the voltage drop (the voltage on the synchronconverter terminals drops to 305 Volt and not 300 Volt). This is achieved without changing the frequency (as seen in Figure 21) by producing reactive power.

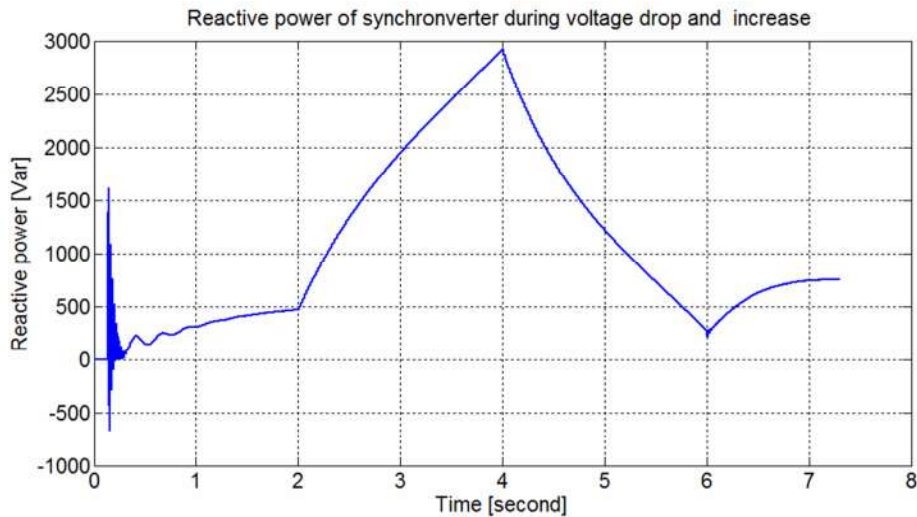


Figure 22. The reactive power of the synchronconverter stabilizes at its nominal value at $t = 2\text{s}$. It then increases because grid voltage drops. After $t = 4\text{s}$ the reactive power decreases because the grid voltage climbs back to its nominal value. The nominal reactive power of the synchronconverter was set to 500 VAr, but the synchronverter does not stabilize at 500 VAr due to the voltage drop on the line impedance.

It is important to note that the behavior shown in Figures 20, 21 and 22 is not a *Fault Ride Through*. A Fault Ride Through mechanism means changing the algorithm to make sure certain regulations are met. Since this algorithm was not designed for a specific regulation such a mechanism was not designed. A simple check is done to detect voltage drops (will be discussed in Section 12.1) and short circuits. It is left for future designers of the synchronconverter to decide what to do when such a fault occurs. For now only the most basic regulation is kept, i.e. the synchronconverter disconnects after a fault of more than 30 milliseconds with the terminal voltage amplitude under 30% of the nominal value, or if the

frequency change rate exceeds 8 Hz per second. An additional check for correct frequency range is also done routinely in the algorithm to make sure synchronverter frequencies are not above or below allowed grid frequencies. As we see it is very easy to fit the synchronverter algorithm to any given regulation. This simplicity is very important in the fast changing world of renewables and smart grid applications.

Next we will investigate **a micro grid (in simulations) composed of two synchronverters and two loads**. We expect that this grid behaves like an interconnection of 2 synchronous generators. To test this we perform some load changes and track the frequencies at which the micro grid stabilizes. We have designed this experiment so that the frequency will be around 50 Hz. We choose a non-symmetric system in which the synchronverter that starts the micro grid, called the grid synchronverter, is working slightly above full capacity, i.e. it is designed to supply 5kW at the nominal frequency 50 Hz, but it supplies 5.5kW to the two loads and so cannot work at the nominal frequency. The first load closest to the grid synchronverter is 4kW and the second is 1.5kW. Between the two loads there is a small impedance with resistance 1 mΩ and inductance 2mH. Figure 23 below describes this system.

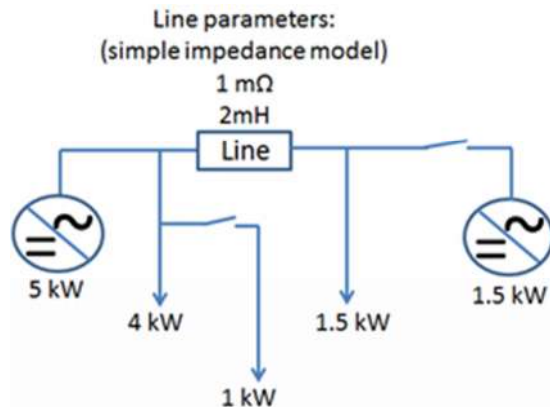


Figure 23. The two synchronverter micro grid. The first synchronverter with $P_{set} = 5\text{ kW}$ starts the micro grid. The second synchronvertor connects after 4 seconds. The 1 kW load is connected at t = 9s, 5 seconds after the second synchronverter connects to the micro grid.

After 4 seconds we allow the second synchronverter to connect to the micro grid and see that indeed the micro grid frequency rises slightly above 50 Hz (see Figure 25) and the loads are shared between both synchronverters as expected. The first synchronverter has an active power of 4.5kW while the output of the second is 1kW, see Figure 24. Another 5 seconds later we add an additional load of 1kW and this causes the grid frequency to drop and the extra load is shared between the two synchronverters. This additional load causes the demand for power in the micro grid to be equal to the sum of the nominal power of the grid synchronverter (5kW) and the second synchronverter (1.5kW). This causes the system frequency to stabilize to its nominal value 50 Hz. Both synchronverters have identical parameters except their active power set points. Both synchronverters were set to output 500 VAr.

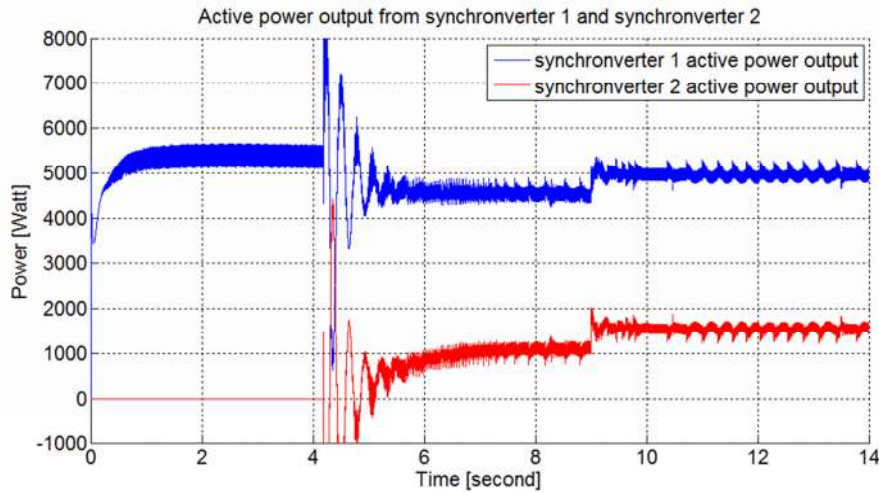


Figure 23. Synchronverter 1 starts building the micro grid at t=0s and stabilizes to provide 5.5kW.

At t =4.2s synchronverter 2 is added and the power from synchronverter 1 drops to 4.5kW while synchronverter 2 supplies 1kW. Near t=4s we notice inter-area oscillations which quickly decay. At t=9s another load of 1kW is connected and the power output of both synchronverters rises by 500 watt until they both output their nominal power which is 4.5 kW for the grid synchronverter and 1.5 kW for the second synchronverter.

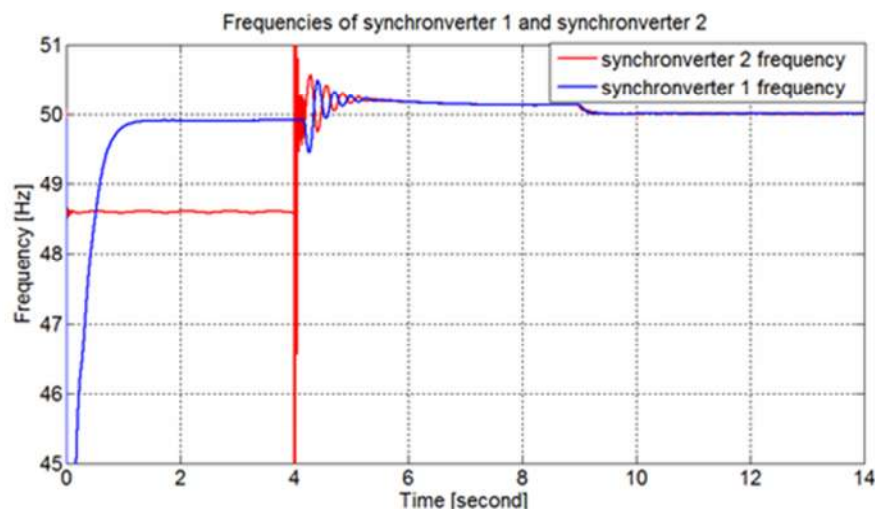


Figure 25. Synchronverter 1 starts building the micro grid at t=0s and its frequency stabilizes slightly below 50Hz since the load is above the synchronverter's set active power. At t =4.2s synchronverter 2 is added to the micro grid and the frequency increases slightly above 50 Hz. Near t=4.5s we notice inter-area oscillations which decay quickly. At t=9s another load of 1kW is connected and the frequency decreases to 50 Hz. At this point the loads are balanced by the set active power of the synchronverters so that the system stabilizes to the nominal frequency of 50 Hz.

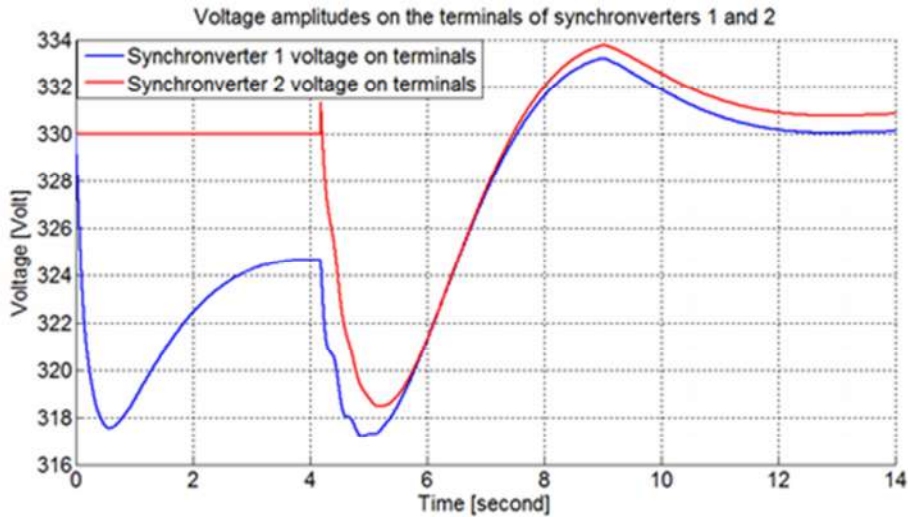


Figure 26. Synchronverter 1 starts building the micro grid at $t=0$ s. Its terminal voltage stabilizes slightly below the nominal value of 330 V (amplitude). At $t=4.2$ s synchronverter 2 is connected and the voltage starts fluctuating, it increases until $t=9$ s when another load of 1kW is connected.

7. Inter-area oscillations

We hope that the synchronconverter can be used to solve practical problems in an actual power grid. To verify this we need to consider specific problems, the current approach to solve them and then propose new solutions using the synchronconverter. We have chosen to focus on inter-area oscillations. We will explain what they are and how they are dealt with today. Finally we will present our solution to inter-area oscillations using synchronconverters. Local oscillations are associated with a single generator, due to its dynamics vaguely resembling the dynamics of a damped pendulum (the swing equation). The frequency range of these damped oscillations is approximately 0.7 to 2 Hz. In contrast inter-area oscillations involve groups of generators which oscillate against one another when the physical link between them is weak (i.e., it has relatively high impedance), see [15] for details. These oscillations are much more complex since they involve several non-linear systems. The oscillation frequencies range from 0.1 Hz to 0.8 Hz. A key feature of these oscillations is that the power variations in one (group of) generator will be opposite to the power variations in the other (group of) generator.

Inter-area oscillations are caused by the electro-mechanical nature of the generators. They constitute a well-known problem, see for instance [16], [15], [21] and [29], and the usual solution is to regulate the field voltage with a controller called *Power System Stabilizer* (PSS). This requires additional hardware and each type of PSS has its own pros and cons. Designing a PSS controller is a hard task which requires comprehensive knowledge of the system, including all modes of oscillations involved, and careful thinking about which of the several generators should have a PSS installed.

We explore inter-area oscillations by simulation experiments: we look at a simple grid composed of two synchronous machines of 1 GW nominal power, each using a steam

turbine and a governor with an IEEE type 1 synchronous machine voltage regulator and exciter, see Figure 27. These generators operate at 22 kV and are connected to a 22/130 kV transformer. Each generator has a local load of 300 MW and both generators are connected via a 220 Km line with 0.05W/Km resistance and 1.4 mH/Km inductance. The capacitance of the line was neglected to improve the simulation run time (including the capacitance does not change the results significantly according to our tests). In the middle of the line there is a substation composed of a 130/22 kV transformer and a small load of 55 MW. Another small load of 60 MW located near one of the generators is switched on after 10 seconds. This sudden change causes power oscillations between the generators until a new equilibrium is reached. Our system vaguely resembles the one used in the example in the simulation package SimPower (the example is called power_PSS).

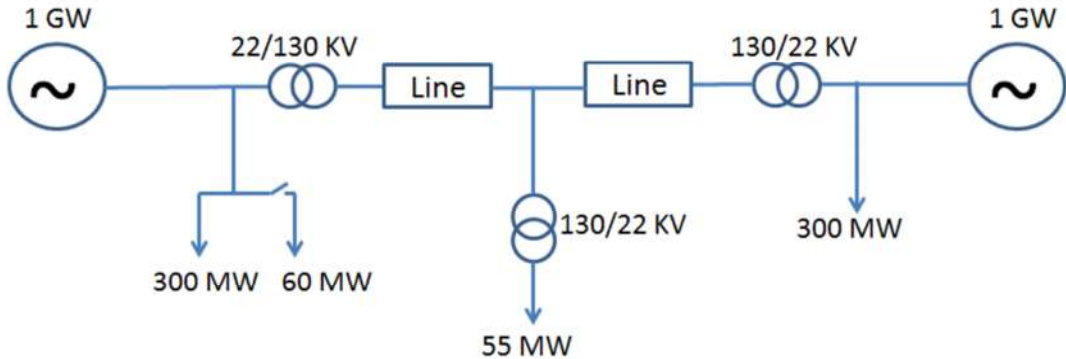


Figure 27. The simple power network (without synchronverters) exhibiting inter-area oscillations. The model includes steam turbines as prime movers for the two synchronous generators. The oscillations are triggered by closing the switch connecting an additional load of 60 MW.

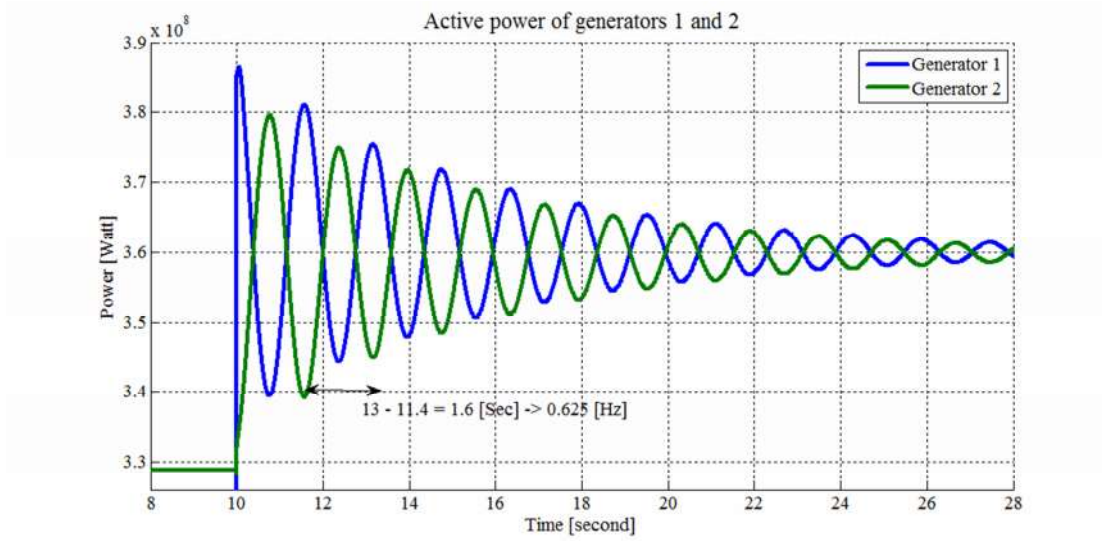


Figure 28. Power oscillations in the system from Figure 27.

Figure 28 shows that in our model, the active power outputs of the two generators in Figure 27 oscillate (with damping) against each other when the switch is closed connecting the additional 60 MW load at $t=10.5s$. The frequency of this oscillation is 0.625 Hz, which is well within the range of inter-area oscillation and below the range of local oscillations. The

system was stable before the load jump and no power was transferred from one generator to the other. The oscillations last for more than 20 seconds and even after 10 seconds they have an amplitude of 10 MW which can cause heating in the lines and transformers.

7.1. Power system stabilizers

There are solutions to the problem of inter-area oscillations, as we stated earlier, but they are far from perfect and require changes to the generators themselves. The most common solution is the PSS which we will now review. The excitation control system in a conventional SG controls the rotor current i_f and its main purpose is to make sure that the generator maintains a terminal voltage close to the nominal voltage. The reactive power of a generator is closely related to the terminal voltage: in sinusoidal steady state,

$$Q = 3 \left[\frac{VE}{X} \cos(\delta) - \frac{V^2}{X} \right] \text{ where } V \text{ and } E \text{ are rms values as in equation (4.6).}$$

This expression is fundamental in the field of AC power systems, for more information see [16].

The excitation control system provides the direct current to the field winding which in turn determines the voltage of the generator and the reactive power. If we look at the formula for the active power, which in steady state is $P = \frac{3VE}{X} \sin(\delta)$, (E , X , V and δ have the same values as in equation (4.6)) we see that P depends on the voltages V and E . However, since the variations in V and E are small, P is mainly changed via δ (which changes as a result of changes in the active torque of the prime mover).

Power System Stabilizers (PSS) use the dependence of P on E to dampen inter-area oscillations as well as local oscillations, see for instance [16], [30]. The general structure of a PSS shown below is taken from [30]:

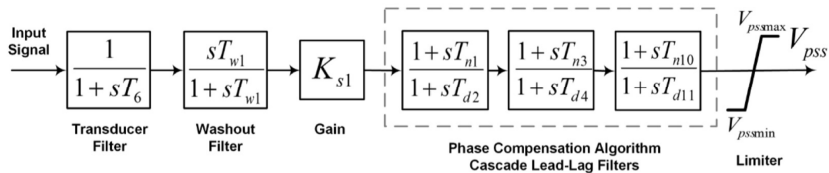


Figure 29. General model of a PSS.

We have demonstrated the efficiency of various PSS by adding them to our simulation model from Figure 27. We have used 3 types of PSS available in the Matlab SimPower library. The first is called Multi Band PSS (MB PSS) and the input to it is the rotor angle velocity deviation from nominal frequency. It handles 3 bands of frequencies (low, intermediate and high) adjusted in advance. The second is a generic PSS the input to which is the rotor speed deviation (from nominal frequency) multiplied with a constant gain and filtered, as shown in Figure 29. The last PSS is almost like the second, but works on the difference between electrical and mechanical power instead of rotor angle velocity deviation.

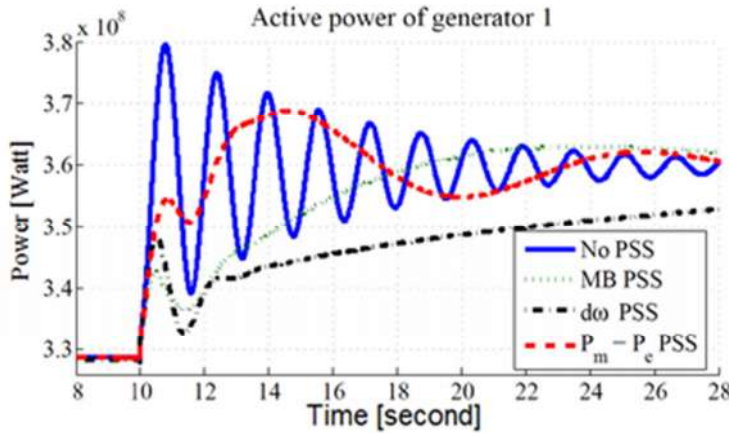


Figure 30. Comparison of power oscillations using three types of PSS, as well as no PSS, in the system from Figure 27.

We can see that the various PSS perform well, but have certain disadvantages. MB PSS is the best of those tested here but it requires very precise design based on an accurate model of the system. The second PSS (also called $d\omega$ PSS) takes a long time to reach the new equilibrium point. Even after 20 seconds it is far from settled. The third type of PSS (also called $P_m - P_e$ PSS) causes large and very low frequency power oscillations. All three PSS have the disadvantage of having an adverse effect on voltage regulation since they work by changing the field current and hence E . Maintaining a constant voltage is important for transformers and certain loads. After presenting our solution to the inter-area oscillation problem, we will show the voltage profile of the various PSS.

7.2. Synchronverters with virtual friction

7.2.1 Frequency droop based solution

We would like to solve the problem of inter-area oscillations by using the synchronconverter which is an available resource rather than modifying the generators by adding a PSS unit. Adding a PSS unit to a synchronous generator is not a simple process. It requires identifying the generator on which the extra controller must be added. This means deciding which is the most important generator from a power stand point and from a voltage regulation stand point since PSS damages voltage control.

From (4.4) we see that the droop factor D_p plays a main role in the damping of frequency oscillations in the synchronconverter. The frequency droop loop in the synchronconverter is fast since it has no mechanical parts, only electronic components. This is unlike a real generator in which the droop loop acts on the prime mover and therefore has delays due to physical limitations (of the order of one minute). This means that generators are more sensitive to oscillations and adding our synchronconverter to the grid, even without any changes, can potentially improve system behavior.

To study the above idea, two synchronconverters were added to the small grid from Figure 27, one near each generator, using transformers (inverters do not work at high voltages due

to limitations of the electronic switches). Each synchronconverter was designed to give 45 MW maximum power and we operate them at 35 MW. This means that the synchronconverters supply roughly 10% of the power required by the loads.

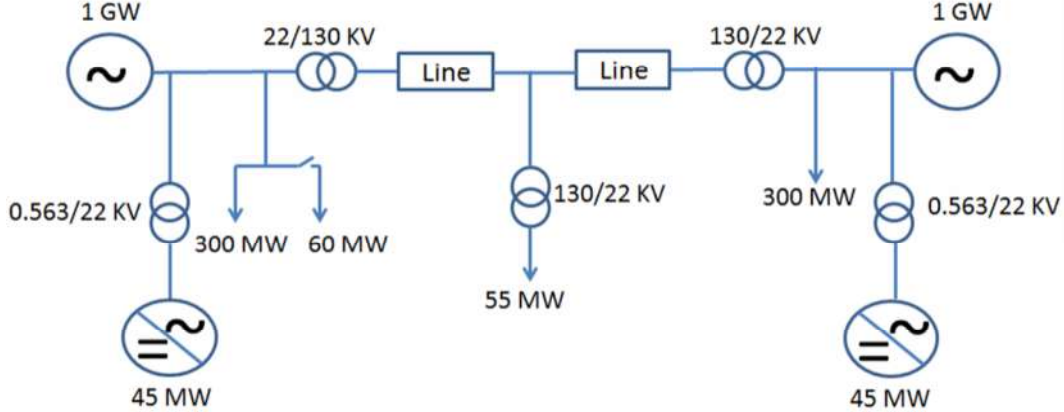


Figure 31. The network from Figure 27 after adding synchronconverters next to each synchronous generator.

From the simulation of this system, we see that adding the synchronconverters improves the overall response of the system (see Figure 32). Obviously this is not a significant improvement. In the next section we will make an additional change to the synchronconverter algorithm which will greatly improve the performance of the system when combating inter-area oscillations.

7.2.2 Virtual friction based solution

If there are several generation areas and each contains a synchronconverter, an additional torque can be introduced that acts as if there was viscous friction between the imaginary rotors of the synchronconverters. This will require fast communication between synchronconverters which may incur costs, however, communication systems have improved and have become very cost efficient.

The additional virtual friction torque will be added to the total torque acting on the imaginary rotor of the synchronconverter. To make this more precise, consider for simplicity a micro grid with only two synchronconverters with rotor angles θ_1 and θ_2 . The mechanical equations including the virtual friction torques are:

$$J\ddot{\theta}_1 = T_{m1} - T_{e1} - D_{p1}(\dot{\theta}_1 - \omega_r) - D_{pv}(\dot{\theta}_1 - \dot{\theta}_2),$$

$$J\ddot{\theta}_2 = T_{m2} - T_{e2} - D_{p2}(\dot{\theta}_2 - \omega_r) - D_{pv}(\dot{\theta}_2 - \dot{\theta}_1).$$

Here $D_{p1}, D_{p2} > 0$ are the droop constant of the synchronconverters, while $D_{pv} > 0$ is the virtual friction coefficient that helps damping unwanted inter-area oscillations. In steady-state operation the virtual friction torque is zero. When there is a sudden load change and the system starts to go off balance then the virtual rotors of the synchronconverters rotate against each other and the virtual friction torque starts working to counteract this. This idea was first reported in our conference paper [5].

Notice that the rotor of a real synchronous generator stores the kinetic energy $J\dot{\theta}^2/2$, proportional to its moment of inertia J . The importance of inertia in power systems is discussed for instance in [26]. Inverters have no moving mechanical part, so they cannot store kinetic energy. To imitate the effect of the kinetic energy, a synchronverter needs large capacitors on its DC bus or storage batteries (a better but more expensive solution). Consider the test system in Figure 31 with virtual friction added to the synchronverters.

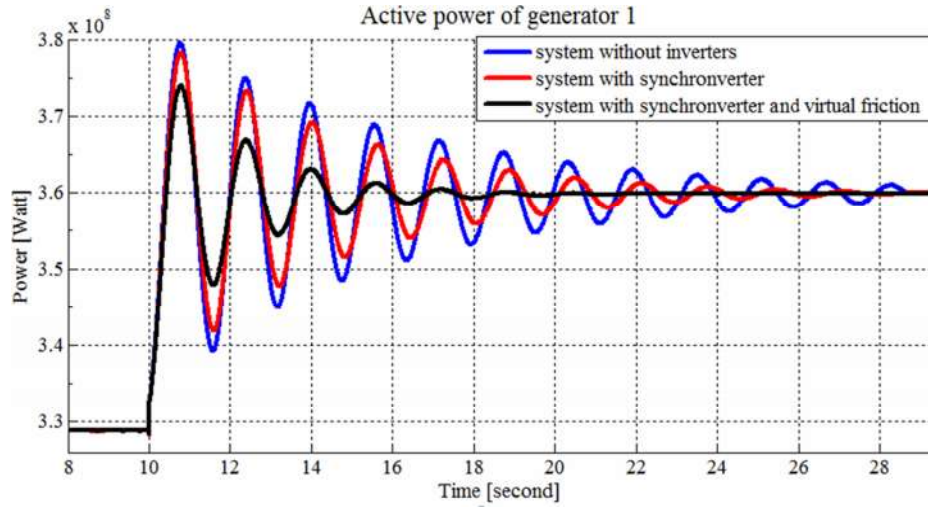


Figure 32. System with two synchronverters with and without virtual friction.

In Figure 32 we see the effect of the frequency droop of the synchronverters (in red) on the active power oscillations in one of the generators. This effect is small but considering that most of the power in the test grid comes from the generators and not from the synchronverters it is not negligible. The effect of virtual friction on the oscillations in the active power of the generators is strong enough to dampen them completely within 10 seconds, at $t=20s$.

As mentioned earlier the PSS damages the voltage regulation. Figure 33 shows the active power while using various types of PSS and also while using synchronverters with virtual friction for damping inter-area oscillations. Figure 34 shows the corresponding voltage profiles near generator 1.

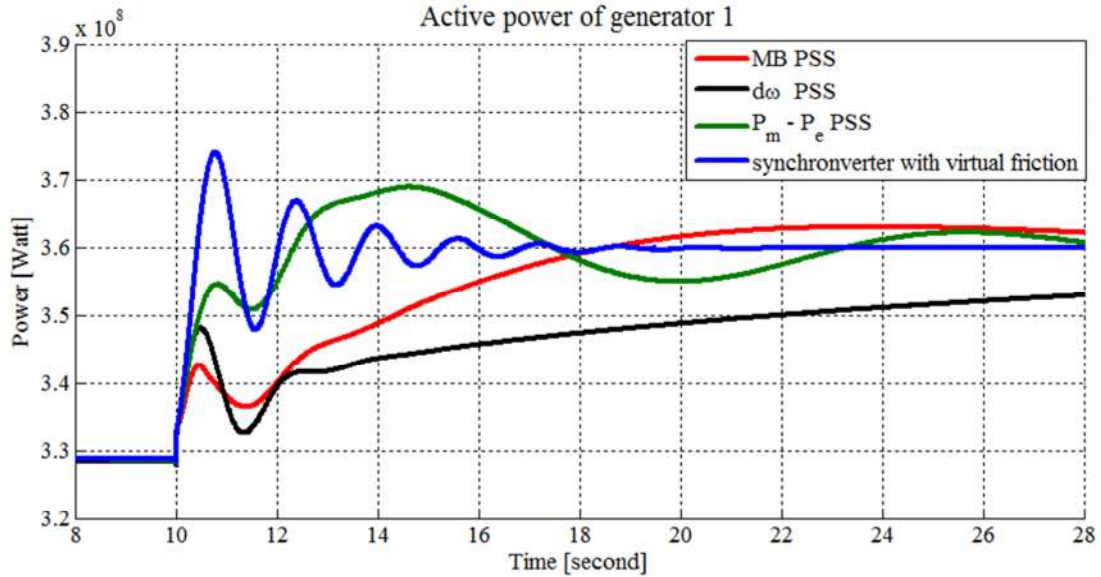


Figure 33. Comparison of system power flow with synchronverter and PSS.

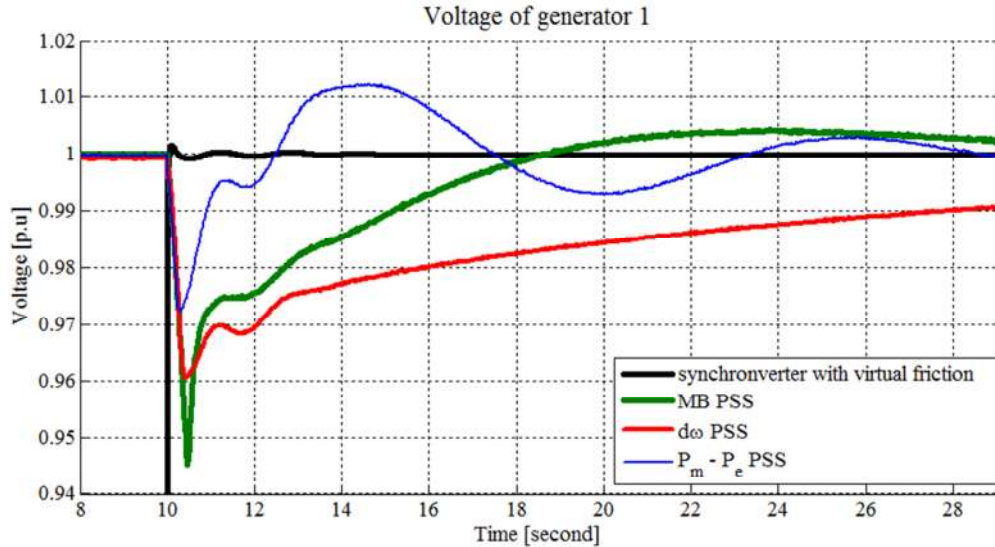


Figure 34. Comparison of system voltage profile with synchronverter and PSS.

We wanted to take the system to an extreme scenario, to generate stronger inter-area oscillations and demonstrate how the voltage profile can be distorted by the PSS while the synchronverter solves the problem without voltage distortions. The test system in Figure 31 is changed to cause stronger inter-area oscillations. This is done by increasing the substation load to 150 MW from 55MW and also by increasing the switched load to 150 MW from 60 MW. Figure 35 shows the oscillations in active power of generator 1 under the changes mentioned above. As seen in Figure 35 the oscillations in power are better damped by the synchronverter with virtual friction than the PSS, but not significantly.

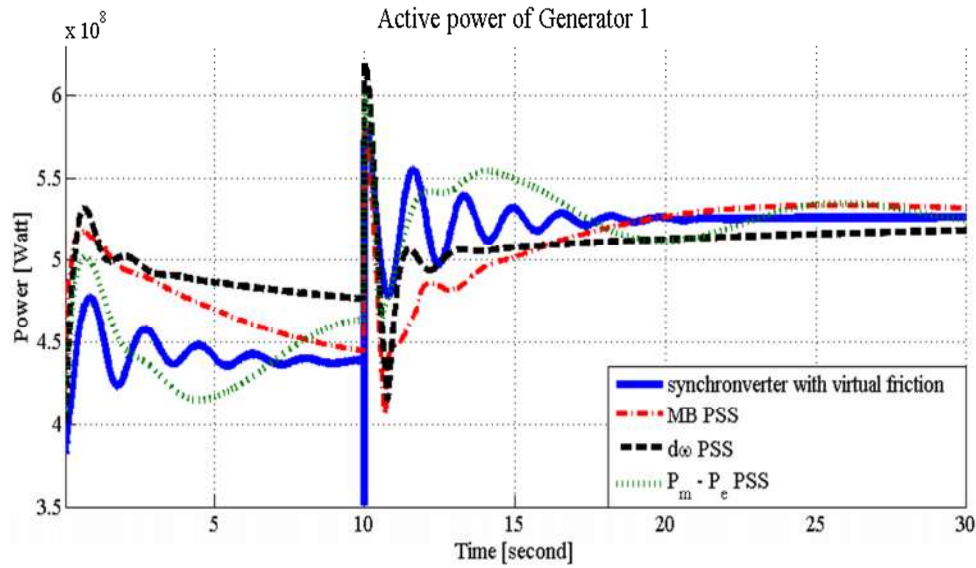


Figure 35. Comparison of system power flow with synchronconverter and PSS, with the switched load increased to 150 MW (from 60 MW) and the substation load increased to 150 MW (from 55 MW).

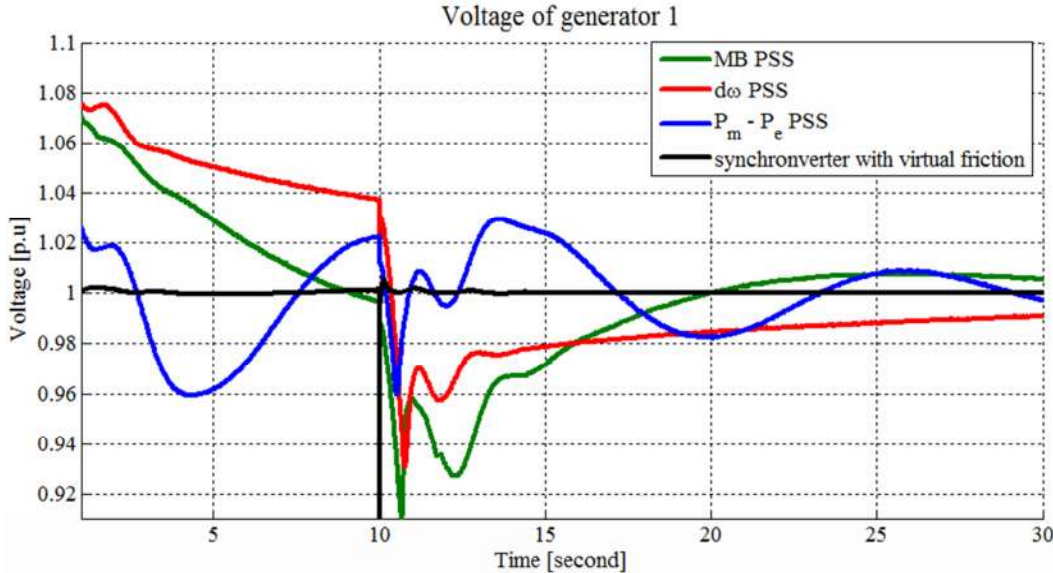


Figure 36. Comparison of system voltage profile with synchronconverter or PSS, under the same conditions as in Figure 35.

As seen in Figure 36 the voltage profile on the generator terminals is distorted significantly when the PSS solution is applied during strong inter-area oscillations. Figure 36 shows that even for strong inter-area oscillations the voltage profile of the generator terminals remains unchanged when the oscillations are damped using synchronconverters and virtual friction. One must remember that in this example the PSS works on generators which supply 90% of the power while the virtual friction works on inverters supplying only 10% of the power. In cases where the synchronconverters supply much more power the results will be much better in favor of the synchronconverter. Since we have compared synchronconverters with virtual friction to synchronous generators with a PSS controller, it is hard to say which solution would work better if both of them are implemented on the same power source, either a synchronconverter or a synchronous generator. We would like to test

both solutions on the same power source. We cannot create virtual friction between two synchronous generators, however we can add an additional PSS controller to our synchronverter algorithm. We assume that the synchronverter behaves similar enough to a synchronous generator, so that we could actually apply to it a PSS control. The PSS controller works on the induced voltage in the rotor. In our synchronverter algorithm we assume that the derivative of the rotor current is 0 which is equivalent to assuming that the voltage across the rotor is constant. But in reality small fluctuations in the rotor current influence the flux in the rotor and thereby change the rotor voltage. This is good for us since it means we can use the current to change the voltage on our imaginary rotor to stabilize frequency fluctuations caused by inter-area oscillations using PSS control. In Figure 37 we can see where we place our PSS controller in our algorithm. The proportional gain D_q stabilizes the voltage amplitude in the synchronverter terminals. By adding another reference voltage from PSS control which depends on frequency fluctuations we couple the voltage amplitude E with the frequency disturbance, Δf .

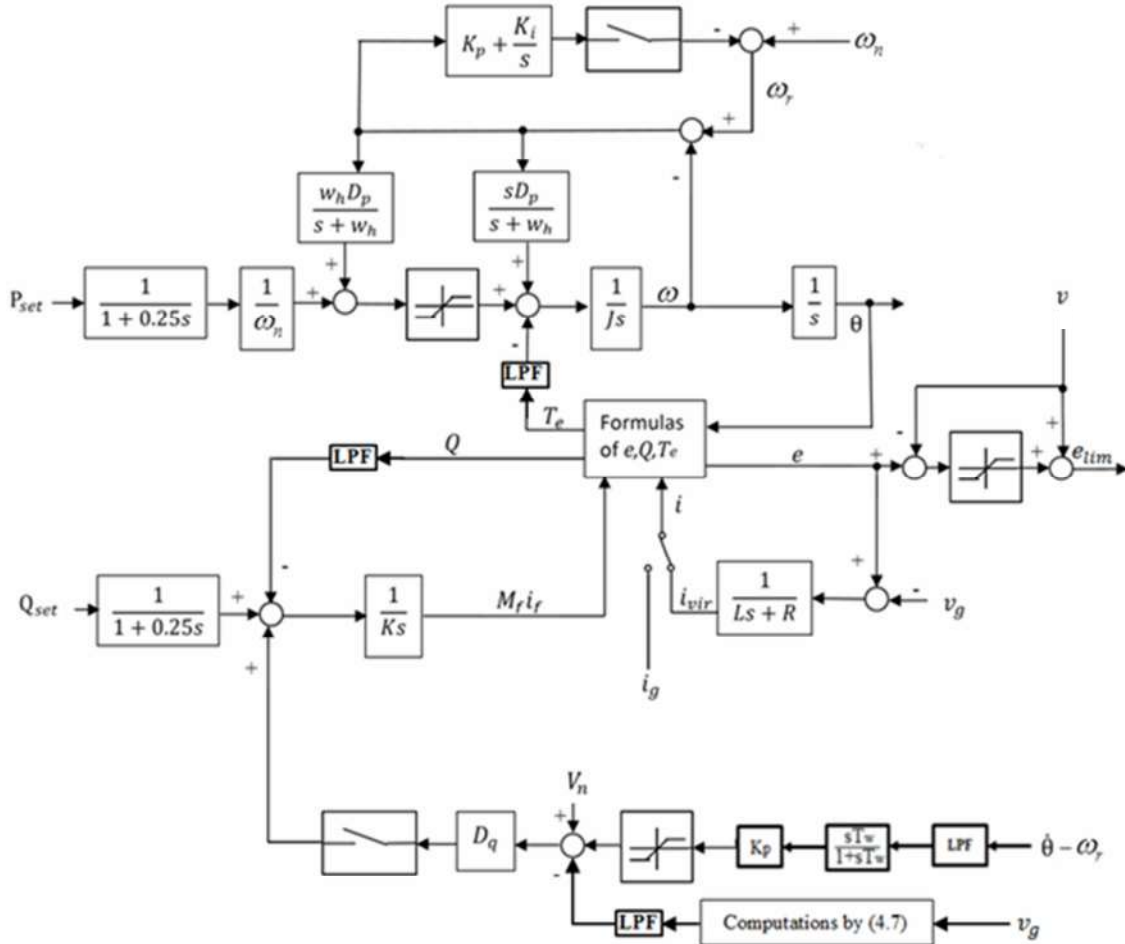


Figure 37. Synchronverter with PSS controller

The washout filter constant T_w in Figure 37 is chosen in the range of 1 to 10 seconds. The synchronverter algorithm is run on a processor so it is discrete and not continuous. The constant K_p should be chosen such that it amplifies the disturbance in frequency

sufficiently, but not higher than what the synchronverter can handle. We have found $K_p = 10$ to be suitable. It is important to saturate the additional voltage from the PSS control to be not more than 5% of the nominal voltage and not less than -10% of the nominal voltage. The implementation in Figure 37 is a basic standard control structure of a PSS. There are better implementations of PSS controllers but this is good enough for our test. In order to check that this PSS controller actually does what it is supposed to do we designed a test system of two synchronverters with a switched load between them connected via a high impedance line. This should generate inter-area oscillations when the loads are switched. I will not give an exact description of this simple system since the exact parameters are not important, only the fact that inter-area oscillations are generated between 2 synchronverters. The figure below presents the phase difference between the synchronverters virtual rotor angle, θ .

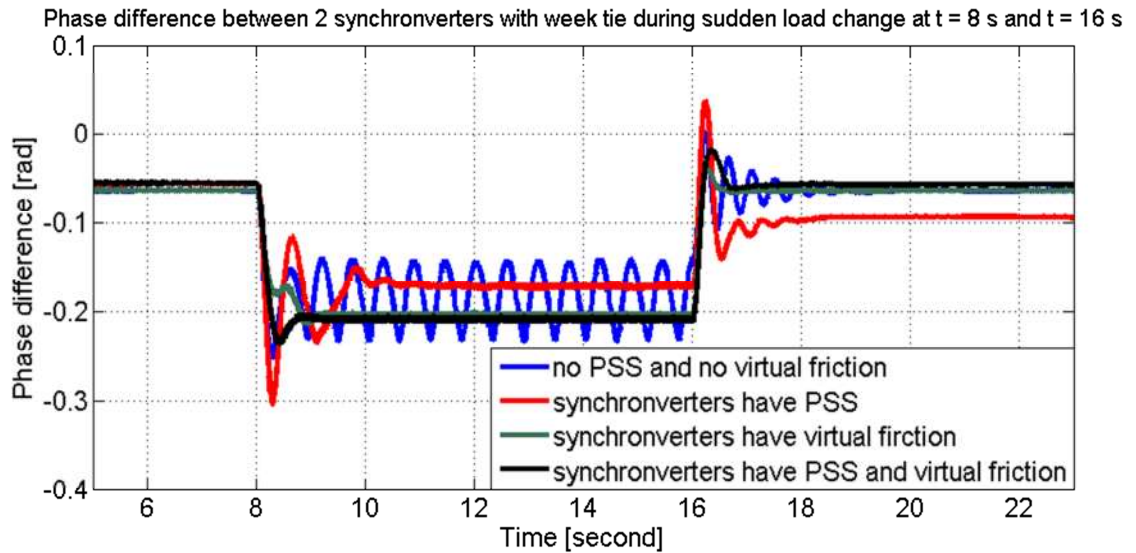


Figure 38. Proof of concept for PSS implementation in a weakly connected two synchronverter system.

We see in Figure 38 that until $t=8s$ there are no oscillations. At $t=8s$ the load changes and the load sharing between both synchronverters changes as well. We see that the blue line representing the case where the synchronverters have neither PSS nor virtual friction, has oscillations that do not decay until the load changes back to its previous value at $t=16s$. The red line represents the case where both the synchronverters have a PSS controller. We see that the oscillations decay but the sharing of the load, located between the two synchronverters in the middle of the line connecting them, is different. It is hard to say whether this is good or bad since it depends on the application. In such a simple system there is no ideal load sharing. The teal line represents the case where the synchronverters have virtual friction between them and we obtain better decay of the oscillation. The black line represents the scenario where the synchronverters have virtual friction between them and also a PSS controller. There is a slight improvement in the decay of oscillations but it is hard to tell whether this is a real improvement (compared to only having virtual friction) or some side effect due to simulation approximations. To summarize we see that the proposed

PSS controller does indeed work as it should in a synchronverter. We would like to test if the synchronverter with PSS controller performs as well as the synchronverter with virtual friction in the system described in Figure 31. Then we can truly understand which solution is better for the synchronverter operating in a system with synchronous generators. Here we wanted to see the performance of each solution clearly so we run the simulations under the extreme conditions described in Figure 35.

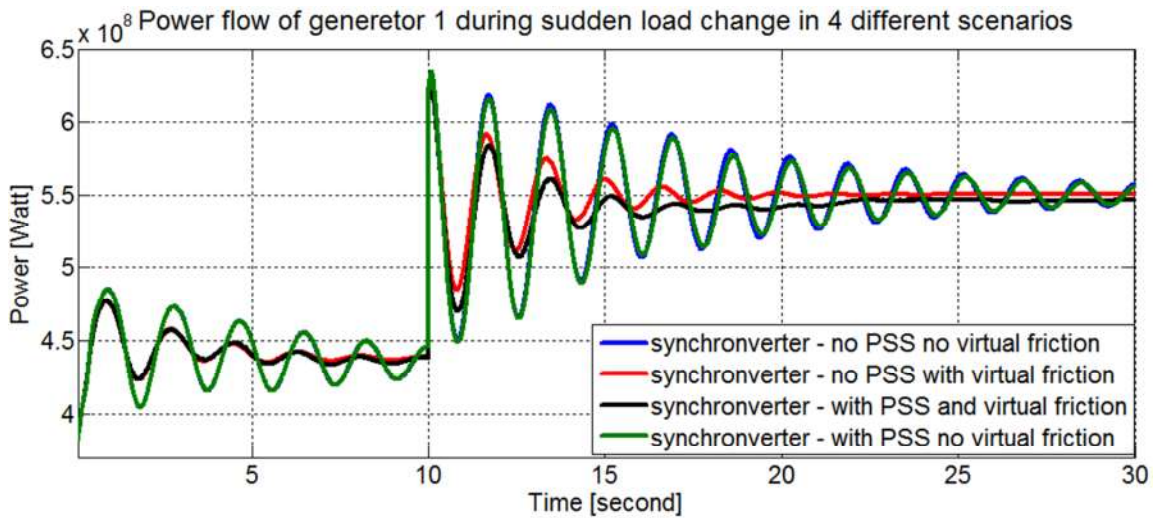


Figure 39. Comparison of the synchronverters from the test system in Figure 31 in 4 different operation modes, with and without PSS and virtual friction.

We see in Figure 39 that the difference between the blue line which describes the results under no PSS or virtual friction between synchronverter, and the green line with PSS only is very small. Since the PSS is placed in the synchronverters which only supply 10% of the power and are not the cause of the oscillations it does not do much. This is unlike the simulation in Figure 38 where only synchronverters (and no synchronous generators) are involved with PSS added to them. The red line in Figure 39 shows that using virtual friction dampens inter-area oscillations like in Figure 35. The black line which combines both PSS and virtual friction shows very little improvement. The results in Figure 39 are different from the results for the two synchronverter system in Figure 38, since here the synchronverters are not the cause of oscillations, the synchronous generators are. We see that not only virtual friction is a better solution than PSS (when they both operate on the synchronverters) but also that it can help in cases where the PSS does not help.

It is important to note that communication systems have delays. These delays may interfere with our virtual friction implementation. It has been checked that for small delays of up to 2 milliseconds the results do not differ by much. I have chosen not to attach these results since this issue requires more research than I have conducted so far.

7.3. The Pogaku-Prodanovic-Green (PPG) inverter and inter-area oscillations

We would like to investigate the performance of the system described in Figure 31 if instead of synchronverters we use a conventional inverter. For this purpose we have selected a very advanced inverter controller developed by N. Pogaku, M. Prodanovic and T.C. Green in [23]. This controller has frequency-power droop control as well as advanced load sharing capabilities. Below are the control block diagrams of this inverter as they appear in [23]:

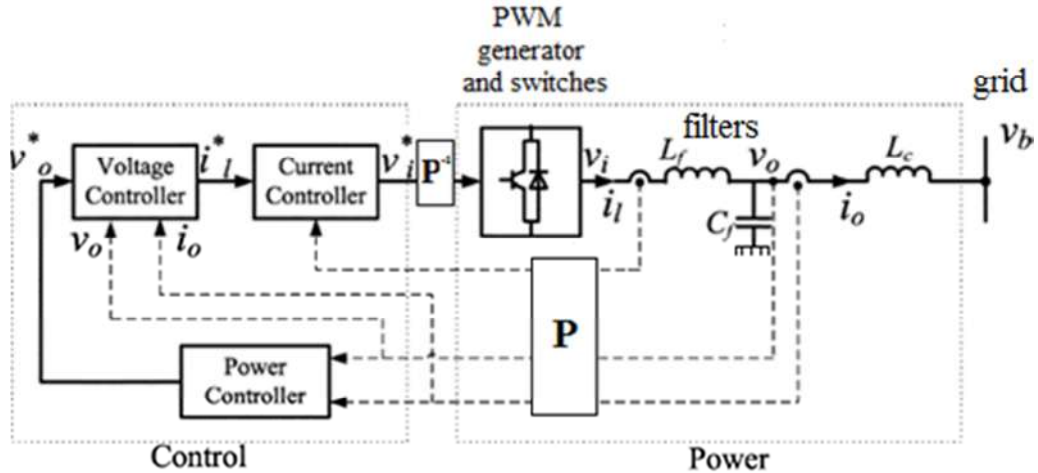


Figure 40. General inverter block diagram. P is the Park transform and an inverse Park transform is done after the calculations in the current controller, before the PWM generator and switches.

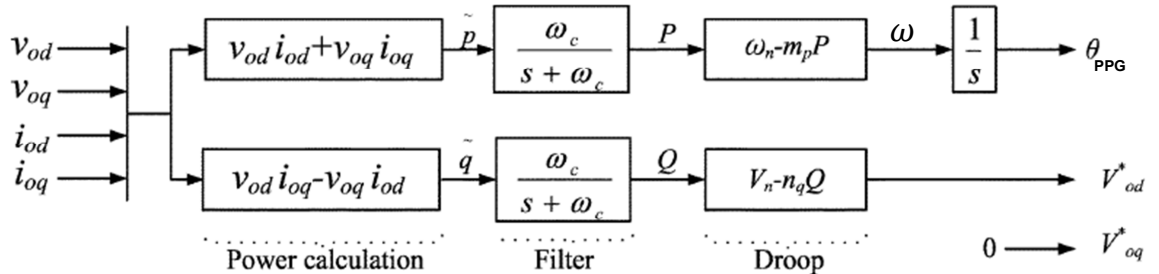


Figure 41. Power controller of the PPG inverter. ω_c is an LPF cut-off frequency for high harmonic filtering of active and reactive power. ω_n is a reference frequency frame within the range of allowed operational frequencies, that will set the power P_n transferred to the grid at nominal grid frequency corresponding to the equation $\omega_n - m_p P_n = \omega_{grid}$, where ω_{grid} is the grid nominal frequency and P_n is the active power after the LPF. The actual power that will flow to the grid is bigger. In order to calculate the actual power supplied to the grid we must also add the power that is cut by the filter. This is not easy to compute, since we do not know the effect of the switches and other non linear elements in the grid. We simply tuned the value of ω_n until we got the wanted nominal power for the simulations. m_p is a droop gain calculated by $m_p = (\omega_{max} - \omega_{min})/P_{max}$ where if we consider negative frequency drooping (extra power for frequency below nominal) we need to put $2P_{max}$. V_n is the nominal voltage amplitude (phase to ground) of the inverter and n_q is calculated by $(V_{max} - V_{min})/Q_{max}$. This value represents the voltage drooping, the higher the value of n_q , the less compensation in VAr is given for maintaining constant voltage. This parameter requires tuning. θ_{PPG} is the estimated grid angle, used in the Park and inverse Park transformations.

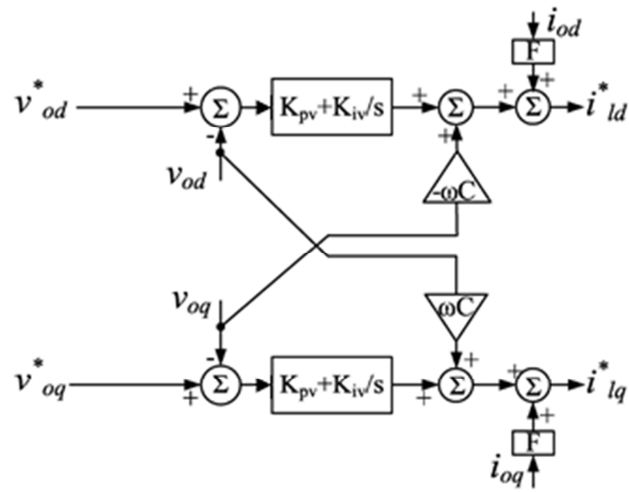


Figure 42. Voltage controller of the PPG inverter. K_{pv} and K_{iv} are PI controller constants for the voltage controller and C is The value of the filter capacitor, C_f used to compute the effect of filtering on the output voltage and F is the current feed-forward gain. F is used to improve the disturbance rejection of the inverter system.

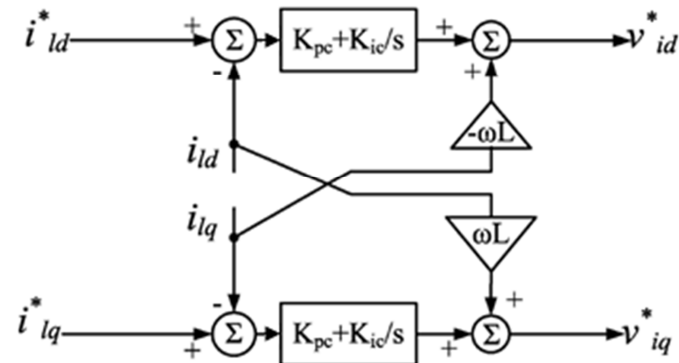


Figure 43. Current controller of the PPG inverter. K_{pc} and K_{ic} are PI controller constants for the current controller and L is the value of the output inductor, L_c . The value of this inductor is used since we want to control the output filter inductor current and not the current before the filter.

Values For 40 MW PPG inverter	
Parameter	Value
L_f	0.0725 nH
C_f	5.52 mF
L_c	0.04575 nH
K_{pv}	500
K_{iv}	1000
K_{pc}	10.5
K_{ic}	5000
F	0.75
ω_n	323.4593 rad/second
V_n	563 V

ω_c	31.4 rad/second
m_p	$0.35 \left(\frac{\text{rad}}{\text{second}} \right) / \text{MW}$
n_q	60 V/GVar

Table 2. Values of parameters for a 40 MW PPG inverter working in a 50 Hz grid.

One can easily see that this inverter uses an LCL filter like the synchronconverter and it also has frequency-power drooping and voltage-reactive power drooping like in the synchronconverter. This makes it easy for us to build an inverter model with parameters equal to those of the synchronconverter.

An additional synchronization block should also be added to this inverter. We have designed a synchronization process which is almost identical to the one in our self-synchronized synchronconverter. We found that the resulting system behaves similarly to the one containing synchronconverters without virtual friction. This means that synchronconverters have the advantages of other advanced inverters, and this is probably due to their fast frequency-power droop, which does not suffer from mechanical limitations and delays like the frequency-droop loop of a real generator. The following figure is the comparison of the synchronconverter and this inverter, which we will refer to as PPG inverter, when we put them in the system shown in Figure 31.

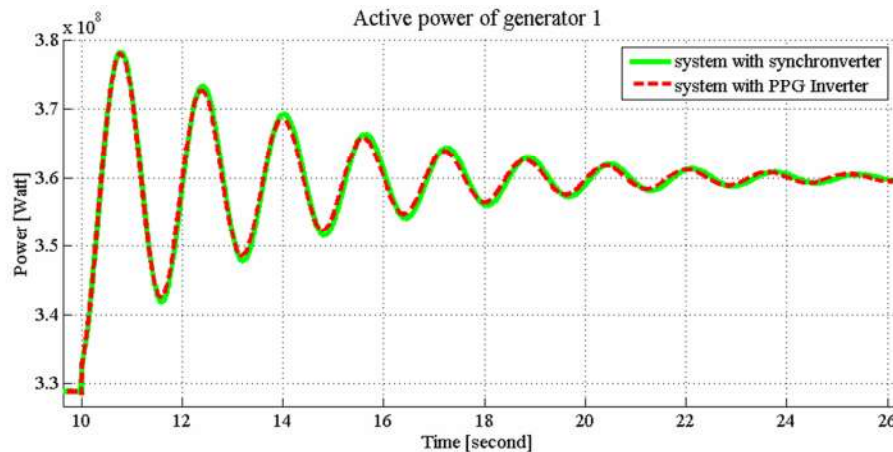


Figure 44. For the system in Figure 31, comparison of behaviour with inverter and synchronconverter (without virtual friction).

8. Eilat –Ktura grid section: a case study

So far we have tested the synchronconverter in simulated systems, some of which we designed ourselves for some specific tests and others were based on systems in SimPower examples. To verify that the synchronconverter actually helps in a real system we should test it on a real system. For this purpose we have chosen the grid section between Eilat and Ktura. Eilat is the southernmost city in Israel. This means that electricity produced mostly in Hadera power station has to travel long distances to reach Eilat. This is very costly which makes Eilat a perfect candidate for renewable sources, along with the fact Eilat is sunny

most of the year. We obtained data from the IEC concerning line parameters, synchronous generators found in Eilat, renewable sources currently located in Ktura and other sources that will be available in the future. The north line from the center of Israel to Ktura was given similar values as the line from Ktura to Eilat, only that the former is six times longer. The grid from the north is modeled as an infinite bus. In Figure 45 we see the full scheme of the system.

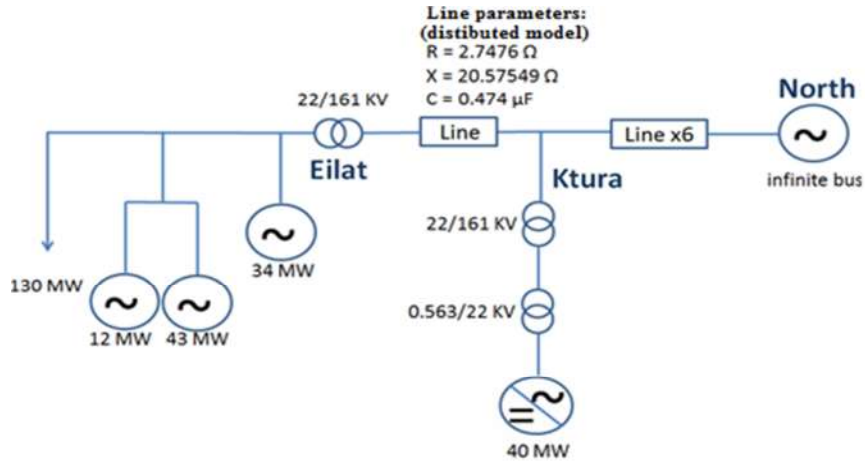


Figure 45. Schematics of Eilat-Ktura grid section.

The simulation scenario is as follows: first we connect the generators in Eilat to the infinite bus, wait for 8 seconds until the system stabilizes. After the system stabilizes, at $t=8s$, the inverter in Ktura is connected. It takes another 8 seconds for the system to stabilize. Assume that when the inverter in Ktura is connected along with the generators in Eilat, we get a scenario where the local load is balanced by the local power production. This is a reasonable scenario since it is expensive to bring power from the north to Eilat. Two seconds later at $t=18s$ the line from the north to Ktura is disconnected thereby creating an electrical island. This could happen for maintenance reasons or faults somewhere along the line from Ktura to the north. It is important to note that currently the IEC does not allow islanding but this situation would probably change in the future. The newly created electrical island in Eilat-Ktura grid section starts oscillating in frequency and power. It takes almost 15 seconds until the oscillations decay. After another 17 seconds at $t=35s$ a three phase fault occurs in Eilat. This is an extreme but possible scenario. Short circuits occur frequently in a power grid. Most of them are one phase faults that last for a short duration and consume little power. **We consider this three phase short circuit in three scenarios: with the resistance between the phases (in Eilat) being 10Ω , 1Ω and 0.1Ω .** In the first scenario the three phase fault causes a 2% frequency decrease at the Ktura and Eilat generators, due to the extra power dissipated in the high voltage line and also in the resistors of the short circuit. The frequency in Eilat also decreases in the case of 1Ω short circuit, but it increases for 0.1Ω , as is normal for generator near a total short circuit (where terminal voltage drops near zero). In each of the three cases, a phase difference develops between Eilat and Ktura during the short circuit and the islanded system oscillates after the short circuit is removed. The recovery of the system from the fault depends on the type of inverter used in Ktura. We want to compare the synchronverter with our PPG inverter

described in the previous chapter. Today there are no inverters that allow positive frequency-power drooping, meaning that if the frequency drops the inverter cannot supply additional power since it has no energy storage. This is why we need to update the PPG inverter to only support negative power-frequency drooping. This is done by saturating the power output if the signal P from the frequency droop is larger than P_n as shown in Figure 45 below. Notice that P_n is the nominal power after the LPF, this is lower than the actual power flowing to the grid at nominal grid frequency, see Figure 41 for more details.

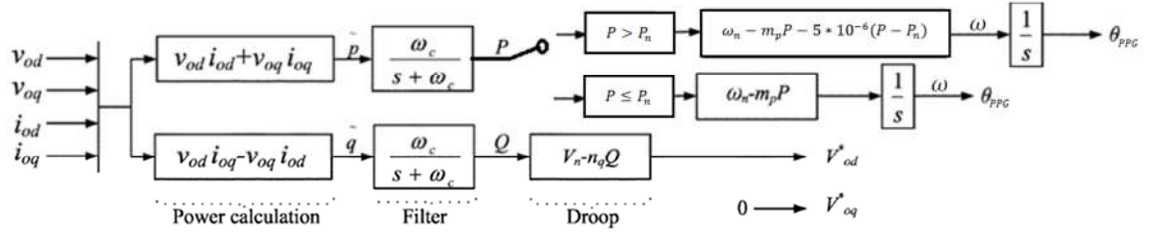


Figure 46. Updated power controller of the inverter designed in [23] (compare with Figure 41).

In Figure 46 we see that if the power the inverter has to generate (due to frequency drop) is larger than the nominal power then, the frequency-power droop characteristic changes so that the frequency is still tracked by the inverter but the power does not exceed nominal power.

We have run three simulations: one with the synchronconverter as the inverter at Ktura, the second with the PPG inverter as the inverter at Ktura and a third with a synchronous generator instead of the inverter at Ktura. We have run these simulations to compare the performance of the synchronconverter and the PPG inverter. The synchronization process (see below in Figure) is equally good for the synchronconverter and the updated PPG inverter and they both synchronize better than a synchronous generator.

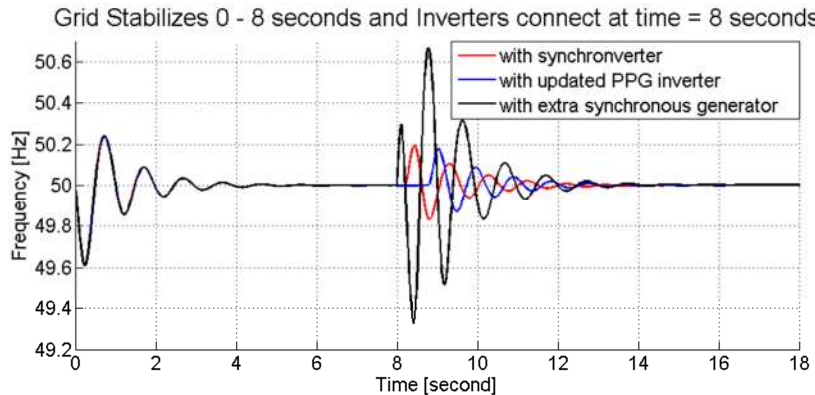


Figure 47. Synchronization of the inverter at Ktura to the grid (frequency in Ktura).

Assuming that 89 MW are generated by synchronous generators in Eilat, and 40 MW are generated by an extra unit 52 km to the north in Ktura, generation and consumption are balanced. We have simulated 3 options for this extra unit: synchronconverter, updated PPG inverter and synchronous generator. The Eilat-Ktura grid section is islanded at $t = 18s$ and at $t = 35s$ a 150 ms short circuit occurs. In each of the following scenarios when the extra unit in Ktura is a synchronous generator the local grid of Eilat-Ktura loses stability, leading

to a blackout. We will first show the results of the first scenario, a 10Ω short circuit resistance.

Frequency in Eilat during a 10 Ohm 3 phase short circuit after islanding

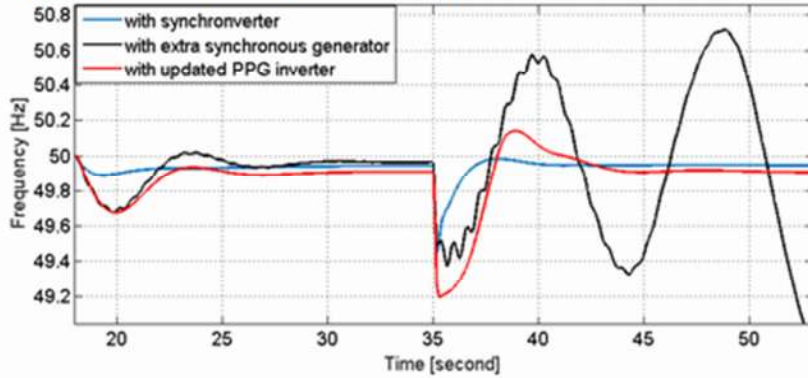


Figure 48. Frequency in Eilat after islanding and short circuit at Eilat when the inverter in Ktura is a synchronverter, PPG inverter or a synchronous generator. Both synchronverter and PPG inverter stabilize the system, the synchronverter stabilizes faster. The synchronous generator trips the system (instability after the short circuit).

Frequency in Ktura during a 10 Ohm 3 phase short circuit after islanding

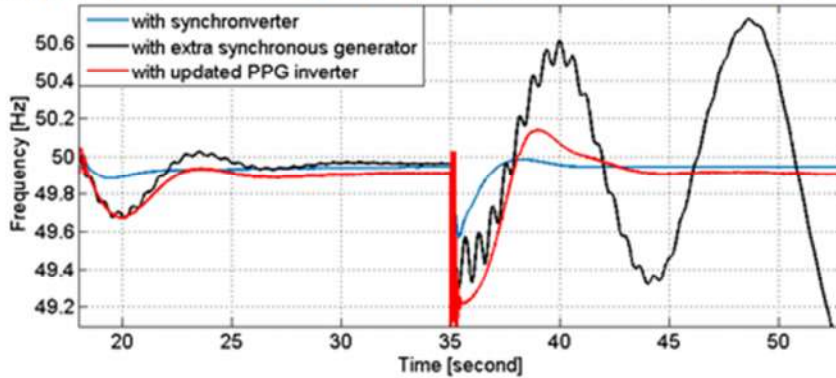


Figure 49. Frequency in Ktura after Islanding and short circuit at Eilat when the inverter in Ktura is a synchronverter, PPG inverter or a synchronous generator. Similar to the behavior seen in Eilat in Figure 48 (this is the same simulation).

Voltage rms on synchronous generator terminals in Eilat

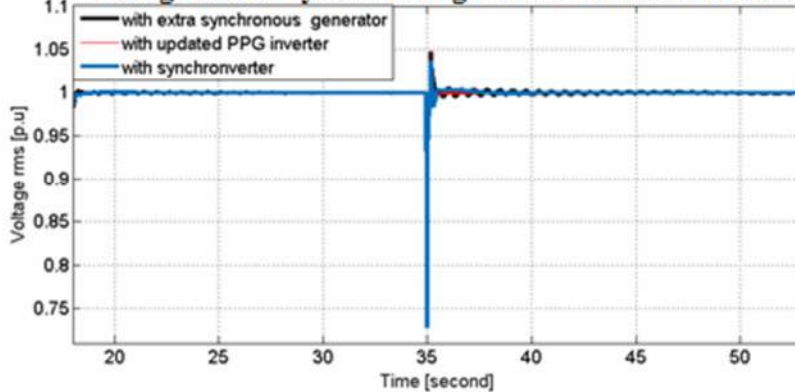


Figure 50. Voltage rms value per unit on the terminals of the synchronous generator in Eilat under the same scenario as in Figures 48 and 49. We see very small influence of the type of power source in Ktura, when a synchronous generator is the extra power unit in Ktura the voltage signal of the generators in Eilat has ripples.

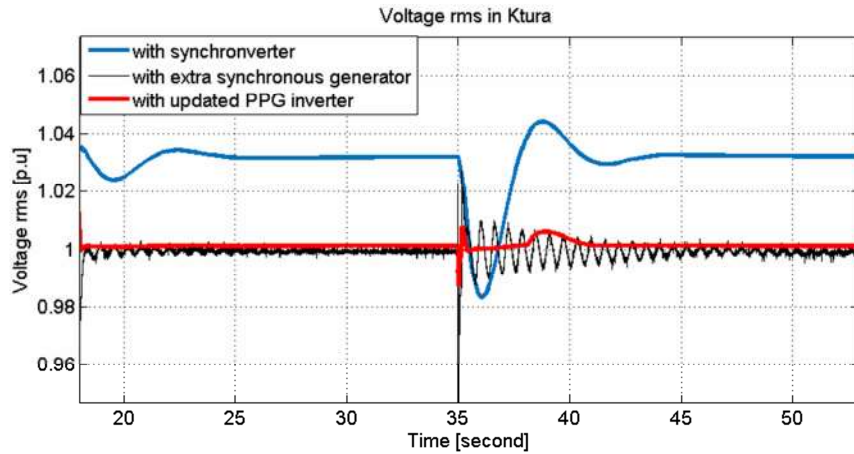


Figure 51. Voltage rms value per unit on the terminals of the extra power unit at Ktura. We see that the synchronconverter maintains higher voltage levels than both PPG inverter and synchronous generator and that the PPG inverter has the most stable voltage level on its terminals.

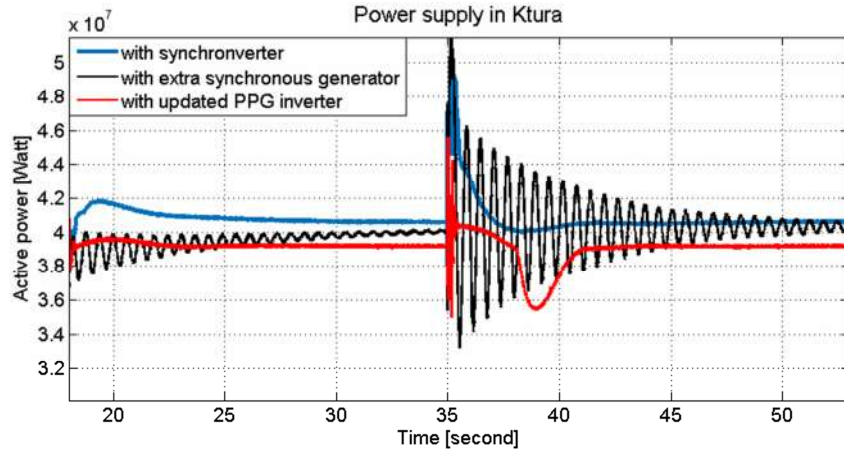


Figure 52. The active power supplied from Ktura by the synchronconverter, PPG inverter or synchronous generator under the scenario from Figures 48, 49. The synchronconverter delivers more power although both inverters and the synchronous generator are designed to supply 40 MW nominal power, and maintains better stability. The synchronous generator causes many ripples.

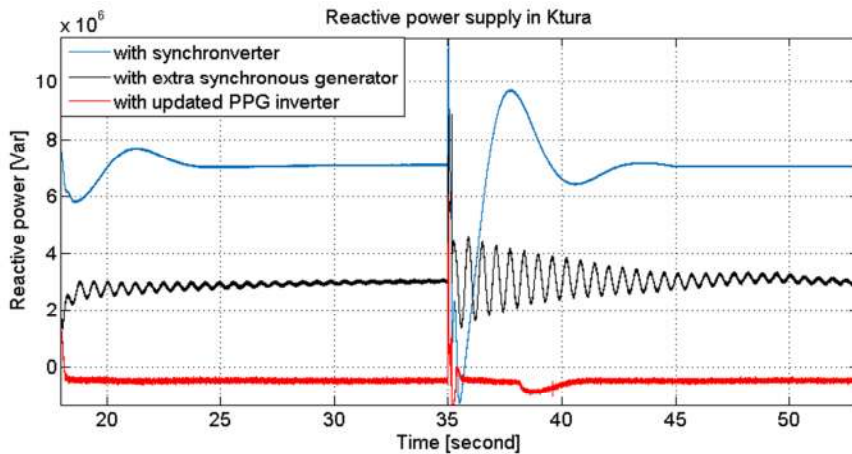


Figure 53. The reactive power supplied from Ktura by the synchronconverter, PPG inverter or synchronous generator under the scenario from Figures 48, 49. The synchronconverter supplies more reactive power, which explains the high level of voltage on its terminals shown in Figure 51. The synchronous generator causes ripples.

When we take the system to a more extreme situation, a 1Ω resistance in the short circuit, we get similar results that highlight the advantage of the synchronconverter versus the PPG inverter.

Frequency in Eilat during a 1 Ohm 3 phase short circuit after islanding

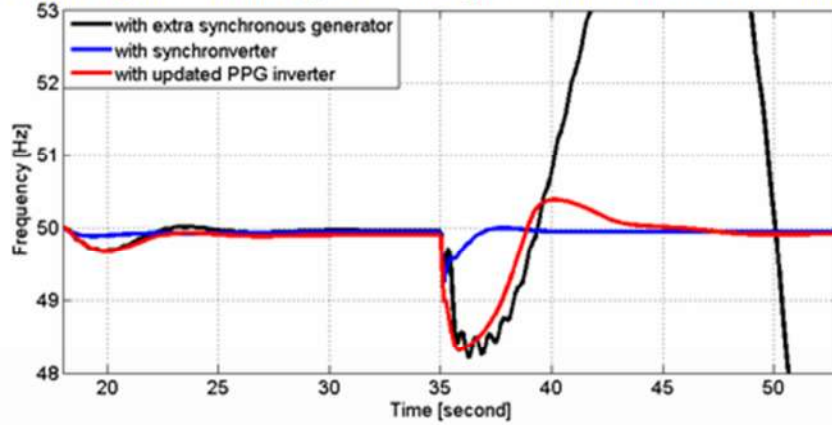


Figure 54. Frequency in Eilat after Islanding and 1Ω short circuit at Eilat at $t = 35s$ when the inverter in Ktura is a synchronconverter, PPG inverter or a synchronous generator. Both synchronconverter and PPG inverter stabilize the system, the synchronconverter stabilizes faster. The synchronous generator trips the system (instability after the short circuit).

Frequency in Ktura during a 1 Ohm 3 phase short circuit after islanding

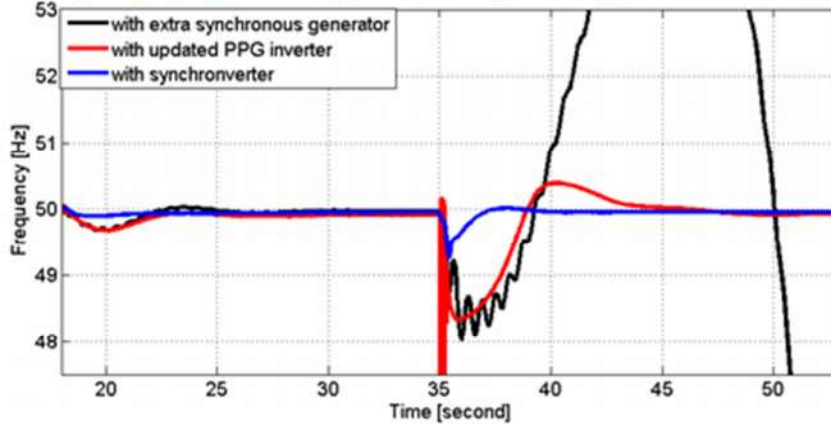


Figure 55. Frequency in Ktura after Islanding and short circuit at Eilat when the inverter in Ktura is a synchronconverter, PPG inverter or a synchronous generator. Similar to the behavior seen in Eilat in Figure 54 (this is the same simulation as Figure 54).

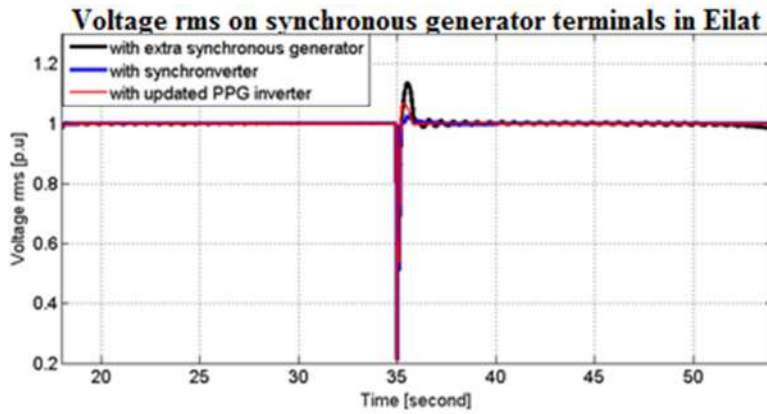


Figure 56. Voltage rms value per unit on the terminals of the synchronous generator in Eilat under the scenario from Figure 54. We see very small influence of the type of power source in Ktura, when a synchronous generator is the extra power unit in Ktura then the voltage signal of the generators in Eilat causes ripples.

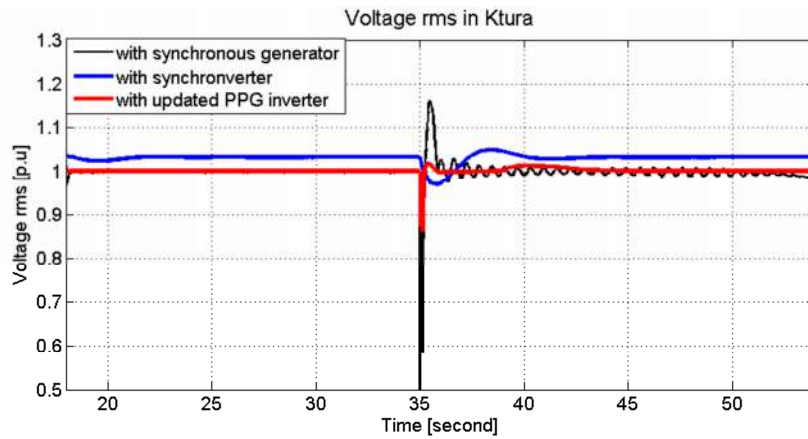


Figure 57. Voltage rms value per unit on the terminals of the extra power unit at Ktura under the scenario from Figure 54. We see that the Synchronconverter maintains higher voltage levels than both the PPG inverter and the synchronous generator and that the PPG inverter has the most stable voltage level on its terminals.

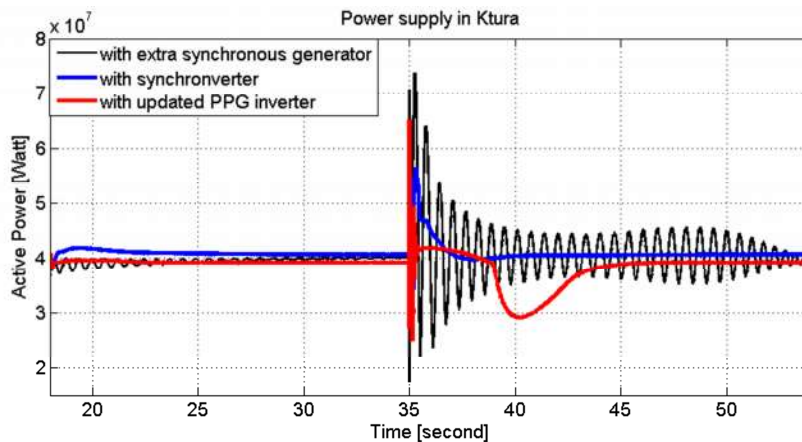


Figure 58. The active power supplied from Ktura by the synchronconverter, the PPG inverter or the synchronous generator under the scenario from Figure 54. The synchronconverter delivers more power although both inverters and the synchronous generator are designed to supply 40 MW nominal power, and maintains better stability. The synchronous generator causes many ripples.

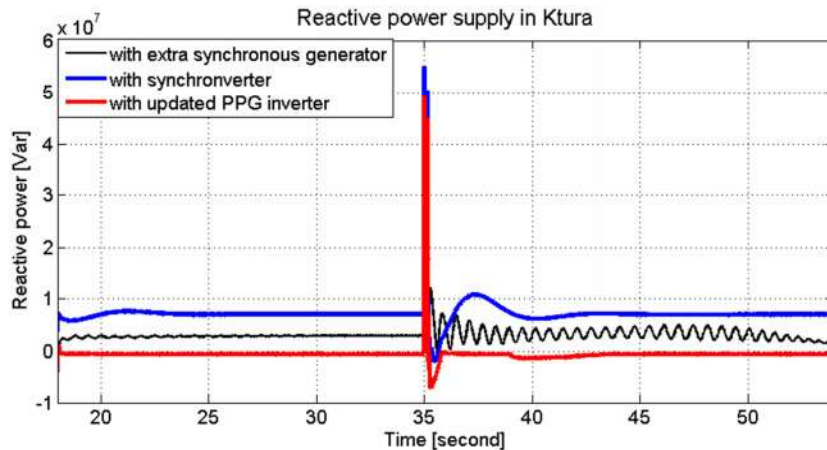


Figure 59. The reactive power supplied from Ktura by the synchronverter, the PPG inverter or the synchronous generator under the scenario from Figure 54. The synchronverter supplies more reactive power, which explains the high level of voltage on its terminals shown in Figure 56. The synchronous generator causes ripples.

We wanted to see the behavior of the systems in a classical short circuit, when the voltage on the synchronous generators terminals drops almost to zero during the 150ms of the short circuit. For that we reduced the resistance of the short circuit to 0.1Ω . This case is different from the previous two since during a full short circuit the synchronous generators cannot supply any power to the system because the voltage is zero. This causes the generators to work in under loaded conditions, such conditions cause the frequency to jump up and mechanical damage could be inflicted to the rotating parts of the generator. This only happens if the frequency jumps too high or for a long time period, the limitations depend on the age of the generator and the manufacturers design.

Frequency in Eilat during a 0.1Ω 3 phase fault short circuit after islanding

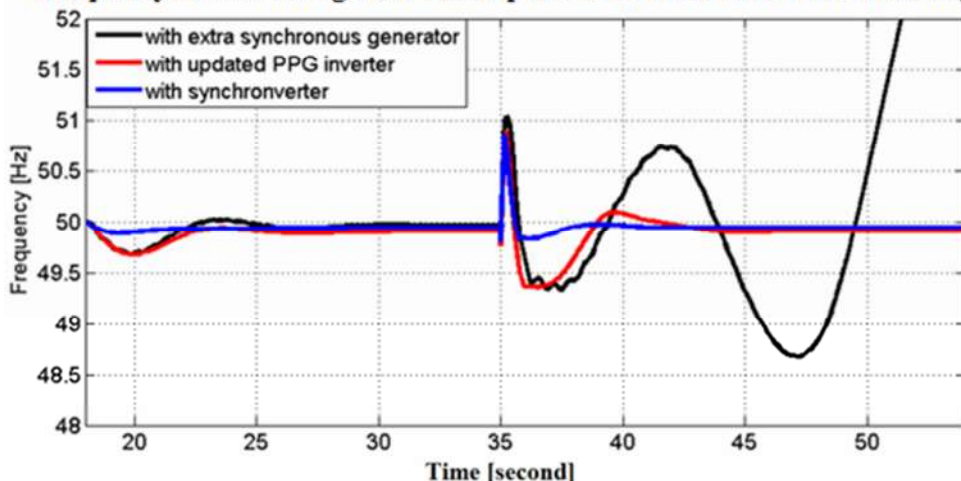


Figure 60. Frequency in Eilat with a full short circuit (0.1Ω) in Eilat occurring at $t = 35s$. We see that the frequency rises during the fault as expected. The recovery of the system with the synchronverter in Ktura is better than with the PPG inverter. When Ktura has a synchronous generator then the system trips like in the previous short circuit scenarios.

Frequency in Ktura during a 0.1 Ohm 3 phase short circuit after islanding

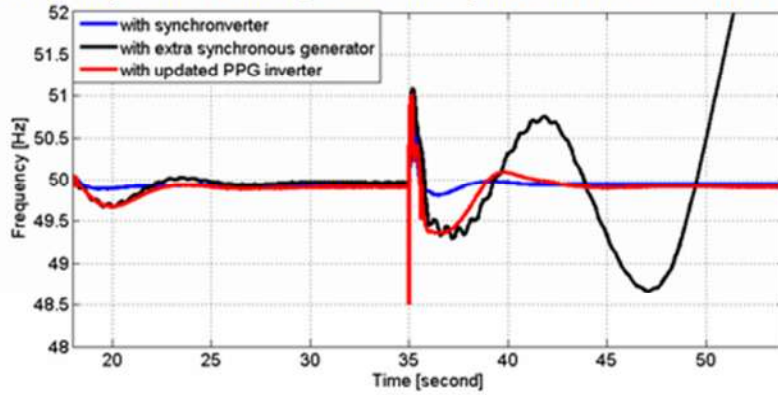


Figure 61. Frequency in Ktura with a full short circuit in Eilat occurring at $t = 35s$. We see that the frequency in Ktura behaves the same as in Eilat. Frequency rises during the fault, the synchronconverter gives fastest recovery and with the synchronous generator there is a blackout.

Voltage rms on synchronous generator terminals in Eilat

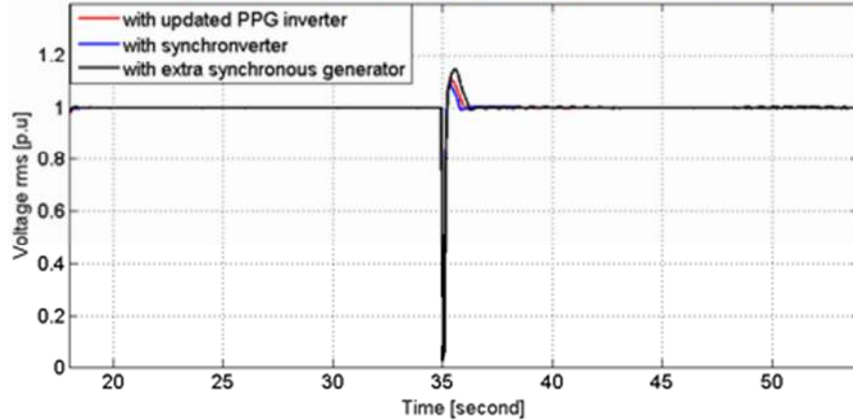


Figure 62. Voltage rms value per unit on the terminals of the synchronous generators in Eilat with the scenario as in Figure 60. We see very small influence of the type of power source in Ktura. The synchronconverter gives better results, lowest voltage jump during recovery.

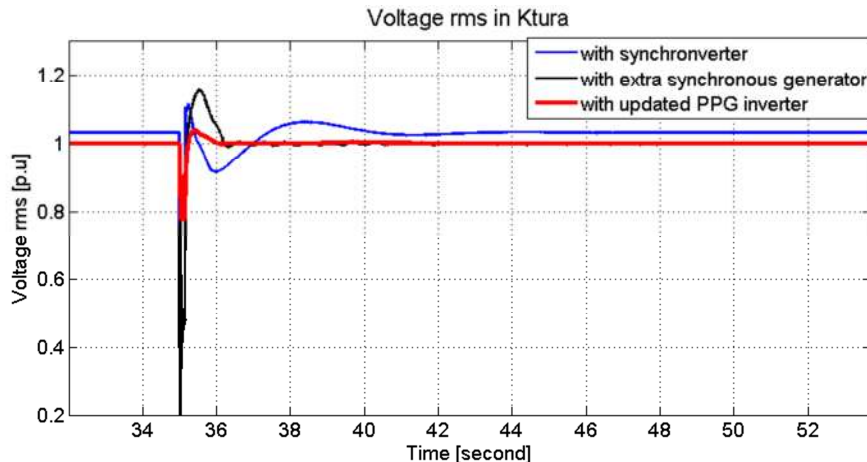


Figure 63. Voltage rms value per unit on the terminals of the extra power unit at Ktura with the scenario as in Figure 60. We see that the synchronconverter maintains higher voltage levels than both the PPG inverter and the synchronous generator and that the PPG inverter has the most stable voltage level on its terminals.

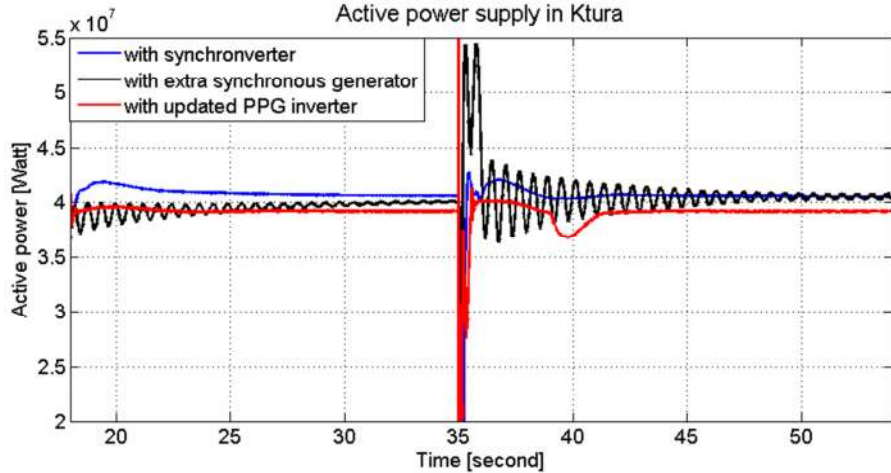


Figure 64. The active power supplied from Ktura by the synchronconverter, PPG inverter or synchronous generator with the scenario as in Figure 60. The synchronconverter delivers more power although both the PPG inverter and the synchronous generator are designed to supply 40 MW nominal power, and maintains better stability. The synchronous generator causes many ripples.

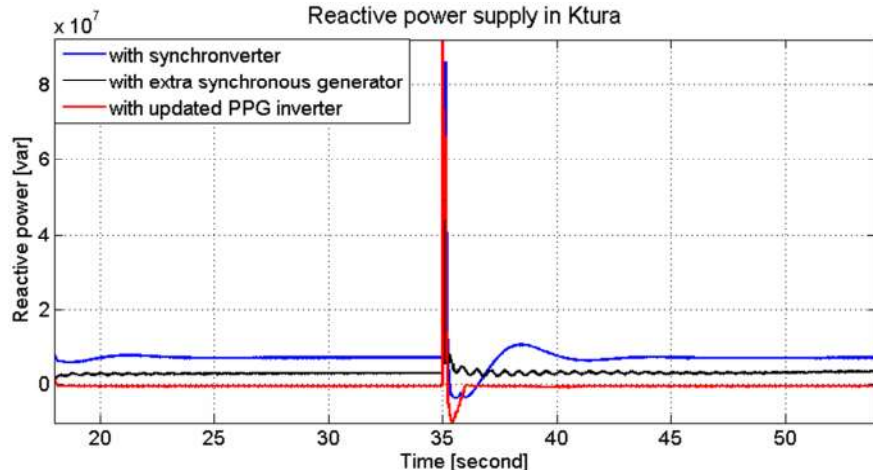


Figure 65. The reactive power supplied from Ktura by the synchronconverter, PPG inverter or synchronous generator with the scenario as in Figure 60. The synchronconverter supplies more reactive power, which explains the high level of voltage on its terminals shown in Figure 63. The synchronous generator causes ripples.

Figures 48 to 65 shows that the synchronconverter not only gives faster recovery time from faults but also reduces the effect of the faults themselves. We also see that after islanding, the power flow from Ktura decreases in the case of the PPG inverter, and increases in the cases of the synchronous generator and the synchronconverter, see Figures 52, 58 and 64. This is due to negative drooping that allows the synchronconverter and synchronous generator to supply more than the nominal active power to stabilize the frequency. While the PPG inverter does handle the faults well, we see that the synchronous generator trips. This is probably due to the slow response time of the synchronous generator frequency drooping. Inverters have no mechanical parts, which makes their response faster than that of conventional generators. This quality is very important but it may also cause problems if the inverters have no additional energy storage. In some cases the grid may have a fault and

we may want the grid to maintain the existing performance. This will not be possible without additional energy to compensate the losses caused by the fault. For this reason the synchronconverter along with a small energy storage unit offers the best support for grid stabilization.

We also wanted to check what would happen if the extra power that is supposed to come from the synchronconverter has a time delay of 200 milliseconds. This delay can be a result of the dynamics of MPPT or energy storage device discharge. There is no need to recreate all 3 scenarios introduced previously since the effect on the synchronconverter should be the same regardless of the fault itself. We choose to show this in the first scenario where the resistance of the fault is 10Ω . In Figure 66 below we see that the differences, in frequency which also corresponds to active power flow, with and without delay are negligible. There is no effect on the voltage or reactive power from this delay in extra power supply, so we have chosen not to attach the corresponding plots.

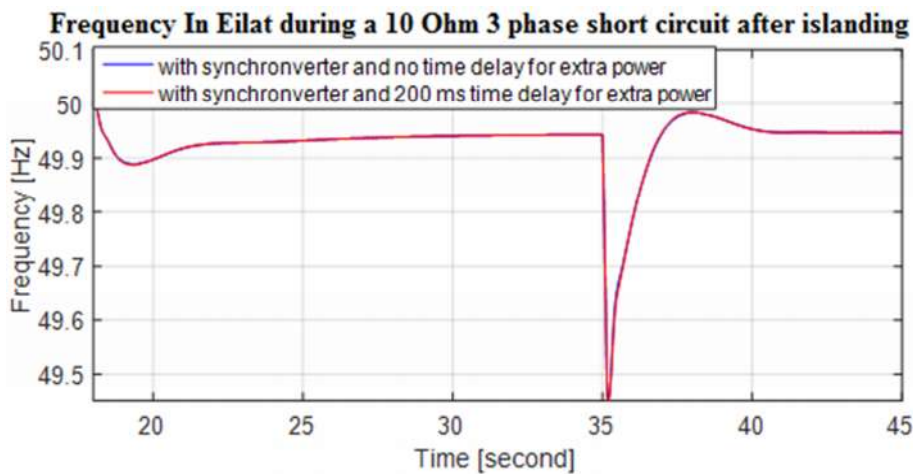


Figure 66. Ktura-Eilat simulation of a 10Ω short circuit in Eilat with a synchronconverter in Ktura. The scenario is repeated twice with and without time delay of the synchronconverter for extra power. This Figure shows the frequency in Eilat.

9. A synchronconverter based energy storage device for grid stabilization

This chapter is based on my intuition and more work is needed to truly understand the advantages a synchronconverter can provide while operating in an energy storage device. Usually energy storage is used in emergencies when a fault of some sort occurs and disconnects the user from the grid. In such a scenario the operating algorithm of the energy storage inverter can be basic and simple. Indeed there are no stability problems for low power energy supply in off grid operation. Another use for energy storage which is less common is providing additional energy when the demand exceeds the available power supply. This can happen on cold nights when people turn on heating boilers or on hot summer days when people turn on air-conditioning systems. There could also be other circumstances but these are the main scenarios. Usually when an energy storage device is used together with the grid it must work under some basic regulations. Since the power

energy storage can supply is negligible relative to the grids power most inverters today will only work under these regulations.

We suggest a new use for energy storage devices. As shown in the last chapter inverters have certain advantages such as zero delay frequency-power drooping which can considerably contribute to grid stability. If we use emergency storage for grid stabilization it will help justify the cost of existence of such devices and may even help make the grid more robust (which is especially important in places with poor infrastructure). We suggest keeping the energy storage devices always connected with nominal power 0W. The inverter is operated with the synchronverter algorithm.

To demonstrate how this could work we need to build a model of a power grid which includes low voltage, medium voltage and high voltage grid sections, each of which plays a different role in delivering power for consumers. After some research we designed the following grid:

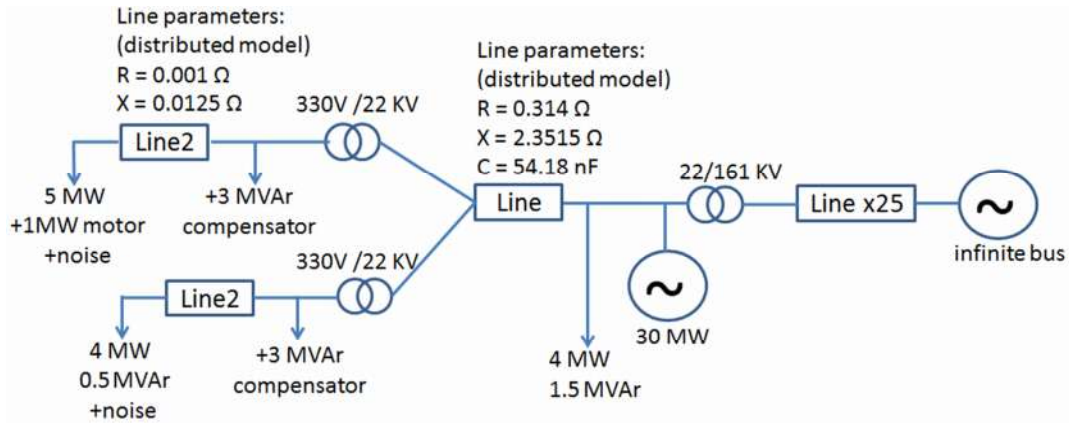


Figure 67. Scheme of power grid with low, medium and high voltage parts. The line is modeled using the distributed model of power lines.

In this scheme the high voltage part comes from a faraway large power station and in the medium voltage part there is a local factory with industrial power station that can provide all electrical needs for the factory and a nearby city. The low voltage part is simulating a small city with a 10MW power consumption divided in to two branches where one branch consumes 2MW more than the other. There are power factor compensators in each branch. On the branch with the bigger load there is a laundromat or a facility which uses a large 1MW motor, which is modeled using a synchronous machine with a constant negative mechanical torque input (which means a constant mechanical load). We also add load switching noises of about 1-1.5% of the branch loads to simulate a more realistic power grid. It is important to note that in an actual grid there are more branches in the low voltage area and FACT devices, see Chapter 11 pp. 627-684 in [16], which helps regulating the voltage and the power factor. To make the simulation faster we ignore this. We do not claim that this omission will not matter but this is not important in the simple proof of concept of an always connected emergency energy storage device whose inverter works as a synchronverter. After some simulations where we connected the synchronverter to various parts of the grid we found that the weakest spots of the grid are the elements which

have complex dynamics such as the motor or synchronous generator. So the best place to put a stabilizing device is near these elements.

To check if there are improvements when a synchronverter is added, we caused a fault near one of the medium to low voltage transformers on the medium voltage side. The fault is a 3 phase fault of 10Ω for duration of 150 milliseconds. Unfortunately placing a synchronverter with 0W nominal power with the regular algorithm did not contribute much to grid stability. This is probably since the infinite bus is strong enough to keep the system stable so the synchronverter was not really needed.

This got us looking for an idea for making the synchronverter more meaningful even in the presence of an infinite bus. On the basis of the effect of virtual friction on inter-area oscillations we expected that there must be a way to cause similar decay in local oscillations, or at least in inter-area oscillations, using only one synchronverter. Indeed this can be achieved by using an one way virtual friction between the synchronverter and some oscillating element, either a synchronous generator or a motor. More precisely, we add another torque to the right side of (4.4). For a generator this torque should be $T_{vf} = (p_e - p_m)/\dot{\theta}$ where p_m is the mechanical power the generator receives from the governor and p_e is the generator's output electrical power. Typically in a synchronous generator, the mechanical power is slowly varying and the electrical power changes fast which leads to oscillations in the system. The synchronverters fast frequency drooping can help the system stabilize faster by compensating for the slow change in mechanical torque. For a motor the torque has an identical expression given by $T_{vf} = (p_e - p_m)/\dot{\theta}$ where p_m is the mechanical load's power and p_e is the electrical power being absorbed by the motor. This means that the mechanical power acts like a constant nominal reference power for the generator or the motor and the electrical power is the dynamical fast changing power that is absorbed or consumed by the motor/generator. One important fact that needs to be mentioned is that the power that the generator (motor) produces (consumes) is different, usually bigger than the power the synchronverter produces. Hence we need to normalize the additional torque. The chosen normalization is as follows $\widetilde{T}_{vf} = T_{vf} \left(2P_{max_{synch}} / P_{max_{gen}} \right)$.

Therefore if the amplitude of oscillation of power in the generator or motor is $P_{max_{gen}}$ or $P_{max_{mot}}$, then the synchronverter can supply for a short period up to twice its maximum power which is usually the nominal power it was designed to output. We recommend that in the future, after checking the feasibility of inverters to supply higher power for short durations, the normalization should change and maybe we can use synchronverters designed for nominal power P to output momentarily power $5P$ or more. Simulations indicate that this helps considerably in the decaying of oscillations and does not require bigger energy storage (since the oscillations last a very short period of time).

We have run 6 different scenarios to check this idea. The first scenario is simply the system from Figure with the fault mentioned in the previous page. This scenario is the reference scenario which we want to improve using the synchronconverter. The second scenario is adding a 2MW nominal power synchronconverter in parallel to the motor and load on the low voltage side. Here we add a one sided virtual friction torque between the synchronconverter and the motor. The third scenario is adding a synchronconverter of 5MW nominal power in parallel to the synchronous generator on the medium voltage side with a one sided virtual friction torque between them. The fourth scenario includes both synchronconverters from scenario 2 and 3 to show that they work better together without disturbing each other. In the fifth scenario We used the system from scenario four and added another synchronconverter of 10 MW nominal power on the high voltage side in parallel to the infinite bus. We also added an additional virtual friction between this synchronconverter and the synchronconverter on the medium voltage side. This was to verify if the main problem is the oscillations between the infinite bus and the synchronous generator and if so the virtual friction between the two synchronconverters parallel to them should help considerably. The last scenario was the same system from scenario five without any virtual friction torques. The point of this scenario is to show that without these torques the synchronconverters with 0W nominal power do not affect the system as much as they would with them. First in Figure 68 we plot the power of the synchronconverter near the synchronous generator and the power of the generator from scenario three in addition to the power of the same synchronconverter in scenario six without the one sided virtual friction. Similarly in Figure 69 we plot the power of the synchronconverter in the low voltage side and the power of the motor from scenario four together with the power of the synchronconverter from scenario six without the one sided virtual friction.

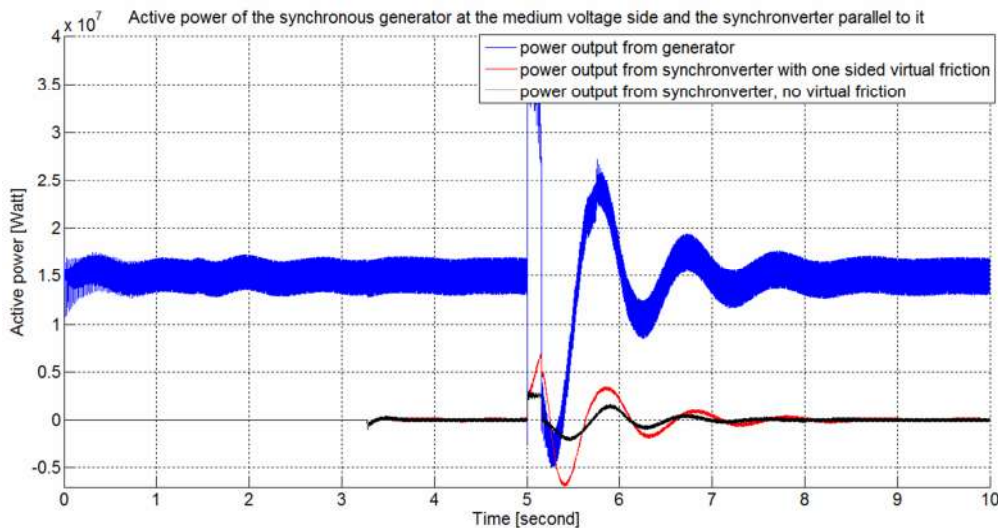


Figure 68. Output power of synchronous generator and synchronverter attached to it with and without one sided virtual friction. synchronverter connects at $t=3.2s$ and the fault starts at $t=5s$ and lasts until $t=5.15s$.

We can clearly see in Figure 68 that the power from the synchronverter has a very small phase difference with the power from the generator whether or not there is a one sided

virtual friction between them. When this friction is absent we see that the synchronconverter reacts weakly.

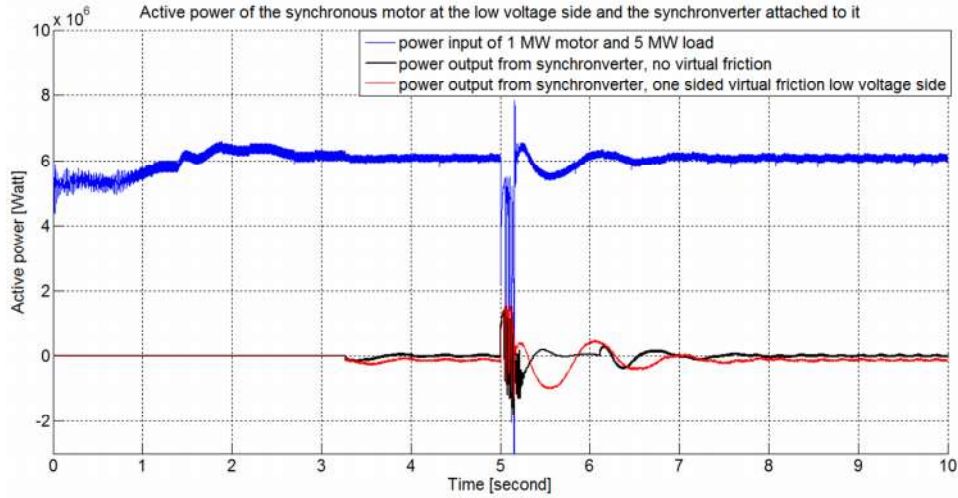


Figure 69. Input power of 1MW synchronous motor and 5 MW load, and synchronconverter attached to it with and without one sided virtual friction. Synchronconverter connects at t=3.2s and the fault starts at t=5s and lasts until t=5.15s.

We see in Figure 69 that the motor is behaving like the generator in Figure 68 only much smaller fluctuations in power. Without the one sided virtual friction the synchronconverter hardly reacts to motor power changes. Before presenting the frequency and voltage of both the generator and motor in the 6 different scenarios in the next several pages, we summarize the scenarios in the table below:

Scenario 1	No synchronconverters present
Scenario 2	2 MW synchronconverter on low voltage side with one sided virtual friction with motor
Scenario 3	5MW synchronconverter on medium voltage side with one sided virtual friction with generator
Scenario 4	Synchronconverter on medium and low voltage sides with corresponding virtual friction with the generator and the motor.
Scenario 5	Synchronconverter on low voltage side with one sided virtual friction with the motor and one sided virtual friction between medium voltage side synchronconverter and synchronous generator and virtual friction between medium voltage side synchronconverter and high voltage side synchronconverter
Scenario 6	3 synchronconverters are present without virtual friction of any kind

Table 3. Summary of the 6 tested scenarios for synchronconverter use in energy storage.

For readability I have divided the plots to 3 scenarios each. Figure 70 present the three worst attempts to stabilize the synchronous generator frequency and Figure 71 presents the three best solutions for stabilizing the synchronous generator frequency.

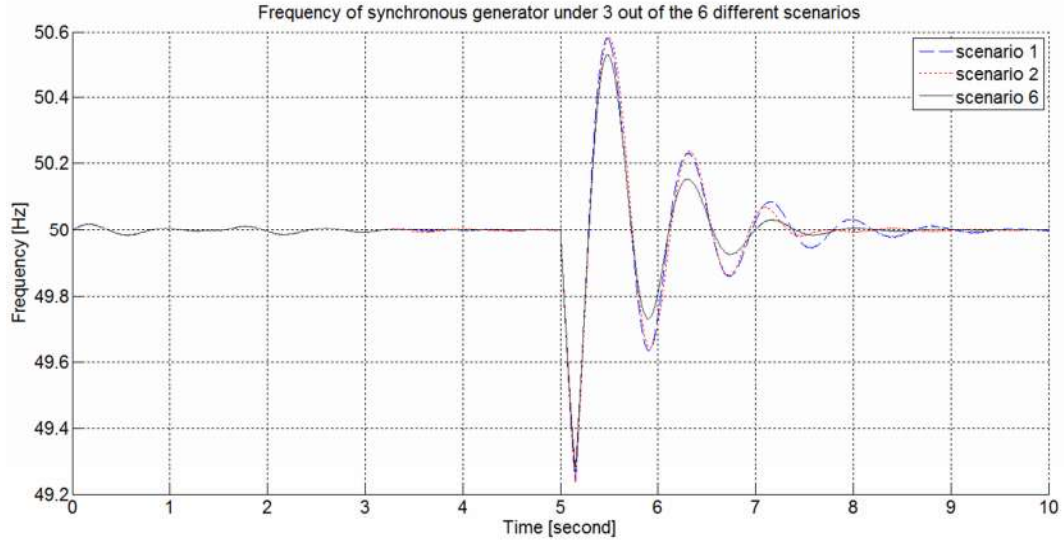


Figure 70. Synchronverters connect at $t=3.2s$, fault occurs between $t=5s$ to $t=5.15s$. We see that with three synchronverters but without any virtual friction there is a small improvement and with a synchronverter in the low voltage side with one sided virtual friction to the motor we see some improvement after 7 seconds.

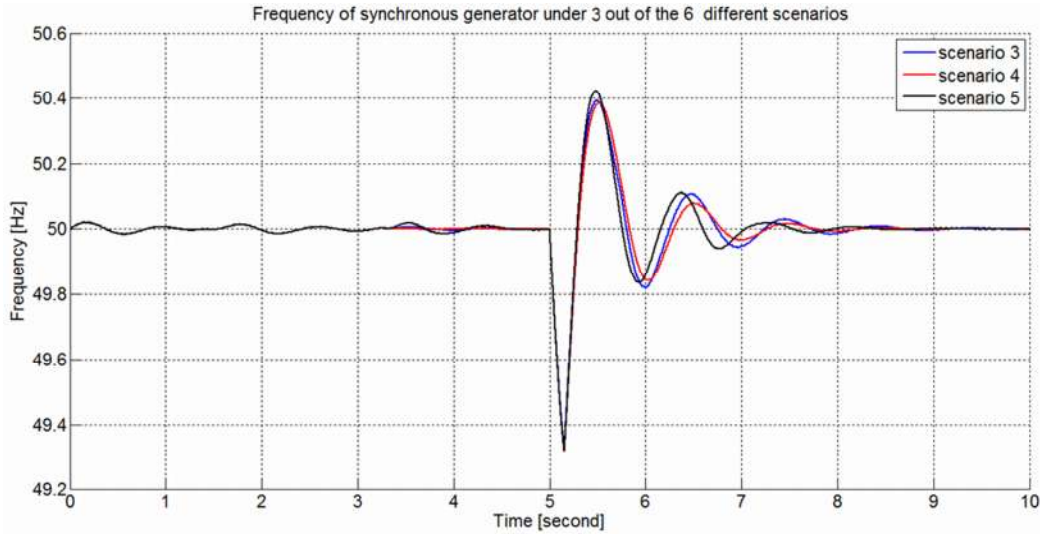


Figure 71. Synchronverters connect at $t=3.2s$ and fault occurs between $t=5s$ to $t=5.15s$. We see that scenario 4 which includes 2 synchronverters with one sided virtual friction to the motor and generator gives the best results. Adding another synchronverter in the high voltage side with virtual friction to the synchronverter in the medium voltage side does not improve the results. This is probably due to the fact that these oscillations are not inter-area but are more local in nature.

Figure 72 present the three worst attempts to stabilize the synchronous motor frequency and Figure 73 presents the three best solutions for stabilizing the synchronous motor frequency.

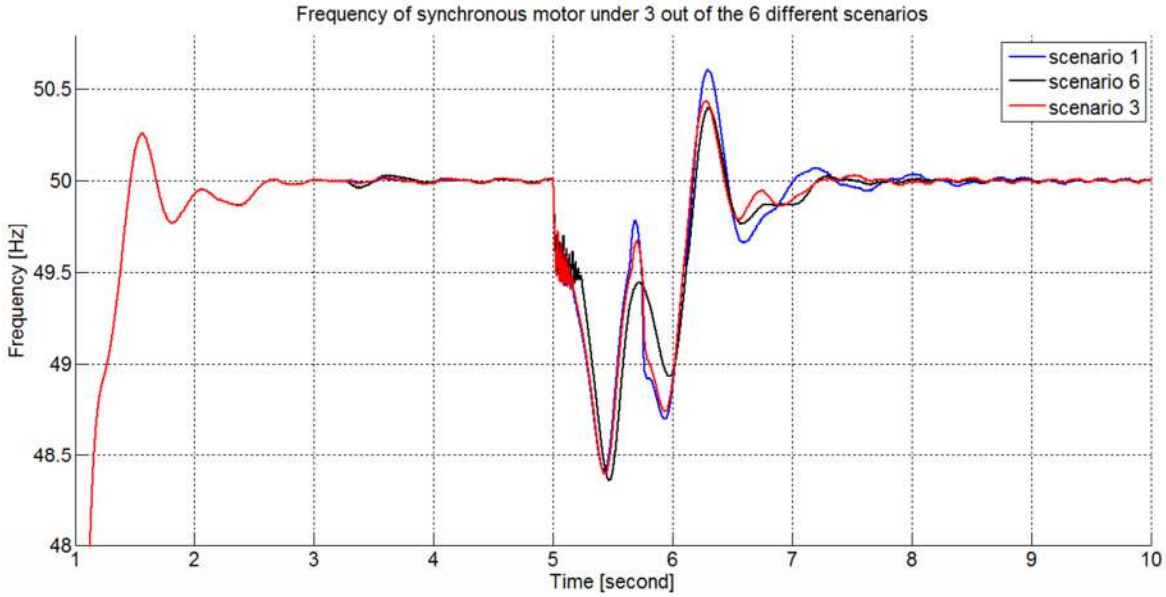


Figure 72. Synchronverters connect at $t=3.2s$ and fault occurs between $t=5s$ to $t=5.15s$. We see that the synchronverter on the medium voltage side does not help the motor performance irrespective of whether there is one sided virtual friction between that synchronverter and the synchronous generator.

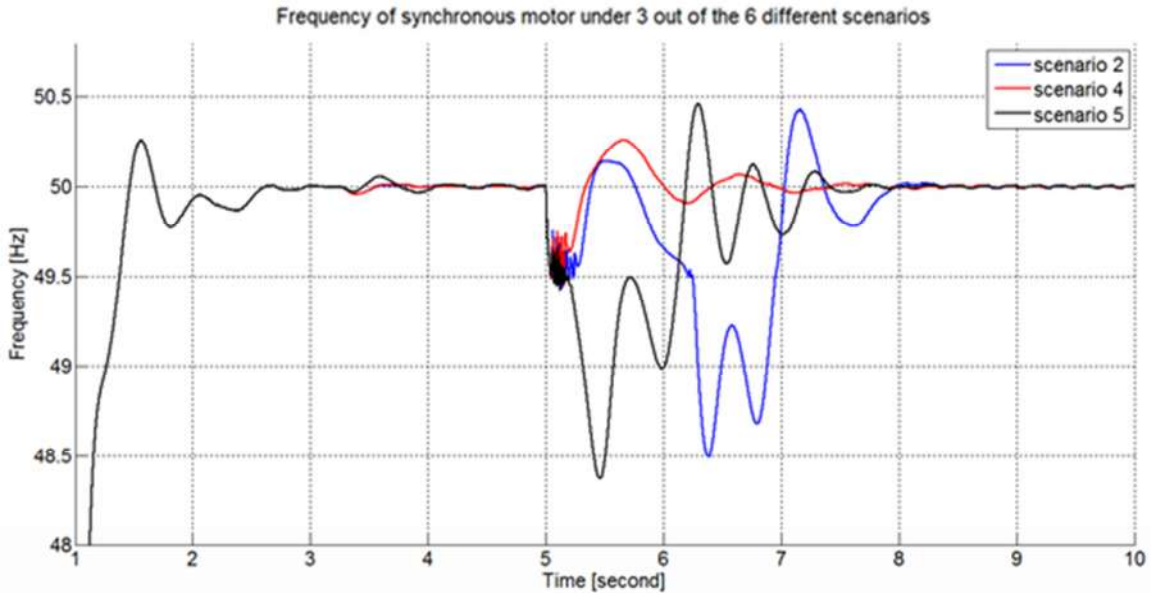


Figure 73. Synchronverters connect at $t=3.2s$ and fault occurs between $t=5s$ to $t=5.15s$. We see that scenario 4 which includes 2 synchronverters with one sided virtual friction to the motor and generator gives the best results. Adding a synchronverter with one sided virtual friction to the motor in the low voltage side does help, however since the oscillations in the synchronous generator are much stronger and are not damped by the synchronverter on the low voltage side, the effect of the synchronverter is limited. When we add both generator and motor with synchronverters we see the strong effect of one sided virtual friction in the low voltage side between the synchronverter and the motor.

We would like to see how the synchronconverter improves voltage stability as well as frequency. Figure 74 presents the two worst solutions for stabilizing the motor voltage with a synchronconverter. Figure 75 presents the four most effective synchronconverter solutions to stabilize the voltage on the synchronous motor terminals.

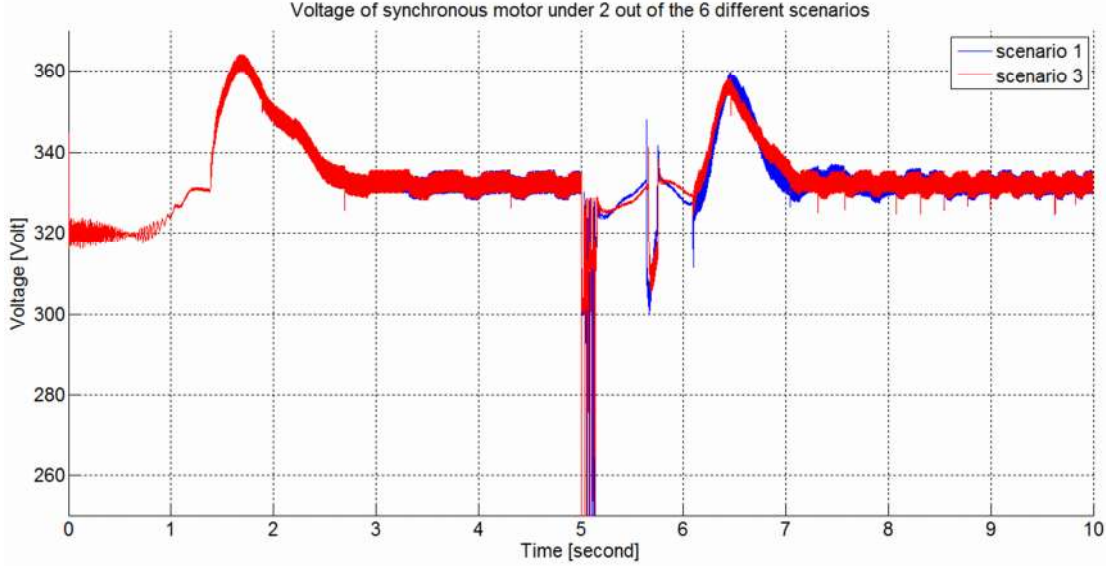


Figure 74. Voltage amplitude at motor terminals, we can see that a synchronconverter connected near the generator helps stabilize the generator but hardly helps the motor.

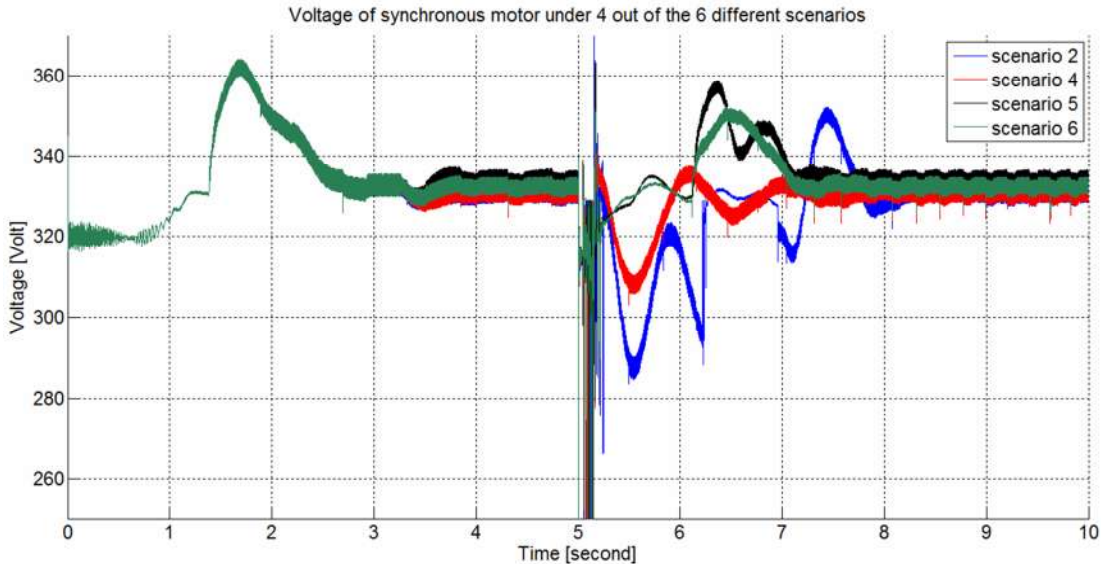


Figure 75. We clearly see the high impact of the synchronconverter in the low voltage side. Similar to the case of frequency stability in Figure 73, when one synchronconverter stabilizes the synchronous generator and another one stabilizes the motor we get the best results. Introducing a third synchronconverter in the high voltage side does not help, not even if virtual friction is working between it and the medium voltage side synchronconverter. This further justifies our assumption that no inter-area oscillations are involved.

Since the synchronous generator has an exciter which helps stabilize the voltage, we will not see much improvement or changes in the synchronous generator voltage, so we do not present it.

We wanted to verify that by increasing the droop factor D_p , we will not get a similar effect as the one sided virtual friction, although D_p assists in damping the oscillations in the synchronverters swing equation, see (4.4). For this we simulated scenario four again, but this time without one sided virtual friction but instead with D_p increased by a factor of 10.

In Figure 76 we see that increasing D_p does not give the same results as one sided virtual friction. Furthermore increasing D_p does not contribute to frequency stability of the synchronous generator at all.

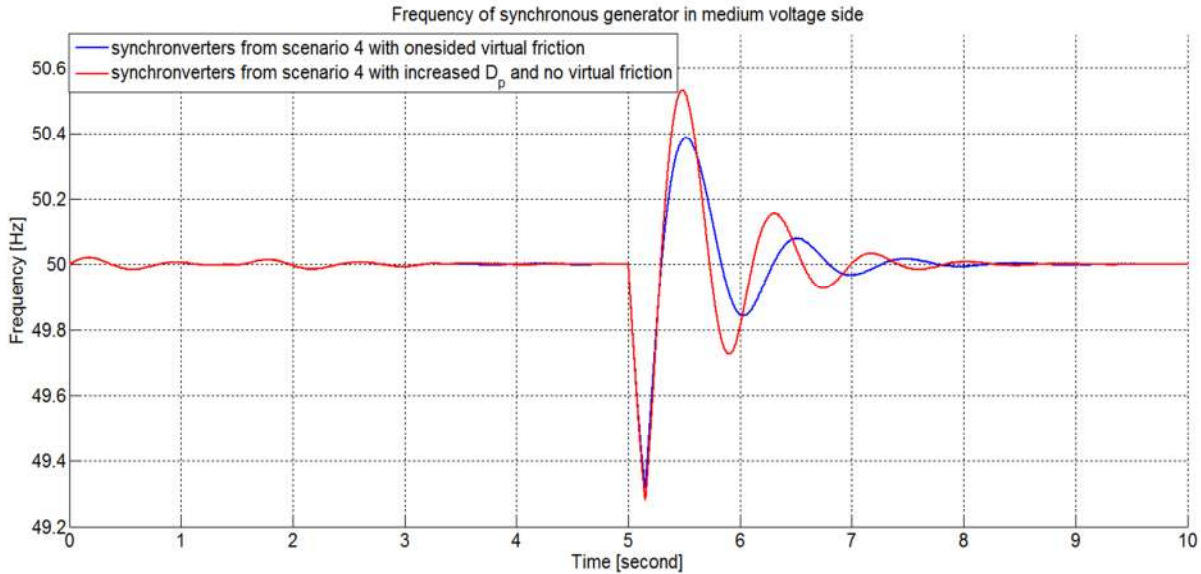


Figure 76. Comparison of one sided virtual friction to increasing the droop factor D_p in the system described in scenario 4.

To conclude I believe that one sided virtual friction gives a new approach for energy storage that can benefit the robustness of the power grid. Although connecting batteries to the grid all the time is not cost effective, we can choose to do so only on certain occasions, for instance when there is a storm or when there is an event which may lead to many faults. It can be seen from Figure 68 and Figure 69 that the synchronverter outputs a small current although the nominal power is set to 0. This could be because rotating a rotor, even a virtual one, requires some mechanical torque to maintain constant angular speed. We have no friction in our virtual rotor but it could be that our filter or switches will consume energy, and so there should always be some power output from the synchronverter to allow synchronization to the grid.

10. Future work and conclusions

We have seen that synchronous generators are not always stable, but when they are near a stable equilibrium, which is usually the case in a well-designed electrical grid, they are not only stable but can be analyzed using a simpler reduced model. We have also seen that in this reduced model rotor current does not depend on stator current and other state variables which means that the rotor current will stabilize to a constant value. In the future we will try to accurately identify the region of attraction where the reduced third order model remains stable. We also want to see if the synchronverter behaves like the fifth order model of the synchronous generator, which we know is a fairly accurate model of a real generator that has known and verified control schemes. This can help choose the parameters for the synchronverter. In this work we have only examined a case where the synchronous generator is connected to an infinite bus. We would like to study the case of two connected generators for understanding the interconnection of generators and related problems better.

We have seen from simulations that the synchronverter indeed works like a synchronous generator in terms of frequency and voltage drooping. We have also seen that a grid formed by two synchronverters behaves like a grid formed by a synchronous generator. We would like to test this in a lab in the future, with actual equipment. Another issue for the future is to diagnose and create a fault ride through behavior in the synchronverter which will probably be similar to that in a synchronous generator.

We have introduced the idea of virtual friction between two generators or synchronverters as another way to reduce inter-area oscillations. This idea has only been demonstrated using simulations. It would be useful to develop a mathematical model of this concept.

We have also examined the well-known solution to inter-area oscillations, PSS. The efficiency of PSS in a synchronverter has not been properly studied. We have only shown that it can be implemented, but we have not explored the best way to do it.

We have given some insights for the use of a synchronverter in energy storage devices. Although there is no mathematical model, it is clear that once we have more energy available during a fault, the less damage the fault will cause. We have also shown a way to implement one sided virtual friction between a synchronverter and a synchronous machine (generator or motor). Again there is a need to build a mathematical model of this.

Using data from IEC we have seen that the synchronverter is suitable for micro grids or in cases when islanded operation is allowed in a large grid. In the future when the demand for electricity would increase, the complexity of the grid will increase as well and simple stability solutions will be hard to find. The synchronverter, with its flexibility, has a good potential to provide elegant and simple solutions.

11. Bibliography

- [1] J. Alipoor, Y. Miura and T. Ise, "Distributed generation grid integration using virtual synchronous generator with adaptive virtual inertia", *IEEE Energy Conversion Congress and Exposition*, Denver, Colorado, 2013, pp. 4546-4552.
- [2] H.P. Beck and R. Hesse, "Virtual synchronous machine", *9th International Conf. on Electrical Power Quality and Utilization*, Barcelona, Spain, 2007, pp.1-6.
- [3] F. Blaabjerg, R. Teodorescu, M. Liserre and A.V. Timbus, "Overview of control and grid synchronization for distributed power generation systems", *IEEE Trans. on Industrial Electronics*, vol. 53 , 2006, pp. 1398-1409.
- [4] F. Bullo and F. Dörfler, "Synchronization and transient stability in power networks and nonuniform Kuramoto oscillators", *SIAM J. Control and Optim.*, vol. 50, 2012, pp. 1616-1642.
- [5] E. Brown and G. Weiss, "Using synchronverters for power grid stabilization", *IEEE 28th Convention of Electrical & Electronics Engineers in Israel (IEEEI)*, Eilat, 2014, pp. 1-5.
- [6] J. Driesen and K. Visscher, "Virtual synchronous generators", *IEEE Power and Energy Society General Meeting - Conversion and Delivery of Electrical Energy*, Pittsburgh, PA, 2008, pp. 1-3.
- [7] A.J. Ellison, "Electromechanical Energy Conversion", George G. Harrap and Co. Ltd., London, 1965.
- [8] R.W. Erickson and D. Maksimovic, "Fundamentals of Power Electronics", 2nd edition. Kluwer Academic Publishers, New York, 2004.
- [9] S. Fiaz D. Zonetti, R. Ortega, J. Scherpen and A. van der Schaft, "A port-Hamiltonian approach to power network modeling and analysis", *European Journal of Control*, vol. 19, 2013, pp. 477-485.
- [10] A.E. Fitzgerald, C. Kingsley and S.D. Umans, "Electric Machine", McGraw-Hill, New York, 2003.
- [11] J.J. Grainger, W.D. Stevenson, "Power System Analysis", McGraw-Hill, New York, 1994.
- [12] J.M. Guerrero, J.C. Vasquez, J. Matas, M. Castilla, and L.G. de Vicuna, "Control strategy for flexible microgrid based on parallel line-interactive UPS systems", *IEEE Trans. on Industrial Electronics*, vol. 56, 2009, pp. 726-736.
- [13] H.K. Khalil, "Nonlinear Systems", third edition, Prentice Hall, New Jersey 2002.
- [14] V.K. Khanna, "Insulated Gate Bipolar Transistor (IGBT): Theory and Design", Wiley-IEEE Press, Hoboken, NJ, 2003.
- [15] M. Klein, G.J. Rogers and P. Kundur, "A fundamental study of inter-area oscillations in power systems", *IEEE Trans. on Power Systems*, vol. 6, 1991, pp. 914-921.
- [16] P. Kundur, "Power System Stability and Control", McGraw-Hill, New York, 2009.
- [17] G.A. Leonov, D.V. Ponomarenko and V.B. Smirnova, "Frequency-Domain Methods for Nonlinear Analysis: Theory and Applications", World Scientific, Singapore, 1996.
- [18] Y. Mandel and G. Weiss, "Adaptive internal model based suppression of torque ripple in brushless DC motor drives", *Systems Science and Control Engineering*, vol. 3, 2015, pp. 162-176.
- [19] I.J. Nagrath and D.P. Kothari, "Electric Machines", third edition, Tata McGraw-Hill, New Delhi, 2004.
- [20] V. Natarajan and G. Weiss, "Almost global asymptotic stability of a constant field current synchronous machine connected to an infinite bus", *Proc. 53rd IEEE Conf. Decision and Control*, Los Angeles, 2014, pp. 3272 -3279.

- [21] B. Pal and B. Chaudhuri, "*Robust Control in Power Systems*", Springer Verlag, New York, 2005.
- [22] F.Z. Peng, L.M. Tolbert, and F. Khan, "Power electronics circuit topology – the basic switching cells", *IEEE Power Electronics Educational Workshop*, Recife, Brazil, 2005, pp. 52 - 57.
- [23] N. Pogaku, M. Prodanovic and T.C. Green, "Modeling, analysis and testing of autonomous operation of an inverter-based microgrid", *IEEE Trans. on Power Electronics*, vol. 22, 2007, pp. 613-623.
- [24] P.W. Sauer and M.A. Pai : "*Power System Dynamics and Stability*". Stipes Publishing, Champaign, IL, 1997.
- [25] J. Strand, "Energy efficiency and renewable energy supply for the G-7 Countries, with emphasis on Germany", *International Monetary Fund*, Working paper, WP/01/299, 2007.
- [26] A. Ulbig, T.S. Borsche and G. Andersson, "Impact of low rotational inertia on power system stability and operation", *IFAC World Congress*, Cape Town, South Africa, 2014.
- [27] K. Visscher and S.W.H. de Haan, "Virtual synchronous machines for frequency stabilization in future grids with a significant share of decentralized generation", *CIRED Seminar SmartGrids for Distribution*, Frankfurt, Germany, 2008, paper no 118.
- [28] J.H. Walker, "*Large Synchronous Machines: Design, Manufacture and Operation*", Oxford University Press, Oxford, 1981.
- [29] X. Yang and A. Feliachi, "Stabilization of inter-area oscillation modes through excitation systems", *IEEE Trans. Power Systems*, vol. 9, 1994, pp. 494-502.
- [30] A.A. Zea, "Power system stabilizers of the synchronous generator, tuning and performance evaluation", *MSc thesis*, Chalmers University of Technology, Goteborg, Sweden, 2013.
- [31] Q.-C. Zhong and T. Hornik, "*Control of Power Inverters in Renewable Energy and Smart Grid Integration*", John Wiley & Sons, Ltd, West Sussex, United Kingdom, 2013.
- [32] Q.-C. Zhong, P.-L. Nguyen, Z. Ma and W. Sheng, "Self-synchronized synchronverters: Inverters without a dedicated synchronization units", *IEEE Trans. Power Electronics*, vol. 29, 2014, pp. 617-630.
- [33] Q.-C. Zhong and G. Weiss, "Synchronverters: Inverters that mimic synchronous generators", *IEEE Trans. Industrial Electronics*, vol. 58, 2011, pp. 1259-1267.

12. Appendix - synchronconverter parameters

Values used for the simulation of a 5 kW synchronconverter	
Variable	Value
J synchronization	1e-5 kgm ²
D_p synchronization	1 Joule second
K synchronization	1000
R virtual	0.015 Ω
L virtual	4 mH
K_p	4e-9
K_i	2e-7
Synchronization limit	0.05 Volt
J	0.2 kgm ²
D_p	1.7 Joule second
K	5e4
D_q	120 A
R_s	0.152 Ω
L_s	4.4 mH
C	10 μF
L_g	2.2 mH
Switching period = sample time	1e-4 second
v_n	330 Volt
$M_f i_f$ initial condition	1.05 Volt second
ω_h	20 rad/second
e max	±400 Volt
P and Q LPF constant, see Figure 15	0.25 second
P maximum	8 kW
P minimum	0 kW
Ilimiter – current limiter	25 Volt

Table 4. Parameters for 5 kW synchronconverter.

Additional Comments:

The parameter synchronization limit is the voltage maximum difference we allow between the EMF and the grid voltage when we connect the synchronconverter. The voltage on the capacitor is slightly higher than e , the synchronous internal voltage of the synchronconverter. The values for the synchronization process are application dependent. For faster

synchronization J and D_p should be smaller, but there are cases where we may want higher D_p (for instance when the grid is noisy high synchronization D_p is better). Ilimiter is the maximum allowed voltage difference between the capacitor and the calculated EMF. This is used to prevent large currents as described in Chapter 5. The values of K , R and L should not be tuned since they are less application dependent and more nominal value related. The PI controller values are not sensitive and should be tuned as required. The values of K and D_q are also application dependent, but the values given here are a good starting point.

Values used for a PSS in a synchronverter	
Variable	Value
K_p	10
T_ω	1 second
LPF before PSS	Simple averaging (old + new)/2
D_{vf} (for virtual friction)	Same as D_p
K_p PSS (optional)	25
K_i PSS (optional)	0.15
High saturation value for PSS	0.05 v_n
Low saturation value for PSS	-0.1 v_n

Table 5. Parameters for PSS and virtual friction in the synchronverter.

A more advanced method for a PSS is to add a PI controller after the LPF, the rest stays unchanged. I have implemented this but noticed no improvement.

Values used for the simulation of a 1 MW synchronverter	
Variable	Value
J synchronization	1e-5 kgm ²
D_p synchronization	1.5 Joule second
K synchronization	1000
R virtual	200 Ω
L virtual	4 mH
K_p	4e-6
K_i	2e-5
Synchronization limit	0.02 Volt
J	40.5 kgm ²
D_p	337 Joule second
K	1e7
D_q	5e4 A
R_s	4e-4 Ω
L_s	0.18 mH
C	140 μF
L_g	0.029 mH
Switching period = sample time	1e-4 second
v_n	563 Volt
$M_f i_f$ initial condition	1.79 Volt second
ω_h	20 rad/second
e max	±680 Volt
P and Q LPF constant	0.0001 second
P maximum	1.4 MW
P minimum	0 kW
Ilimiter – current limiter	150 Volt

Table 6. Parameters for a 1 MW synchronverter.

For any higher power synchronverter simply take the 1 MW values (except: internal synchronous voltage maximum point e max, the amplitude reference v_n , the frequency reference ω_h , the current limitation value limiter and the initial condition for rotor flux $M_f i_f$ since they are used for synchronization only, so there is no need to change them) and

multiply those with the nominal power of the synchronverter in MW. This works very well and saves a lot of time recalculating.

LPF filtering of calculated values:

As mentioned in Chapter 5 some additional filtering is needed in the synchronverter algorithm. I have chosen to implement these filters as a basic order one LPF with one tunable parameter according to the following formula:

$$NewValue = OldValue + \frac{MeasuredValue - OldValue}{FilterParam}$$

This means that if FilterParam is 1 we simply get no filtering meaning and NewValue = MeasuredValue. For FilterParam = 2, we get a median between the old and measured values. As FilterParam is increased the LPF is stronger, filtering more.

Although in some cases I chose high values for FilterParam, this is not ideal since filtering too strong will cause loss of information. It is recommended to tune the parameter to as low a value as possible (of course the algorithm should work properly at this low value).

Conversion of this discrete filter to continuous time:

Denote y_i to be the new value, y_{i-1} to be the previous value, u_i to be the measured value, and C to be the filter constant. Let the sample time be T_s (this is the switching period of the electronic switches). Then we rewrite the filter equation as

$$y_i = y_{i-1} + \frac{u_i - y_{i-1}}{C}$$

This can be rewritten as:

$$u_i - Cy_i = -(C-1)y_{i-1}$$

We divide and multiply with T_s to get:

$$u_i - y_i = T_s(C-1) \frac{y_i - y_{i-1}}{T_s}$$

This is the discrete version of the continuous-time differential equation:

$$\dot{y} = \frac{1}{T_s(C-1)+1}(-y+u)$$

From this we get the following transfer function for the filter from u to y :

$$H(s) = \frac{1}{sT_s(C-1)+1}$$

We see that the DC gain is 1, so low frequencies are not being filtered and the time constant of our filter is $T_s(C-1)$. From here we can calculate the 3dB frequency which is $f_{3dB} = 1/T_s(C-1)$. In my simulations $T_s = 0.1\text{ms}$.

The calculated values that were filtered are:

Calculated Values with additional filtering	
Variable	FilterParam value and comments
v_g (grid measured phase voltages)	1.66, 16.66 for extremely noisy grid
Q during synchronization	$20 \Rightarrow f_{3dB} = 526 \text{ Hz}$
i_g (grid measured phase currents)	6
v_m (calculated voltage amplitude)	10000
$M_f i_f$	1000 , only if a sharp drop in voltage occurs
$\ddot{\theta}$	40, if the synchronverter sets the grid then this filter works only after initial stabilization of frequency is achieved.
T_e	12.5 - 50 only until initial stabilization
Q	$100 \Rightarrow f_{3dB} = 101 \text{ Hz}$

Table 7. Parameters for additional filters for the synchronverter.

The above filters were carefully built and tested in various simulations. They work for 5kW as well as for 1MW synchronverters. Some tuning may be useful under certain conditions but it is not recommended to deviate from these values. Overtuning or removing these filters is dangerous for the synchronverters stability.

12.1. Basic system for detecting grid faults

In order to determine whether or not there is a grid fault we needed an additional function. Commercial inverters have fault detection and handling system of their own, but for our simulation process we had no predefined regulations for handling faults. We implemented a basic function to detect the fault and disconnect only in the worst case scenarios of either less than 30% grid amplitude for 150 ms or frequency decrease of less than 2%.

Detecting grid amplitude drop is easy, we only need to know the nominal voltage. Since the voltage at the synchronverter terminals is always measured it is possible to calculate the amplitude, store it as a variable and once it drops below 30% a timer starts counting to 150 ms. After that the system outputs a logical signal to the switches and disconnects the synchronverter physically. Additionally the system will change the set mode of the synchronverter to 'not set' and the synchronverter will start synchronizing again. The synchronverter is set not to synchronize as long as the grid frequency is not in the proper boundaries of 47.5 Hz and 51.5 Hz and the voltage amplitude is above 92% nominal value. Frequency changes are more difficult to detect. We assume that the nominal grid frequency is 50 Hz on each phase. For 50 Hz frequency the time period of the voltage is 20 ms. Let the voltage on phase a be 0 Volt at $t=0$ s, since the voltage on the other two phases have a phase difference of $2\pi/3$ rad and $-2\pi/3$ rad from phase a they will be 0 at time 3.3ms and 6.6ms respectively. We define 3 variables and store the voltages of phase a, b and c at time 0s, 3.3ms and 6.6ms respectively. The variables are updated every 20 ms. Before updating the 3 variables we check if the difference between the current and the previous values is less than 5% of the nominal grid voltage amplitude. If they are not, then we know that the grid frequency had changed. In this case the synchronverter checks if the new calculated frequency (calculated by the synchronverter algorithm) is larger than the minimum frequency allowed and if the rate of change is slower than 8 Hz per second, which is the highest rate inverters are supposed to track. If one of these conditions is not met, then the synchronverter is disconnected and it tries to synchronize again. This basic implementation is sufficient for our needs since we only need to know drastic changes in frequency. For a proper Ride Through Algorithm this simple grid fault check system needs a better implementation.

The simulations were run with ode23tb solver, relative tolerance was set to 1e-3 or 1e-4 for noisy simulations. The recommended tolerance is 1e-3. According to Matlab this solver is considered the best for simulations including SimPower elements. For some simulations I had limited the max step size to 1e-4. Usually that works well but sometimes it slows the simulation without improving results so it is better to choose auto step size. All other values were set to auto and zero crossing control was not enabled. the correctness of these simulations was verified using fixed step solvers like ode4 (Runge-Kutta) with 1e-4 step size and a variable step size solver, ode45 (Dormand-Prince). The results are almost completely identical but the run time is very slow.